

The Response of Lake Water Levels to Precipitation  
—Case Study of Lake Biwa

Maho IWAKI



## **Acknowledgements**

The authors would like to thank the Japan Meteorological Agency, Geospatial Information Authority of Japan, the Lake Biwa Work Office, Ministry of Land Infrastructure, Waterworks Bureau, City of Kyoto, Kansai Electric Power Corporation, and United States Geological Survey for providing the data used in this thesis.

In Kyoto University, Lake Biwa Museum, Lake Biwa Environmental Research Institute, University of Shiga Prefecture and Lake Biwa Sigma Research Center of Ritsumeikan University, I used their facilities for the survey and analysis. I would also like to thank the Lake Biwa Branch Office of the National Institute for Environmental Studies, the Maizuru National College of Technology, and the Japan Weather Association for their great support in the writing of my doctoral dissertation. I would like to express my gratitude.

I am deeply grateful to Prof. Kenji Tanaka of Graduate School of Engineering, Kyoto University, for the opportunity to publicize my dissertation submission. I am grateful for the guidance of Prof. Masahito Sugiyama of Graduate School of Human and Environmental Studies, Kyoto University, and Prof. Michio Kumagai of Research Organization for Science and Technology, Ritsumeikan University, in the construction of the thesis, and in the observation and analysis of the data. Dr. Katsuya Nishi of the Biofluid Dynamics Laboratory provided technical guidance for the observations, and Dr. Chunmeng Jiao of the Lake Biwa Environmental Research Institute of Shiga Prefecture, provided support for the observations and data management. Dr. Takashi Toda of the Lake Biwa Museum provided guidance on the mathematical methods of the analysis. Professor Emeritus Toshio Iwakuma of Hokkaido University; Emeritus Professor Satoshi Sakai, Professor Tetsu Kogiso of Graduate School of Human and Environmental Studies, Kyoto University; Associate Professor Yoshitsugu Furukawa of Graduate School of Science, Professor Yosuke Yamashiki, Prof. Kaoru Takara, Prof. Eiichi Nakakita, Prof. Tomoharu Hori, Prof. Takahiro Syama and Prof. Tetsuya Sumi of Kyoto University, Professor Hiroshi Yajima of Estuary Research Center, Shimane University; Dr. Kohji Muraoka of New Zealand Ministry of the Environment, Dr. Tsutao Oizumi of JAMSTEC, Associate Prof. Pedro Luiz Borges Chaffe of Universidade Federal de Santa Catarina, Prof. Warwick F Vincent of Laval University, Prof. Tamar Zohary, Prof. Richard Roberts, Prof. Ilia Ostrovsky, Prof. David P Hamilton; Prof. Naotsugu Koizumi, Prof. Masahiro Maruo, Prof. Emeritus Prof. Fushimi Hiroji, Emeritus Prof. Kurashige Yoshimasa, Emeritus Prof. Takuya Okubo, Prof. Susumu Okumura, University of Shiga Prefecture, Professor Emeritus Tetsuzo Seno, University of Tokyo, Dr. Takamura Noriko, Dr. Takamura Kenji, Dr. Nakada Satoshi, Dr. Oguma Hiroyuki, Dr. Ide Reiko, Dr. Imai Akio, Dr. Mabuchi Kohji of National Environmental Institute for Studies, Ms. Kimiko Watanabe of JT Biohistory Research Hall, Ms. Haruko Yoshida, University of Shiga Prefecture, all of whom provided advice and support for the research.

Dr. Ishikawa Kanako, Dr. Mizuno Toshiaki, Dr. Sakai Yoichiro, Dr. Hayakawa Kazuhide of Shiga Prefecture Lake Biwa Environmental Science Research Institute, Dr. Hiroki Haga of Lake Biwa Museum, Associate Prof. Gael Dur of Shizuoka University. Prof. Sadao Kawamura, Prof. John C. Wells, Prof. Guillaume Auger of Ritsumeikan University, Prof. Daisuke Kitazawa, Institute of Industrial Science, University of Tokyo, Prof. Naoko Hasegawa of Ochanomizu Woman University, Emeritus Prof. Hiromu Nogami, Emeritus Prof. Terufumi Ohno, Emeritus Prof. Tetsuhisa Imasato of Graduate School of Science, Kyoto University, Associate Prof. Mamoru Kato, Emeritus Prof. Hiroki Kamata of

Graduate School of Human and Environmental Studies, Kyoto University, Emeritus Prof. Toshihiko Kawachi, Prof. Masayuki Fujihara of Graduate School of Agriculture, Kyoto University, Prof. Katsuya Kaneko of Kobe University, Prof. Naoto Ishikawa of Toyama University, Emeritus Prof. Mikio Hino, Tokyo Institute of Technology and Emeritus Prof. Ichiro Imai of Hokkaido University, provided valuable advice and encouragement. I would like to thank them for their valuable advice and encouragement.

I have received various kinds of support from the following persons.

I would like to thank the above people, my parents, and the many people who supported me, Cats Winter & Snow helped me under the COVID, and I would like to thank them.

2023 December 14<sup>th</sup> Maho IWAKI

# Index

<b>Acknowledgements</b> .....	i
<b>Index</b> .....	iii
<b>Preface</b> .....	1
<b>Chapter 1 Organisation of the thesis</b> .....	5
<b>Chapter 2 Inherent oscillations of lake water level: the seiches of Lake Biwa</b> .....	13
2–1. Introduction .....	13
2–2. Methods .....	15
2–2. 1. Observation site .....	15
2–2. 2. Measurements of water level .....	15
2–2. 3. Other data acquisition .....	16
2–2. 4. Spectral analysis .....	16
2–3. Results and Discussion .....	18
2–3. 1. Surface seiches of Lake Biwa .....	18
2–3. 2. Internal seiches of Lake Biwa .....	20
2–3. 3. Seismic seiches of Lake Biwa .....	20
2–4. Conclusions .....	30
Appendix 2A .....	31
<b>Chapter 3 Estimation of the average precipitation retention time in the watershed for the surface inflows to Lake Biwa</b> .....	33
3–1. Introduction .....	33
3–2. Method .....	35
3–2. 1. Impulse response function .....	35
3–2. 2. Observation of water level .....	37
3–2. 3. Other data acquisition .....	39
3–2. 4. The calculation method for delay time using response function .....	40
3–3. Results .....	42
3–3. 1. Delay times $\tau_L$ calculated using response function .....	42
3–3. 2. Delay times $\tau_R$ estimated using time series of the incremental water level of the Yasu River .....	45

3 – 3. 3. Relationship between the delay times $\tau L$ calculated using response function and catchment scale (river length and catchment area).....	51
3 – 4. Discussion.....	54
3 – 5. Conclusions.....	56
Appendix 3A. Two-sided t-tests with correspondence between two peaks of delay times .....	57
Appendix 3B. Daily precipitation at the catchment area of Yasu River from Jun 10 <sup>th</sup> to Aug 31 <sup>th</sup> in 2010.....	59
<b>Chapter 4 Estimation of average precipitation retention time due to subsurface flow</b> .....	61
4 – 1. Introduction.....	61
4 – 2. Methods.....	62
4 – 2. 1. Data Assimilation and Calculation of the Response Function .....	62
4 – 2. 2. The calculation method for delay time using a response function .....	65
4 – 2. 3. Other factors .....	66
4 – 3. Results and Discussion.....	66
4 – 3. 1. Data assimilation and calculation delay time using impulse response function.....	66
4 – 3. 2. Determination of delay time calculated by impulse response function using precipitation including the effect of snowfall.....	68
4 – 3. 3. Calculation of the Seasonal Response Function for each month.....	72
4 – 3. 4. Inflow due to snowmelt water .....	75
4 – 4. Conclusions.....	80
Appendix 4A. Effects of the change in the baseline observation points of BSL ....	81
Appendix 4B. Discussion on the change of the baseline observation points of BSL .....	82
Appendix 4C. Relationship between rainfall-water level and precipitation-water level of delay times from 1 to 131 days calculated using impulse response function .....	83
<b>Chapter 5 Conclusions</b> .....	84
<b>References</b> .....	87

# Preface

A deep understanding of terrestrial water storage and hydrological circulation is critically important for sustainable water management. The issue of how previous precipitation events have the strongest effect on the current lake level has long been discussed in the management of lakes (Murakami 1936, Hidaka 1943, Hayami 1951, Dooge 1973). The pathways and magnitude of precipitation inputs into a lake have significant impacts on ecosystem processes such as heat and mass transfer and diffusion, distribution of chemical concentrations, and conservation of the biological environment (Moss et al. 2011, Ostrovsky et al. 2013). However, the actual process is complex and involves many challenges to define, such as how runoff occurs at the surface, and the flow, storage and transport regimes in the ground (Figure. 1).

For this reason, in this study, for a given water mass, the time from the start of direct precipitation to the end of the inflow of the intermediate runoff component (to avoid confusion about terminology, from this point forward described as “subsurface flow”) is defined as the precipitation retention time, and the delay time for the response of the lake water level to precipitation is calculated using an impulse response function to describe the precipitation retention time in the Lake Biwa catchment area.

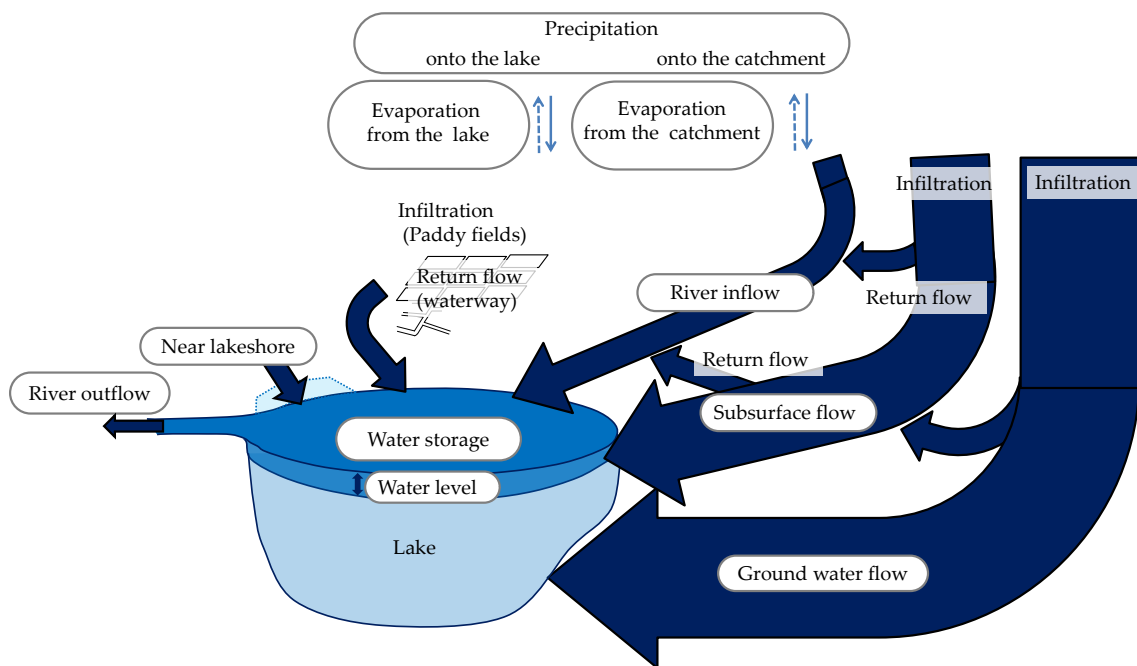


Figure 0 – 1. Hydrological processes that affect water level and and storage in a lake.

The estimation of discharge of rainfall from rivers has been studied for a long time (Murakami 1936, Iwai & Ishiguro 1970, Sugawara 1979, Yamamoto 1972, Sato 1982, Takahashi 1990). Several models have been proposed, including the bucket model (Manabe 1969), which has been used to model the land surface hydrological processes of atmospheric global circulation, and the tank model (Sugawara 1972, 1979), which is well-suited for flood forecasting. In addition, Kondo (1995) proposed a new bucket model and applied it to a catchment area to determine soil moisture and discharge.

Of these models, the tank model was devised as a runoff model to derive flow time series from rainfall time series, and since it contains the storage of rainfall in a watershed (Sugawara 1973), it is also used to index the storage in soil (soil rainfall index) based on observed and estimated rainfall data (Okada et al., 2001). Familiar to the public, the soil rainfall index is used by the Japan Meteorological Agency (JMA) as a basis for issuing warnings and advisories (Japan Meteorological Agency 2013). In addition, Sugawara (1972) indicated that, excluding runoff immediately after precipitation, about 60 % is the short-term runoff component and the remaining 40 % constitutes the base flow. Furthermore, tank models have been used to estimate the inflow into Lake Biwa (Sugawara 1973) and to model the water quality of the inland lakes (Furukawa et al. 2004), but research based on precise measurements of changes in lake surface water levels, which are essential for enhanced accuracy in runoff analysis, has not yet been attempted.

Thus, in the runoff analysis, although the estimation of water flow at the surface and subsurface is a key to understanding the dynamics of the material cycle, there are many different computational methods, different methods are proposed for different regional characteristics such as slope and geology, the estimation is based on empirical equations for each catchment, and it is not applicable when conditions are different, and the verification of the proposed runoff process is also often difficult.

Therefore, this study focused on changes in lake levels due to various factors as a basic method for determining changes in water quantities in lakes and rivers. In general, lake levels are balanced in the long term by the inflow into the lake and the outflow from the lake (Zohary & Ostrovsky 2011). On the other hand, for periodic short-term changes of a few seconds to a few dozen days, surface seiches, wind waves, precipitation (lake surface and catchment area), groundwater, lake surface evaporation, and river runoff are considered to have an effect, and for water level changes of several months to several years, natural phenomena such as evaporation at the lake surface and catchment area and groundwater inflow and outflow are considered contributing factors.

Note that when rain falls on the lake and its catchment area, the lake water level first increases slightly due to direct precipitation on the lake. On the other hand, the effect of precipitation in the catchment on the lake level emerges after a certain period of time through various inflow processes, and depends on ground surface conditions. For example, in forests, precipitation may be retained in the forest canopy or lost by plant evaporation (transpiration). Even after reaching the forest floor from the forest canopy, depending on moisture conditions at the surface of the ground, some of the water may percolate into the groundwater, while other water may flow into rivers as surface runoff.

Thus, there are complex processes by which precipitation impacts lake levels, however, the issue in lake management is how much of previous precipitation has the most influence on the current lake level. In other words, I focus on the delay time (in the response function) where rainfall at a certain time has the most influence on the lake level, while rainfall earlier or later has less influence on the water level change. If the shape of the response function (of the lake level to precipitation) that describes the delay time is determined, the important problem of how previous precipitation strongly influences the current lake level can be solved (Hidaka 1943). Even if the content of the "precipitation to lake level" system is unknown, the statistical properties of the inputs (precipitation) and outputs (lake level) to the system can be examined to understand the characteristics of the system.

To understand conceptually the relationship between input (precipitation) and output

(lake level) to a lake ecosystem, integral-type response functions are excellent and enable a simplified and more precise understanding of the characteristics of the system (Iwaki et al. 2014). For this reason, an impulse response function utilizing the  $\delta$  function was applied to the analysis (Iwaki et al. 2020a; 2020b; 2021a; 2022). The impulse response can decompose an arbitrary input into a multiplicity of impulses of various amplitudes, so the responses to individual impulses can all be expressed in the same form, under the assumption of linearity. Once the shape of this response is determined, the response to an arbitrary input can be calculated by the convolution integral of the input and the unit impulse response (Hino 1977, Iwaki et al. 2020). Furthermore, long-term research on changes in delay times could be useful in studying the effects of climate change. In the long-term, methods such as Fourier and wavelet transforms with this response function can also be used to identify the scale of time variances in the system (Carey et al. 2016; Woolway et al. 2020)

Research on precipitation and river runoff using impulse response functions has been applied to calculate delay times in the adjacent Naka River and Kuji River catchments in Japan (Yokoki et al. 2008), and furthermore, Sayama et al. (2007) separated hydrographs of long-term runoff according to time origin and calculated mean retention times, but there are no studies that relate delay times calculated with response functions to a lake system (Markus et al. 2003, Hantush 2005). The reason for this is the complexity of the watershed and underground water flow, and the difficulty in determining whether the response estimated using the original response function is precisely the response of the river level to precipitation, due to the difficulty of measuring flow rates and runoff volumes. On the other hand, response functions have been applied not only to river response but also to groundwater and debris flows (Moussa 1997, Bakker et al. 2007, Delbart et al. 2016, Hocking & Kelly 2016). However, there has been no previous application of this impulse response function method to lake levels to estimate precipitation retention time. This is because the factors related to weather and runoff that change lake levels have different temporal and spatial scales, change from time to time, and are complex. For example, it is generally difficult to measure all river inflows into a lake, and there is limited existing observational data that can be used for analysis. However, analyzing and understanding water level fluctuations in lakes with various time scales as precisely as possible would clarify the response relationships of lakes to different external inputs, enabling the dynamics of water outflow and inflow to be clearly described and predicted, which could help mitigate natural disasters.

Lake Biwa is an east Asian lake located in the monsoon zone and it is the largest freshwater resource in Japan, so it is important to manage it wisely. Lake Biwa has only one natural outlet from the lake, the Seta River, and its outflow has been measured. Thus, if the change in lake level is observed, the outflow from the catchment area could also be estimated. Therefore, the above-mentioned problems in using response functions for lake level analysis were discussed.

In this thesis study, the delay time  $\tau$  was calculated by the impulse response function using lake level and precipitation data from Lake Biwa. The precipitation retention time from direct precipitation to subsurface flow was estimated, and the results have led to an improved understanding of dynamics of water inflow and outflow for Lake Biwa. Since the characteristics of each catchment differ, the precipitation retention time estimated in this study may not be applicable to all lakes. In addition, studies of temporal and spatial precipitation distribution models are desirable (Nakakita et al. 1997; 2000, Sayama et al.

2005, Nakakita et al. 2010,). Furthermore, more precise application and extension to distribution models, such as precipitation distribution over land surfaces, topographic gradients, evaporation and groundwater, is expected. However, the methodology used in this study for estimating precipitation retention time has the potential to be applied to other lakes and its catchments. The knowledge from this study provides an improved understanding of how precipitation flows into lakes and forests during heavy rainfall and snowmelt. The results may contribute to appropriate monitoring and management strategies for lakes and forests as well for disaster prevention.

# Chapter 1 Organisation of the thesis

This thesis addresses several key aspects of the hydrodynamic properties of Lake Biwa and hydrological features of the Lake Biwa catchment. Specifically, I examined surface seiches in the lake, and precipitation retention times in the catchment through surface and subsurface flows. The detailed structure of thesis is as follows.

In Chapter 2, the seiches (inherent surface oscillations) of Lake Biwa are described and analyzed. This first stage of the work was necessary to discriminate between water level changes caused by precipitation and those caused by natural oscillations of the lake. A “seiche” is a periodic oscillation of the lake water surface and usually has the properties of a standing wave that lasts for several hours or sometimes for several days (Forel 1895, Yoshimura 1937). Wind and pressure are considered the main causes of seiches (Forel 1895). For surface seiches in general, the wind pushes the lake water downwind to the shore of the leeward side, where an increase in water level is maintained until the wind stops. When the force of the wind abates, the water mass flows back under the influence of gravity, thus generating a stationary wave that moves back and forth while gradually decreasing in magnitude. Seiches are therefore described as stationary surface gravity waves.

In the case of Lake Biwa, the first mode, which has the largest amplitude, is the one with the longest node ( $\approx 60$  km); the period of this first mode is about 4 hours, in addition to the oscillation of the southern bay (Imasato 1970; 1971; 1972). Although the volume of lake water itself does not change due to seiches, the water level change due to seiches is periodic. For the surface seiche of Lake Biwa, five modes have already been identified and studied by Imasato (1970; 1971; 1972). Internal static vibration of Lake Biwa has also been identified by Kanari (1970; 1975) and Jiao & Kumagai (1995). For this reason, in this study, a review and synthesis of previous studies of surface and internal seiches was conducted.

In contrast to wind-induced seiches, there have been much fewer studies of seiches induced by seismic activity (Berninghausen 1964; 1966; 1969, McGarr & Vorhis 1968, Kvale 1995, Utsu 2001, Barberopoulou 2004; 2008), and few numerical analyses in oceanography, limnology, and hydrology (Ichinose et al. 2000). For this reason, especially seismic seiche-related oscillations caused by Rayleigh waves from large earthquakes are yet to be explored and comprehensively elucidated. In this thesis study, I investigated water level fluctuations in Lake Biwa associated with surface seiches following the 2011 Tohoku earthquake.

The results of Chapter 2 have been published in the following papers. Iwaki et al (2014) reviewed the surface seiches of Lake Biwa and Iwaki & Toda (2022) described seismic surface seiches (surface) of Lake Biwa, while Iwaki et al (2022) examined the internal seiches of Lake Biwa.

○Iwaki, M., Kumagai, M., Jao, C., Nishi, K. Evaluation of river inflows during heavy precipitation based on water level changes in a large lake. *Jpn J Limnol*, **2014**, 75:87–98. <https://doi.org/10.3739/rikusui.75.87>

○Iwaki, M., Toda, T. Seismic seiche-related oscillations in Lake Biwa, Japan, after the 2011 Tohoku earthquake. *Sci Rep.* **2022**, *12*, 19357. <https://doi.org/10.1038/s41598-022-23939-7>

In Chapter 3, I focused on calculations of the delay time due to river inflow using an impulse response function based on high-resolution water level observations obtained in the south of Lake Biwa. Then, consider the outflow pattern from the calculated delay time and estimate the precipitation retention time due to river inflow.

In the Lake Biwa catchment area, I focused on the Yasu River because its catchment area is the largest and longest in length. The delay time of river discharge of the Yasu River was assumed to be 24 hours based on time series data of water level only (without considering input from precipitation) and compared with the delay time of 23.7 hours which calculated using a response function based on the relationship between precipitation and water level. Based on these results, the delay time due to river inflow of the Yasu River using the response function was hypothesized to be approximately 24 hours, and a shorter delay time was assumed to be the response due to river inflow. Then, based on the relationship between delay time and river scale (river length and catchment area), I estimated the delay time due to more than 450 river inflows.

In Chapter 3, as the delay time, the two types of return flows (slow return flow and fast return flow), river inflow and subsurface flow treated separately. This return flow refers to the flow of water that has infiltrated or stayed in the river after surface outflow and flows back into the river. Fast return flows were a combination of river inflow, surface outflow, and shallow infiltration. On the other hand, Slow return flows had little or no river inflow and were a combination of surface outflow, subsurface flow, and infiltration into the (shallow) ground (but not into the groundwater flow).

The contents of Chapter 3 have been published in the following papers. Iwaki et al. 2014 was the published paper on which this thesis is based. Iwaki et al 2020 is a paper that constitutes chapter 2. The delay time calculated from the response function is discussed, and the factors of delay due to each river inflow are discussed and the delay time for each river is estimated. This paper is the origin of average precipitation retention time estimation due to the river inflow.

○Iwaki, M.<sup>a)</sup>, Yamashiki, Y., Muraoka, K., Toda, T., Jiao, C., Kumagai, M. Effect of rainfall-influenced river influx on lake water levels: Time scale analysis based on impulse response function in the Lake Biwa catchment area. *Inland Waters*, **2020a**, *10*, 283–294. <https://doi.org/10.1080/20442041.2020.1712952>

Other relevant published papers include the surface seiches (Iwaki & Toda 2022), the direct rainfall on the lake surface (Iwaki et al 2022), and understanding river inflow from the Yasu River (Iwaki et al. 2021).

○Iwaki, M., Toda, T. Seismic seiche-related oscillations in Lake Biwa, Japan, after the 2011 Tohoku earthquake. *Sci Rep.* **2022**, *12*, 19357. [https://doi.org/10.1038/s41598-022-](https://doi.org/10.1038/s41598-022-23939-7)

○Iwaki, M., Hayakawa, K., Goto, N. An estimation of precipitation retention time using depth metres in the northern basin of Lake Biwa. *Atmosphere* **2022**, *13*, 724. <https://doi.org/10.3390/atmos13050724>

○Iwaki, M.<sup>b)</sup>, Takamura, N., Nakada, S., Oguma, H. Monitoring of lake environment using a fixed point and time-lapse camera—Case study of south basin of Lake Biwa. *Journal of The Remote Sensing Society of Japan*, **2021**, *41*;5, 563–574. <https://doi.org/10.11440/rssj.41.563>

In Chapter 4, using the daily water level data (five-point average) of Lake Biwa for 31 years from 1983 to 2013 from the Ministry of Land, Infrastructure, Transport and Tourism, I calculated the response function of precipitation - water level (and precipitation - water volume) for four months and estimated the precipitation retention time due to subsurface flow. To evaluate the results of the estimation of average precipitation retention time by subsurface flow, I focused on seasonal changes in snow water equivalent and changes in dissolved oxygen concentrations in the lake during snowmelt at the catchment area of Lake Biwa. Although the timing of the most significant average precipitation retention time varied, the average retention time due to subsurface flow was estimated to be approximately 45 days, based on the observed snow water equivalent and discussion of the snowmelt period which estimated from the observed snow water equivalent. In addition, seasonal results (every 4 months) suggest that the average precipitation retention time due to subsurface flow varies with the season (earlier during snowmelt and later after the paddy season and during dry periods).

○Iwaki, M.<sup>a)</sup>, Yamashiki, Y., Toda, T., Jiao, C., Kumagai, M. Estimation of the average retention time of precipitation at the surface of a catchment area for Lake Biwa. *Water*, **2021**, *13*, 1711. <https://doi.org/10.3390/w13121711>

Other relevant details are the measurement of snow water volume and estimation of snow melt in the published paper by Iwaki et al. 2011.

○Iwaki, M., Hida, Y., Ueno, K., Saijyo, M. Observation of snow water equivalent in the north catchment area of Lake Biwa. *Lakes Reserv. Res. Manag.* **2011**, *16*, 215–221. [doi:10.1111/j.1440-1770.2011.00454.x](https://doi.org/10.1111/j.1440-1770.2011.00454.x)

In Chapter 5, I summarize the findings of Chapters 2, 3 and 4. In Chapter 2 the water level changes due to surface and internal seiches—the natural vibration of the lake, and in Chapters 3 and 4 the average precipitation retention time due to river inflow and subsurface flow was estimated, and discussed in relation to the delay time calculated by the response function.

The overall concept of precipitation retention time estimation (Chapters 3 and 4) is shown below and presented in Figures 1 – 1, 1 – 2 and 1 – 3. Below is the summary of the precipitation retention time estimation (Chapters 3 and 4).

Figure 1 – 1 shows how the delay time  $\tau$  was calculated using the impulse response function, the method used in Chapters 3 and 4. The input data is precipitation, and the output data is the water level of Lake Biwa. First, the input data were standardized. Then, the autocorrelation function  $C_{xx}(\tau)$  and the cross-correlation function  $C_{xy}(\tau)$  were obtained. The power spectrum  $S_{xx}(\omega)$  was obtained by complex Fourier transforming the autocorrelation function  $C_{xx}(\tau)$  and the cross spectrum  $S_{xy}(\omega)$  by complex Fourier transforming the cross-correlation function  $C_{xy}(\tau)$ , respectively. Finally, the system function  $H(\omega)$  was calculated by dividing  $S_{xy}(\omega)$  by  $S_{xx}(\omega)$  in the frequency domain, and the response function  $h(\tau)$ , a function of delay time  $\tau$ , was obtained by inverse Fourier transforming  $H(\omega)$ . The shape of this response function  $h(\tau)$  represents the response of the water level to precipitation.

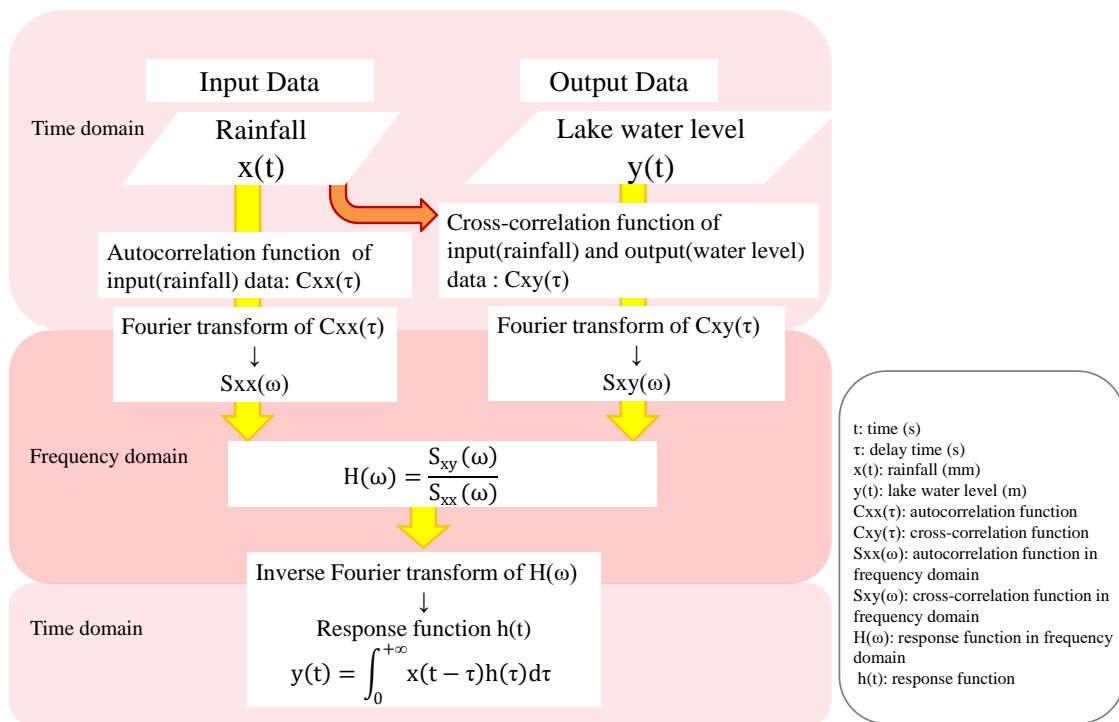


Figure 1 – 1. Flow chart for calculating delay times using a response function.

$t$  : time(s),  $\tau$ : delay time(s),  $x(t)$  : Precipitation(mm),  $y(t)$  : Water level(m),  $C_{xx}(\tau)$  : Autocorrelation function,  $C_{xy}(\tau)$  : Cross-correlation function,  $S_{xx}(\omega)$  : Power spectrum,  $S_{xy}(\omega)$  : Cross spectrum,  $H(\omega)$  : System function,  $h(t)$  : Response function.

The estimation of precipitation retention time in Lake Biwa and its catchment area is complex because several factors are involved. For this reason, Figure 1 – 2 shows a schematic representation of the water flow in Lake Biwa and its catchment area, including various delay time-related factors, as discussed in Chapters 3 and 4. Hydrological processes analyzed in Chapter 3 (river inflow, infiltration, return flow) are colored yellow, and those analyzed in Chapter 4 (snow & snowmelt, subsurface flow) are colored red.

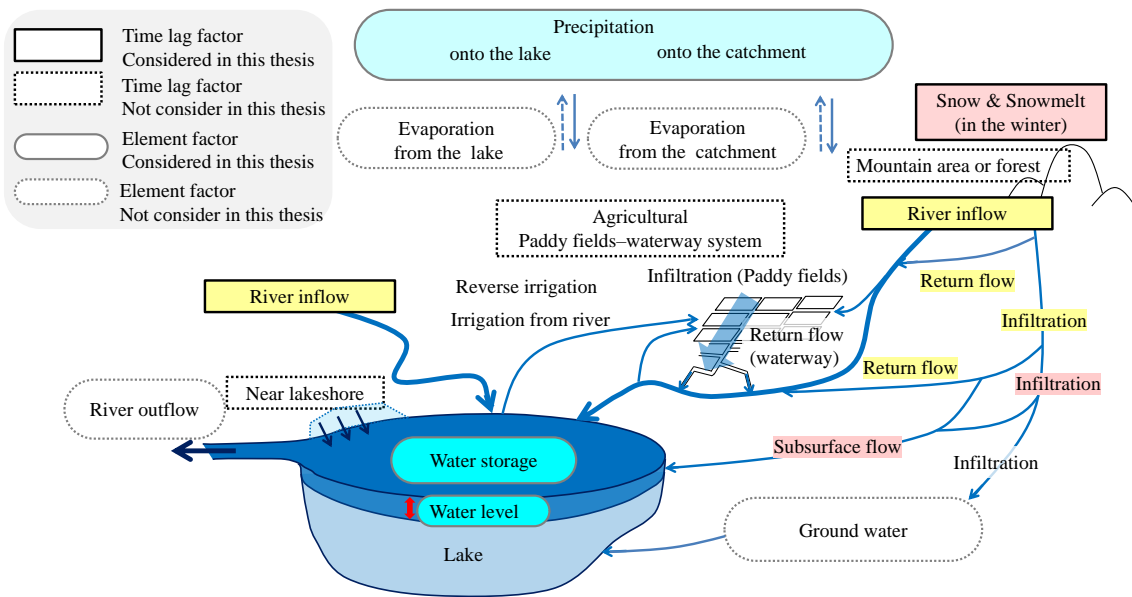
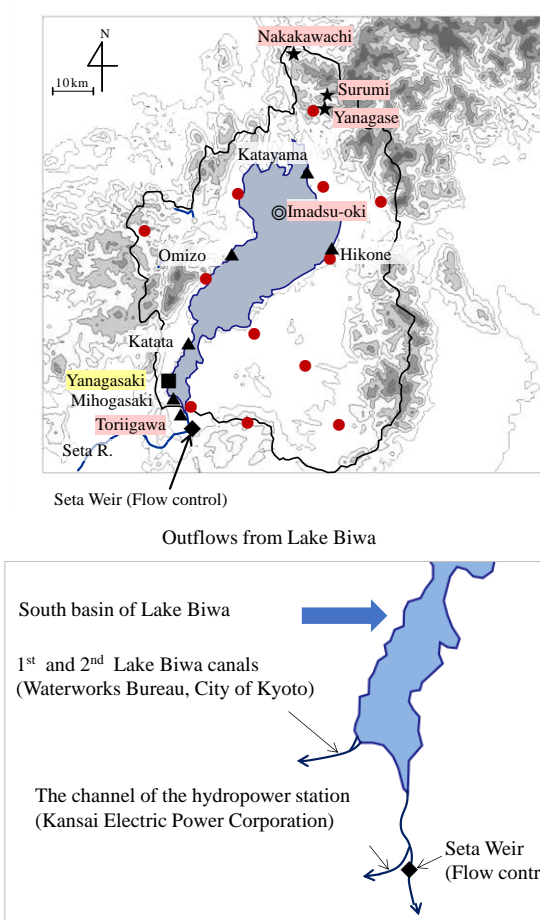


Figure 1 – 2. Diagram of water flows from the catchment area to the lake.

The items in square boxes are processes related to delay time, the elements in rounded square boxes are key hydrological components, and the items and elements addressed in this thesis are solid lines. Processes and elements that are not addressed in this thesis are presented by dashed lines.

Figure 1 – 3 shows the meteorological and water level data, and its locations used in Chapters 3 and 4, respectively. However, because the observation method, observation period and observation interval differ between Chapters 3 and 4, the water level observation points, data names, points, and elements used in each chapter are shown in different colors. Herein,  $t$  is time and  $\Delta t$  is the time interval between sampling (the same applies hereafter). The observation points and data used in Chapter 3 are colored yellow, and the sites and data used in Chapter 4 are colored red (Figure 1 – 3).



■ Observed water-level ( $\Delta t = 1$  or 2 min) at south basin (Yanagasaki).  
 ▲ Water-level data ( $\Delta t = 10$  min, 1 h) at five points average water level data (Mihogasaki, Katata, Omizo, Katayama, Hikone, Toriigawa) conducted by Lake Biwa Work Office (Ministry of Land Infrastructure, Transport and Tourism).  
 ● Meteorological data ( $\Delta t = 1$  h) Automated Meteorological Data Acquisition System (AMeDAS), Japan Meteorological Agency.  
 ◆ Discharge data ( $\Delta t = 10$  min, 1 h)  
 Ministry of Land Infrastructure, Transport and Tourism (MLIT), Waterworks Bureau, City of Kyoto, Kansai Electric Power Corporation.

▲ Water-level data ( $\Delta t = 1$  day) at five points average water level data (Mihogasaki, Katata, Omizo, Katayama, Hikone, Toriigawa) conducted by Lake Biwa Work Office (Ministry of Land Infrastructure, Transport and Tourism).  
 ● Meteorological data ( $\Delta t = 1$  day) Automated Meteorological Data Acquisition System (AMeDAS), Japan Meteorological Agency.  
 ◆ Discharge data ( $\Delta t = 1$  day)  
 Ministry of Land Infrastructure, Transport and Tourism (MLIT), Waterworks Bureau, City of Kyoto, Kansai Electric Power Corporation.  
 ★ Observed snow water equivalent (1–2 times/week) at the northern catchment are of Lake Biwa (Yanagase, Surumi, Nakakawachi).  
 ◎ The water temperature and dissolved oxygen (DO) (1 times/2week) at eight depths in northern part of Lake Biwa (Imadsu-oki) conducted by Lake Biwa Work Office (Ministry of Land Infrastructure, Transport and Tourism).

Figure 1 – 3. Observation sites for data used in this thesis. Those related to Chapter 3 are colored yellow, and those related to Chapter 4 were colored red.

#### Observation sites:

- Water level (South basin, Yanagasaki,  $\Delta t=1$  min or 2 min)
- ★ Snow water equivalent (northern catchments,  $\Delta t=3$  to 7 days)

#### Data:

- ▲ Water level (Toriigawa (BSL; Lake Biwa baseline) used the data of Toriigawa before 1992), Katayama, Omizo, Hikone, Katata, Mihogasaki), BSL; +84.371 m a.s.l. after 1992 BSL used the average of five points (Katayama, Omizo, Hikone, Katata, Mihogasaki),  $\Delta t=1$  day, the Lake Biwa Work Office of MLIT; Ministry of Land, Infrastructure, Transport and Tourism)
- Meteorological data (AMeDAS; Automated Meteorological Data Acquisition System,  $\Delta t=1$  day, JMA; Japan Meteorological Agency)
- ◆ Discharge (Seta River,  $\Delta t=1$  day, the Lake Biwa Work Office of MLIT, Waterworks Bureau, City of Kyoto, Kansai Electric Power Corporation)
- ◎ Water temperature • Dissolved oxygen; DO (North basin, the center of Imadsu-oki, 8

depths,  $\Delta t = 1$  time/2 weeks, White paper of Shiga Prefecture, Lake Biwa Environmental Research Institute, 2009–2010)



# Chapter 2 Inherent oscillations of lake water level: the seiches of Lake Biwa

## 2 – 1. Introduction

Lake Biwa is the largest freshwater resource in Japan, with a surface area of 670.25 km<sup>2</sup> and a maximum depth of 104.1 m (Kumagai et al. 2006). The northern basin is wide and deep, whereas the southern basin is narrow and shallow. More than 450 rivers and streams flow directly into the lake; however, there is only one natural outlet (Seta River) and two artificial canal outflows that supply water to the city of Kyoto. Moreover, a third outflow is used for hydropower generation. A 1-cm change in the water level of Lake Biwa corresponds to a volume of approximately  $6.7 \times 10^6$  m<sup>3</sup>. This implies that even a small change in the water level might severely affect local ecosystems, particularly in the shoreline regions (Tsai et al. 2014). For example, water level dynamics becomes important for the survival of many species that have evolved synchronised life cycles to such fluctuation patterns (Zohary & Ostrovsky 2011, Gronewold 2019).

Factors that influence water level changes include wind waves, surface seiches, precipitation, river flow (inflow and outflow), evaporation, and groundwater. Others include several factors, such as direct precipitation on the lake surface, each with its own specific temporal and spatial scale (Hofmann et al. 2008, Zohary and Ostrovsky 2011). In addition, the water level changes in Lake Biwa are complex due to its large surface area and shape. It is difficult to identify the factors that influence these complex water level changes.

As the lake surface oscillation, the lake has an inherent oscillation, a seiche. This term refers to the periodic oscillation of the surface water of lakes and other closed or half-closed water basins and it is typically characterised by standing wave properties. In Japan, the first studies of seiches were conducted at Lake Ashinoko in 1891 (Hikosaka 1971). Nakamura and Honda (1902) have described seiches in Japanese lakes, including Lake Biwa, and provided detailed technical drawings of the changes in water levels. In response to studies indicating a relationship between the Sanriku tsunami of 1896 and seiches in harbours, several surveys were conducted in major ports and harbours in Japan from 1903 to 1906, thereby culminating into a report by Honda et al. 1908.

Over the past few decades, the surface seiches of Lake Biwa have gained increased research interest. Imasato (1970; 1971; 1972) observed water level fluctuations and developed a numerical simulation model of the seiches from which he identified five dominant seiche modes with periods of 255.5, 79.8, 69.1, 38.7, and 31.9 min. These values were corroborated by field observations that defined the dominant modes as 249.6, 74.1, 65.7, 39.7, and 32.1 min, respectively (Imasato et al. 1971; 1973).

When discussing changes in the water level of a lake, the effects of seiches cannot be ignored. In this study, I investigated basic seiches (surface and internal) and seismic seiches. There are two types of seiches: surface seiches and internal seiches. Surface seiches are mainly caused by strong wind, but earthquakes can also generate these oscillations, called seismic seiches. The surface seiche in Lake Biwa has been the subject of many studies (Table 1–1) and was well detailed by Imasato (1984).

Internal seiches occur when the thermocline is present in a lake (from spring to summer),

and shows wind-induced oscillation, with a period is longer than that of surface seiches. Internal seiches in Lake Biwa were reported by Kanari (1975) and Jiao & Kumagai (1995). However, as for the seismic seiches there are still many unknowns. To distinguish water level changes due to precipitation retention time from these natural oscillations, I have examined surface seiches and internal seiches in Lake Biwa to better understand their periods and other properties. In addition, I examined seismic seiches, with attention to water level changes after the 2011 Tohoku earthquake (2011TE).

## 2-2. Methods

### 2-2.1. Observation site

The surface area and mean water depth of the northern basin are 618.65 km<sup>2</sup> and 43 m, respectively, and the respective values of the southern basin are 51.6 km<sup>2</sup> and 4 m (Haga 2006). The study site was the Yanagasaki pier located at the southwest end of the South Basin. The elevation of the site is 87 m above sea level, and the mean depth is 2 m (Figure 2-1). The pier is typically not busy, and boat arrivals and departures typically occur for several minutes to twice a day; thus, their effect on the water column is marginal.

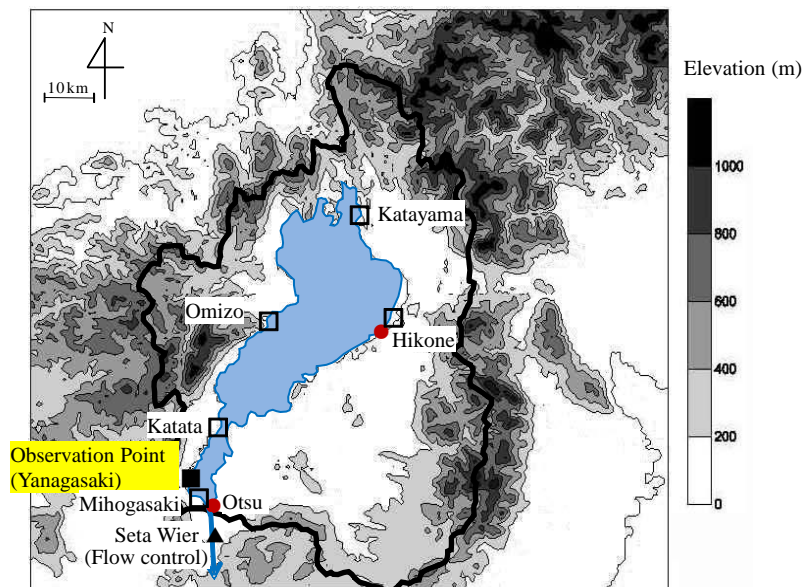


Figure 2-1. Mean water level (■) observation stations around Lake Biwa (dt = 60 s, 120 s). Water level observation sites were monitored by the Lake Biwa Work Office of MLIT (□) (dt = 1 h), AMeDAS and JMA (●) (dt = 1 h), and water discharge data were provided by the Lake Biwa Work Office of MLIT (dt = 1 h), Waterworks Bureau of Kyoto city, and the Kansai Electric Power Corporation (▲).

### 2-2.2. Measurements of water level

To determine water level fluctuations in Lake Biwa, I deployed a capacity-type water level gauge at the end of the Yanagasaki pier (Fig. 2-2). Because the pier where the water level instrument is installed is normally restricted to human traffic except for boarding, it is negligible for the assumed time-domain (or frequency-domain) water level changes. A water level instrument and a HIOKI (LR5042) data logger were installed at the end of the pier at Yanagasaki (Figure 2-2). The water level instrument has a resolution of 1 mm and an accuracy of  $\pm 3$  mm (Table 2A). Sampling intervals were 1 minute from April 22, 2010, to May 20, 2010 and from November 1, 2011 to March 31,

2012, and 2 minutes from May 21, 2010 to October 31, 2011.

The capacitance water level instrument that was used is a device that measures water level fluctuations using two parallel wires (a Teflon wire and a stainless-steel wire) and a linear relationship between the water level and the pulse width of the CR oscillation circuit (Iwaki et al. 2014). Although regular maintenance is required, this method enabled accurate and continuous observation of changes in the lake water level at high-resolution time intervals ranging from a few seconds to several hours (and in some cases a few days to several days). A data logger HIOKI (LR5042) was used to record the water level observation results.

A CR oscillation circuit and a data logger were placed inside a waterproof case (white box in the center of the photo) fixed to a pipe frame, and Teflon and stainless-steel wires (center of the photo) were stretched in parallel between the CR oscillation circuit and the bottom of the pipe frame to measure water level fluctuations. The measurement interval is 2 minutes, the resolution is 1 mm, and the accuracy is  $\pm 3$  mm (Iwaki et al. 2014).



Figure 2 – 2. Photographs of the water level gauge (left) and observation site (right) with rain and water level gauges deployed at the Yanagasaki pier.

### 2 – 2. 3. Other data acquisition

I observed the water level at a single site in the southwest region of Lake Biwa and used additional water level data measured at five stations operated by the Biwako Office of the Ministry of Land Infrastructure, namely: Katayama, Omizo, Hikone, Katata, and Mihogasaki (Figure 2-1). Data on artificially controlled discharge through the Seta River were also provided by the Biwako Office of MLIT. Nine floodgates controlled the flow at the Seta Araizeki weir. Additional discharge data for the two canals and the hydropower station channel were provided by the Waterworks Bureau in Kyoto city, and the Kansai Electric Power Corporation, respectively. Moreover, meteorological data and earthquake information were provided by JMA, Geospatial Information Authority of Japan; GSI, and United States Geological Survey; USGS.

### 2 – 2. 4. Spectral analysis

I used two different spectral analysis methods to identify the characteristics of various

types of surface waves; a) The fast Fourier transform (FFT). This algorithm is a conventional method for analysing oscillatory motions to extract wave spectra, including surface seiches, under the assumption of repeating infinite length data instead of obtaining data for the given time series (Hino 1977, Koike 1997). b) The maximum entropy method (MEM). This was established as a spectral analysis technique by Burg 1975 to obtain wave spectra using short-period data for phenomena, such as seismic waves, because it can help perform spectral estimations to maximise information entropy with an autocorrelation function (Minami 1997, Tokiwano et al. 2002).

## 2 – 3. Results and Discussion

### 2 – 3. 1. Surface seiches of Lake Biwa

The Lake Biwa surface seiche shows oscillations typically up to 6 cm, which is the expected amplitude of lake seiches depending on wind speed and direction (Figure 2–2). The period of the first mode of the surface seiche in Lake Biwa was calculated using the FFT method as approximately 4 h (Figure 2–2), which is similar to the results of Imasato (1984) (Table 1 – 1).

Table 1 – 1. Previous studies on the surface seiche of Lake Biwa (compiled from Imasato (1984) and Iwaki et al. (2014)). Obs: Observation results, Ex: Experimental results, Cal: Calculation results.

Investigator	Year		Period (minutes)					
			Mode- I	Mode- II	Mode- III	Mode-IV	Mode- V	Others
Nakamura & Honda	1911	Obs.	231.2	72.6			30.5	25.2, 22.7
		Ex.		71.9			30.5	
Suda et al (Kobe Mar. Observ.)	1926	Obs.	242.0	71.0		36-37	30.0	25-22, 15
Takaya	1931	Obs.	236.2					
Nomitsu	1935	Obs.	250.0	68.4			30.0	20, 12, 5
Takahashi	1935	Cal.	208.0	68.0				
Nomitsu et al.	1937	Obs.						18-15, 5
Toyohara & Habu	1938	Obs.		66.0			32.0	
Takahashi & Namekawa	1938	Obs.	220.0					
Imasato	1970	Cal.	212.0	71.3	61.0	37.0	32.3	
Imasato	1971	Cal.	255.5	79.8	69.1			
		Obs.	243.9	74.1	65.1			
Imasato	1972	Cal.				38.7	31.9	51.1
		Obs.	232.3	74.1	66.4	40.2	32.6	
Imasato	1973	Obs.	229.8	72.7	65.1	40.1	30.5	
Mutamoto	1976	Obs.	217.5-248.6	74.8-75.8	65.5-72.0	40.0-41.1	30.0-31.9	
Nishio	1992	Cal.	214.4	67.6	60.1	35.2	33.9	
		Obs.	227.6	71.9	64.5	39.8	32.3	
Seki & Taniguchi	2004	Cal.	233.2	71.5	63.3	38.9	32.4	
						37.1	32.0	
		Obs.	240.9	71.9	65.0	39.8	32.3	
Iwaki et al.	2014	Obs.	208.2-255.0	67.8-72.0	64.8-69.0	37.2-40.2	30.0	
Mean		Obs.	237.9	72.0	66.0	40.0	31.1	
		Cal.	224.6	71.6	63.4	37.1	32.7	

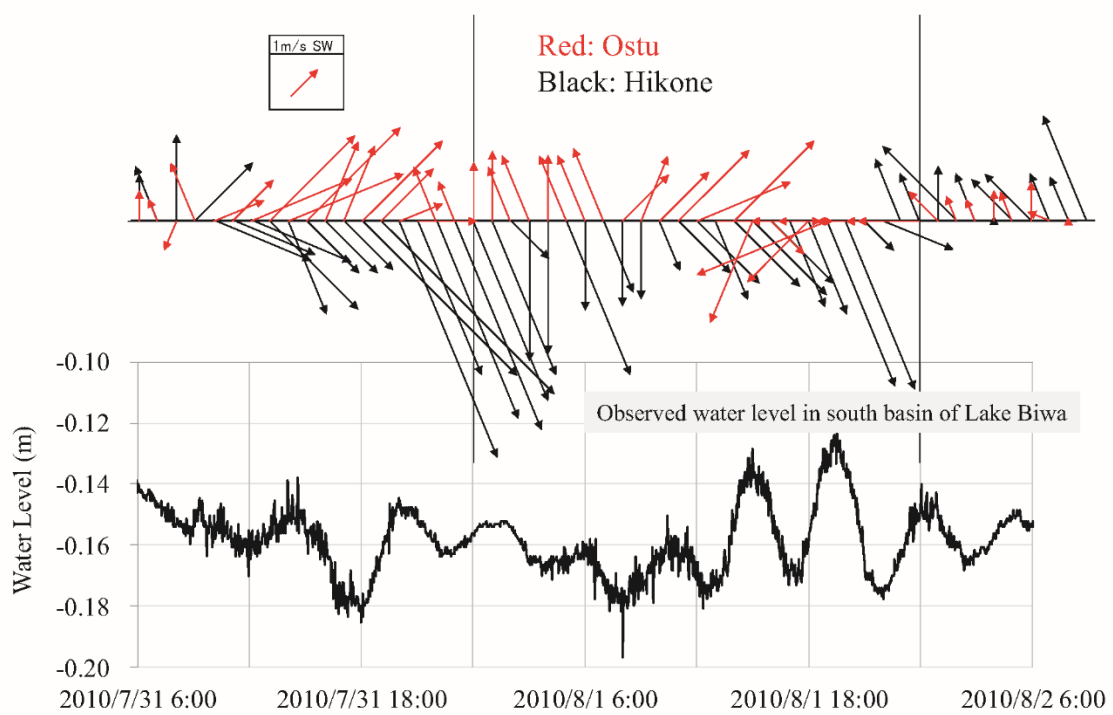


Figure 2–3. Typical seiches for the observed water levels in the South Basin of Lake Biwa from 31 July 2010 to 2 August 2010. Time series of the wind vectors measured at Otsu (South Basin) and Hikone (North Basin) meteorological stations (top panel) and water level changes at Yanagasaki Pier in the South Basin (bottom panel). As can be seen in this figure, the water level varies regularly after a strong wind blows. Seiches involve the inherent oscillations, and these periods are decided in part by the shape of the lake.

### 2–3. 2. Internal seiches of Lake Biwa

Generally, internal seiches are induced by strong wind. In this study, I identified the period in which internal seiches were induced by using the response function for rainfall to the lake water level in the northern basin of Lake Biwa (Iwaki et al. 2022). The results show that the internal seiches correlate with the change in lake water level. Similar to previous research, the periodic change of 56 h corresponds to the longitudinal internal seiche of the northern basin of Lake Biwa, which was caused by the northerly component of the wind that blew over the lake during an internal period of ~24 h, and the period of internal seiches of Lake Biwa as 66.7 h (Kanari 1970, 1975, Jiao & Kumagai). Figure 2–4 showed the delay times calculated using response functions with respect to average rainfall from 24<sup>th</sup> June to 17<sup>th</sup> July 2018, showing  $30 < \tau < 100$  h, and the Figure 2–4 was cited from Iwaki et al. 2022. Based on Figure 2–4, the delay times of 57 h ( $\approx 2.4$  d) or 68–71 h (2.8–3 d) from May 2018 to October (internal seiches were observed during the thermocline, I estimate that the period can be observed until August or September) correspond to the internal seiche.

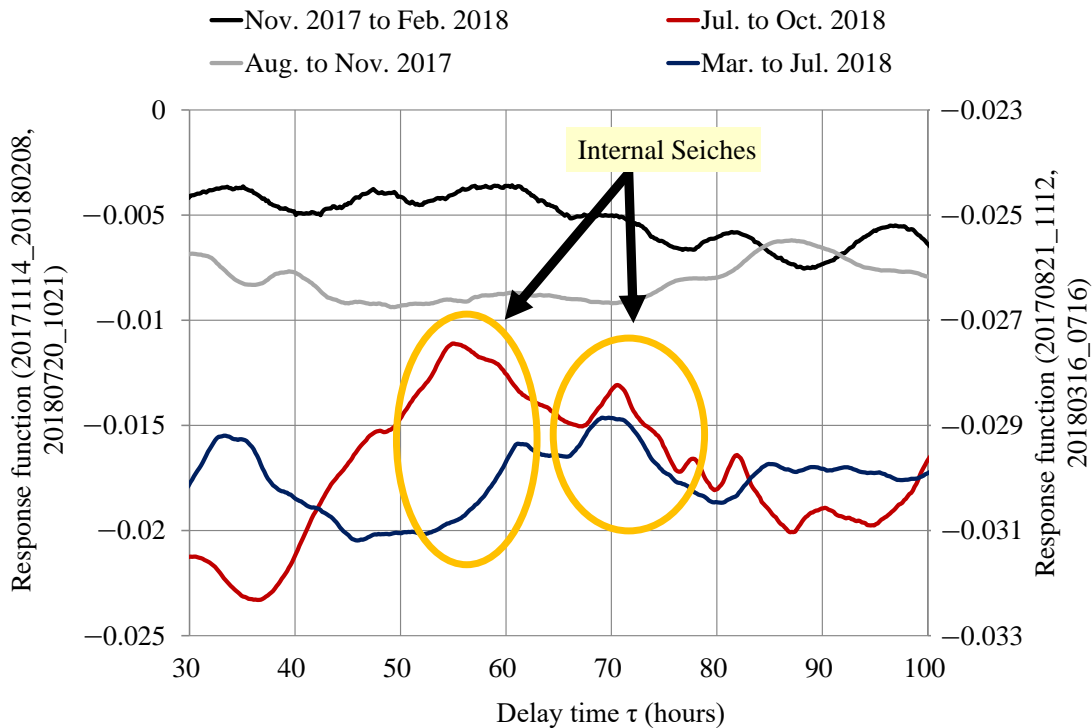


Figure 2–4. Calculated delay times, from water level response functions using average rainfall data from Aug. 2017 to Oct. 2018, showing  $\tau > 30$  (cited from Iwaki et al. 2022). The circled peaks indicate internal seiches.

### 2–3. 3. Seismic seiches of Lake Biwa

Seismic seiche-related oscillations caused by Rayleigh waves from large earthquakes are yet to be explored and elucidated comprehensively, and require ongoing study and cumulative knowledge. Herein, I investigated water level fluctuations in Lake Biwa of

Japan from surface seiches following the 2011 Tohoku earthquake. Lake Biwa is the largest freshwater resource in Japan, and a small change in its water level can affect local ecosystems. Field observations were conducted during 2010–2012 using a water level gauge with 1-mm resolution and a 2-min data sampling interval. Fast Fourier transform and maximum entropy methods were used for data spectral analysis to distinguish the effects of inherent oscillations on water levels generated by the earthquake. I considered that water level changes were influenced not only by the earthquake's motion, but also by long-period Rayleigh waves. I observed a wave with a 3.08–3.10 h duration, which was close to that determined for the Rayleigh waves (3.08 h). The 3.08–3.10 h wave was caused by forced oscillation of Rayleigh waves characterised by a frequency close to the natural frequency and excited by the earthquake. Overall, the study findings suggested that water level fluctuations can be good indicators of high-magnitude earthquakes.

Using the field records from 1730, Forel (1895) showed that seiches could be induced by earthquakes. These earthquake-induced seiches became known as seismic seiches. McGarr and Vorhis (1968) reported seismic seiches generated by the March 1964 Alaskan earthquake. Berninghausen (1964; 1966; 1969) reviewed the relationship between tsunamis and seismic seiches and provided multiple examples, such as the eastern Atlantic south of the Bay of Biscay, Indian Ocean, and Southeast Asia. Using examples from Lake Tahoe, USA, Ichinose et al. (2000) illustrated how local earthquakes beneath a lake have the potential to cause a tsunami, thereby inducing seismic seiches within the lake. Barberopoulou et al. (2004) showed that both seismic waves and seiches occurred in response to the 2002 Alaskan earthquake. Barberopoulou (2008) also investigated large seismic wave motions and various scenarios of seiche generation during strong shaking events in Lake Union, USA. Utsu (2001) reported that under the influence of large earthquakes, an entire body of water within a lake or bay can be agitated by long-period surface waves, thereby leading to free vibrations within the water and resulting in a seiche. Following the 9.0 magnitude Lisbon earthquake of 1755, seismic seiches were observed in the lakes and bays of northern Europe up to 3,000 km away from the epicentre (Kvale 1955). In this case, water level fluctuations up to 1 m were recorded.

A notable marine example is associated with the undersea volcano Funga Tonga Funga Haapai, which erupted at around 1:00 p.m. Japan Time on 15 January 2022. Tidal levels increased and were observed to be over 80 cm near Nuku'alofa, the capital of Tonga, 70 km south of the eruption point, but were smaller at observation points along the 8,000 km to Japan. However, on the Japanese coast, a maximum tidal level increase of approximately 1 m was observed, causing damage to aquaculture facilities and capsizing about 30 ships (Japan Meteorological Agency 2022). The Japan Meteorological Agency (2022) suggested that even in the distant coastal areas of Japan, water levels increased and the Lamb waves damaged public properties before the tsunamis. Under normal circumstances, when the phase velocity of the excited ocean long wave coincides with the movement of the atmospheric disturbance, it resonates and increases in amplitude (Khono 2014). However, the report showed that this is not the only case, and that it is important to note that resonance can occur even when the velocities of the ocean gravity and pressure waves do not exactly match, and that if this condition persists for a long time, the tidal level change can also be significant (JMA 2022). Thus, even if the physical phenomenon occurs at a substantial distance, large earthquakes or volcanic explosions can cause various wave effects, and continuous recording of such oscillations in large

lakes (large waterbodies on land) would allow detection of these long-period waves; however, only a few examples of such phenomena have been recorded.

Earthquakes generate a progressive surface wave that propagates around the Earth; surface waves are characterised by higher amplitudes than those of body waves, with Rayleigh waves exhibiting exceedingly high amplitudes (Yoshizawa 2006, Miyazawa 2012). Obara (2012) showed the transient stress change caused by the passage of surface waves resulting from 2004 Sumatra-Andaman earthquake triggered seismic tremor in two regions in Hokkaido (northern Japan). One tremor coincided with active seismicity linked to previously known deep low frequency microearthquakes related to volcanic activity. In addition, the tremor was related to fluid pressure change, because the periodic enhancement of tremor amplitude was in phase with the largest compressional strain caused by surface waves.

Both minor and major arc rotations of Rayleigh waves can occur along the Earth's perimeter, and the first (minor arc rotation) and second (major arc rotation) Rayleigh waves measured at the observation point are denoted as R1 and R2, respectively. Yoshizawa (2006) reported that the 2004 Sumatra earthquake in Indonesia generated numerous surface wave trains that travelled around Earth several times. On 26 December 2004, a mega earthquake with a magnitude  $> 9.0$  occurred off the coast of Sumatra. Seismographs revealed that the surface waves from this earthquake made eight revolutions worldwide (Yoshizawa 2006). They extracted the long-period Airy phase of the fundamental-mode Rayleigh wave by applying a band-pass filter between 3 and 5 mHz. The long-period records displayed a clear series of multi-orbit Rayleigh waves that had circumnavigated Earth more than six times, and they revealed clear signals of phases up to points R13–R14. In the 2011 Tohoku earthquake, Yomogida et al. 2011 showed clear phase signals at least up to R4, including multi-orbit Rayleigh waves, with a band-pass filter from 3 to 10 mHz.

As progressive surface waves propagating around Earth, Rayleigh waves have dispersibility properties. Dispersibility is observed when the propagation speeds of waves vary in accordance with their wavelength components, during which the initial waveforms gradually change with time. Surface waves indicative of dispersibility typically exhibit phase speeds that increase monotonically with several extrema across wavelength. Waves that correspond to a boundary between normal and inverse dispersions (that is, the extrema of the group velocity called the Airy phases) can propagate with large amplitudes. Rayleigh waves include both longitudinal and transverse motions, for which the amplitude decreases exponentially as the surface distance increases. Oliver 1962 highlighted the dispersion relationships of Rayleigh and Love waves in continental and oceanic areas.

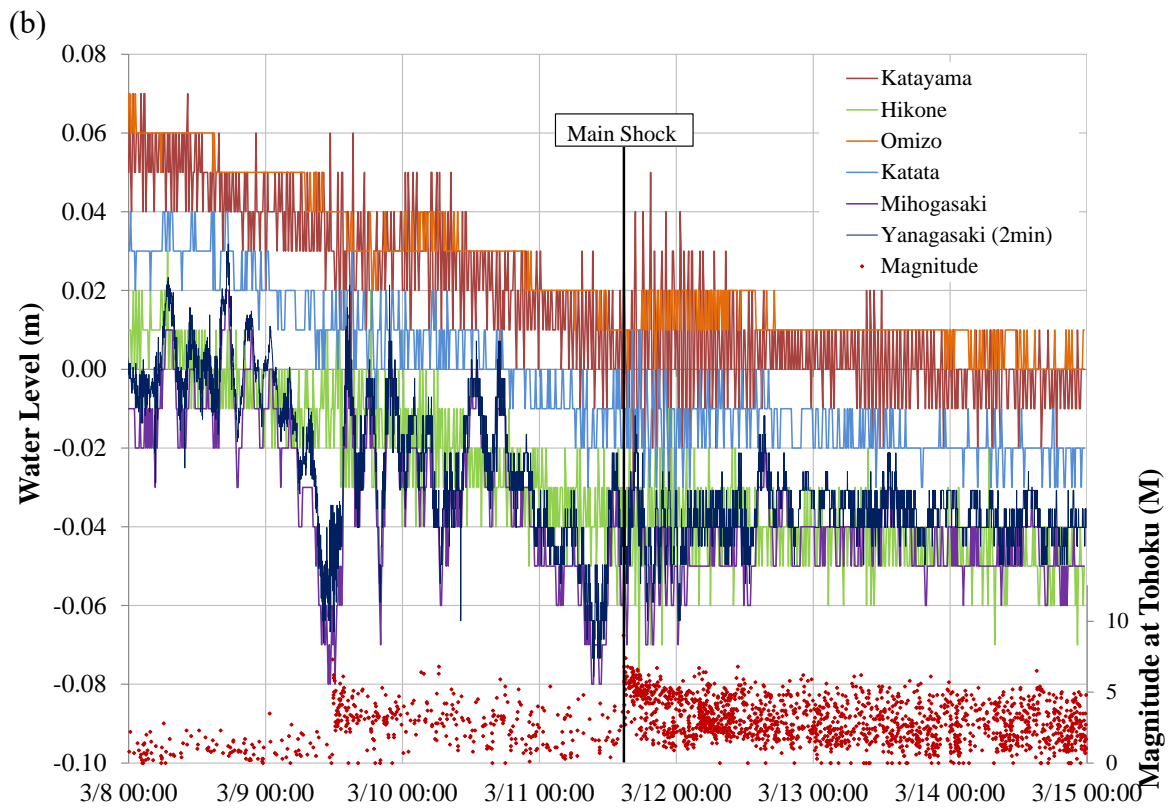
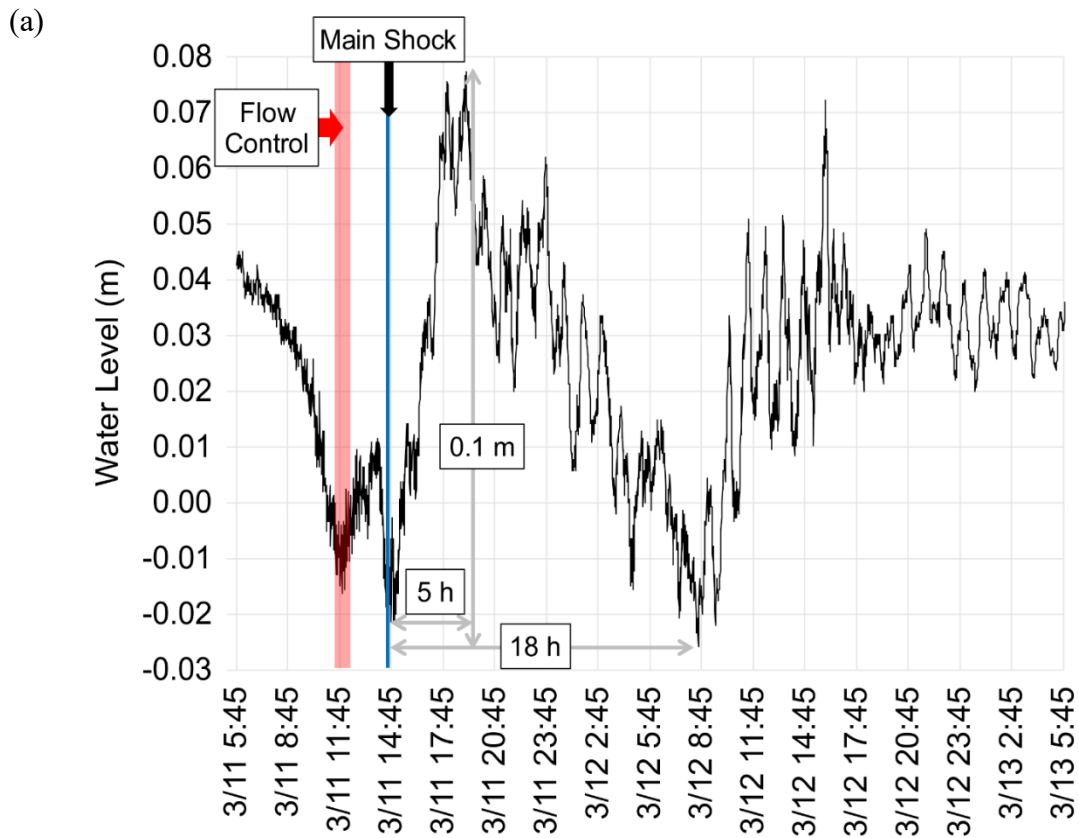
On 11 March 2011, an earthquake of magnitude 9.0 occurred off the Sanriku coast in the Tohoku area of Japan at 14:46 local time. The epicentre was located in the Tohoku region (70 km east of Sendai City) in the Pacific Ocean at  $38^{\circ}6'12''\text{N}$ ,  $142^{\circ}51'36''\text{E}$  (JMA). In the Lake Biwa region, approximately 850 km southwest of the epicentre (Figure. A1), the average land displacements following the earthquake were 6 cm downward and 16 cm horizontal in a southeast direction (Geospatial Information Authority of Japan 2011). As for the 2011TE, Miyazawa showed that seismic events were triggered by P-waves (Miyazawa 2012). Bondevik (2013) showed that S and Love waves were the main reason for a seiche in Norway; this indicates that seismic events can be induced by forced vibration (Bondevik 2013). Although numerous studies on seismic seiches have been

conducted since the 1800s, definitive research has not been performed on seismic seiche-related oscillations resulting from Rayleigh waves generated by large earthquakes. Understanding the effects of Rayleigh waves generated by large earthquakes will play a critical role in understanding the propagation of seismic waves. The objective of this study was to identify the effect of Rayleigh waves on water level fluctuations in Lake Biwa after the 2011TE.

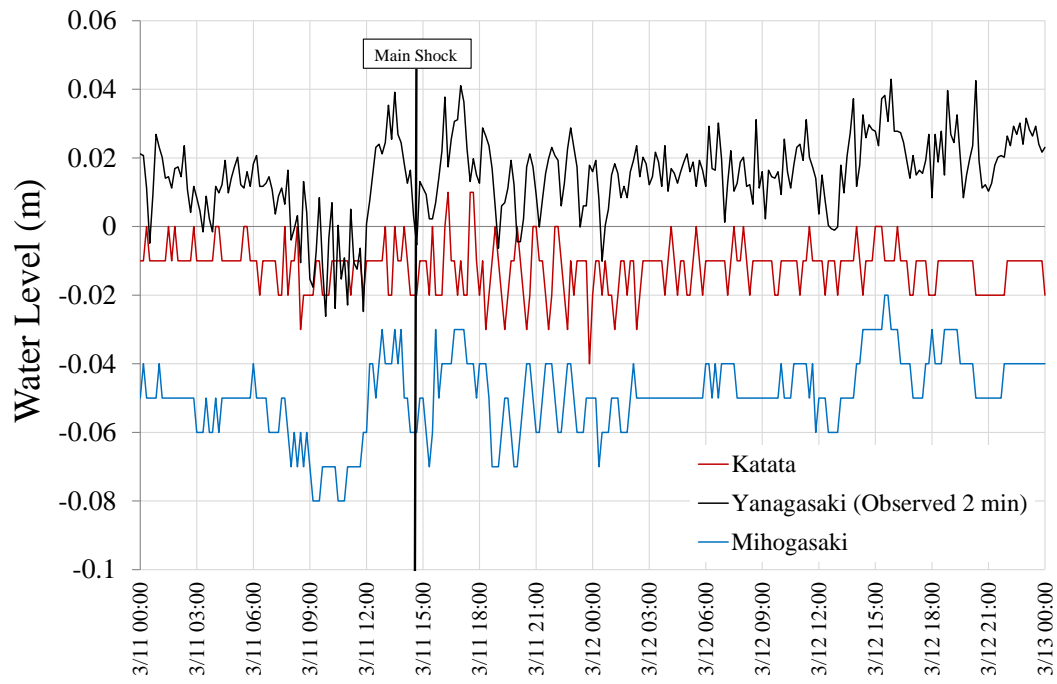
### 2–3. 3. 1 Time series of water levels of Lake Biwa after the Tohoku earthquake

The outflow at the Seta Araizeki weir, where nine floodgates are used to control the discharge, decreased from  $250 \text{ m}^3 \text{ s}^{-1}$  before the earthquake to  $120 \text{ m}^3 \text{ s}^{-1}$  after the earthquake. Approximately 3 h before the earthquake occurred, the water level started to decrease and dropped to 0.03 m (Figure. 2–5). When the earthquake occurred at 14:46 local time, the water level changed dramatically. After the earthquake, the water level increased by approximately 0.10 m (from -0.02 m to +0.08 m) within 5 h after the main shock. Following the peak at 22:00 on 11 March, the water returned to its original level in approximately 18 h (Figure. 2–5). Similar water level changes were recorded in the North Basin (Mihogasaki) monitoring location of the the lake (Figure. 3b). The changes that occurred were highly complex and differed substantially between the shallow southern and deep northern basins of Lake Biwa (Figures. 3b, c). Overall, significant variations in the water level were observed several times along with wavy motions until approximately 13:00 on 13 March.

Wind-caused seiches in Lake Biwa are typically generated by surface waters that are affected by strong winds at Hikone and Otsu (Figure. 2–3). However, a weak wind occurred before the morning of 11 March; therefore, there was little possibility of the occurrence of surface seiche-related oscillation. Conversely, after 13:00 on 11 March (at the approximate time of the earthquake), a strong and dominant southwest wind was present (Figure. A3). These conditions were ideal for the development of a seiche with a dominant first mode. Overall, the earthquake generated a highly complex superposition of waves (Figure. 2–5).



(c)



(d)

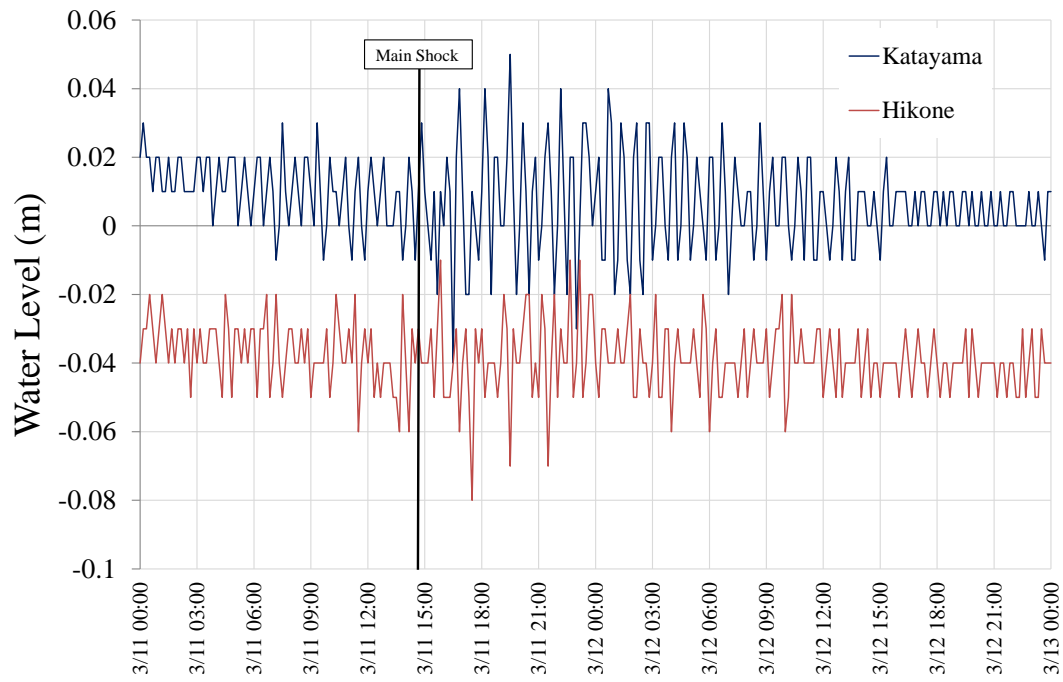


Figure 2–5. Water level changes associated with the Tohoku earthquake. (a) Time series of the water level measured at the Yanagasaki pier in the southern basin from 11 to 13 March 2011. Water discharge at the Araizeki weir was controlled from 11:40 to 12:40. The flow control time at the Seta Araizeki weir is indicated by the shaded bar. 2011TE occurred at 14:46 (main shock) on 11 March, causing the water level to increase for 5 h before returning to its original level 18 h later. (b) Time series of water level changes measured at an interval of 10 min at five stations and an interval of 2 min at the Yanagasaki pier (Figure. 1) in Lake Biwa from 8 to 15 March 2011. The magnitude and frequencies of earthquakes in the Tohoku district are indicated by dots. (c) Time series of water level changes at Yanagasaki (2 min intervals), and Katata and Mihogasaki (10 min intervals) in the southern basin from 11 to 13 March 2011. (d) Time series of water level changes at Katayama and Hikone (10 min intervals) in the North Basin.

### 2–3. 3. 2 Seismic seiche-related oscillations excited by Rayleigh waves

A surface seiche with a period of 3.08–3.10 h has never been observed in Lake Biwa (Table 1–1), and I deduced that this type of wave could have been generated by the 2011TE because no wave peaks with a period of 3.08–3.10 h appeared in the 1,800 monitoring data points prior to the earthquake (from 02:46 on 9 March to 14:44 on 11 March 2011) (Figure. 2–6).

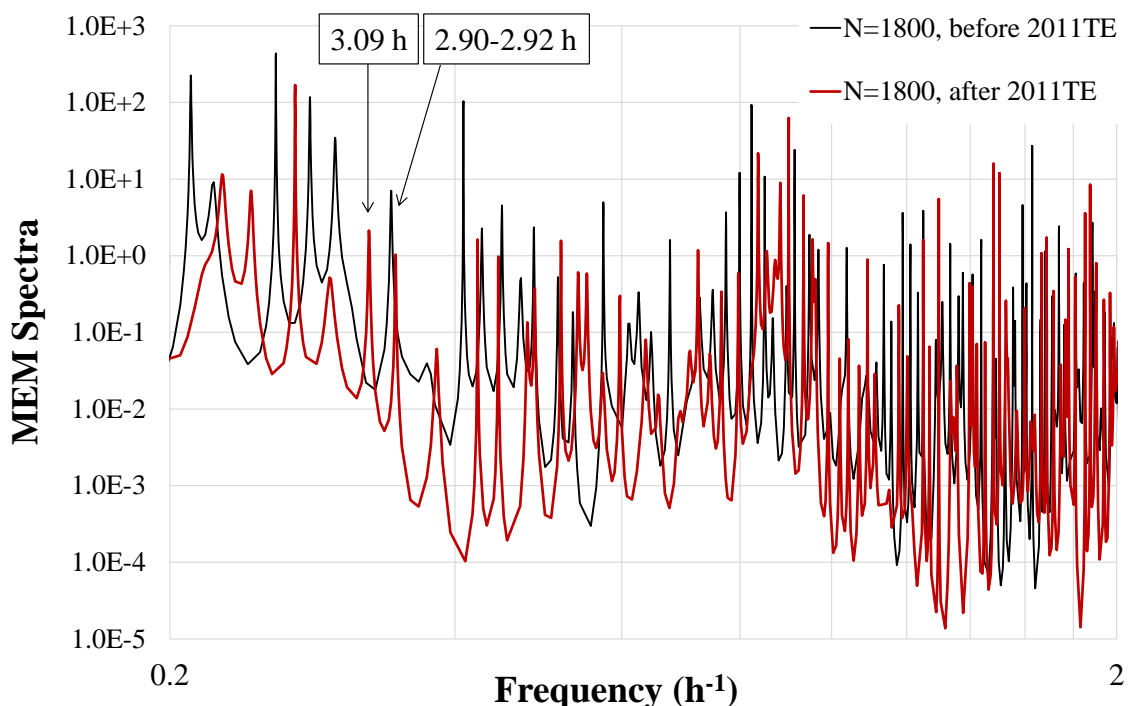


Figure 2–6. MEM spectra of water levels measured at the Yanagasaki pier in Lake Biwa before and after the 2011TE. N is the number of data points used for spectral analysis. The data before the 2011TE covers the period from 14:46 9 March to 14:44 11 March (N = 1,800), and the data after the 2011TE was obtained from 14:46 11 March to 02:44 14 March (N = 1,800).

After the 2011TE, scientists reported a global circulation of Rayleigh waves (Yomogida et al. 2011). When a large earthquake occurs, Love and Rayleigh waves are generated as surface waves that propagate along both the minor and major arcs from the epicentre of the earthquake around Earth (Figure. 2–7a). According to the observed Rayleigh wave dispersibility, the group velocity of the Rayleigh waves (approximately 3.60 km s<sup>-1</sup>) was likely the highest near wave packets with a period of 240 s (Figure. 2–7 b).

If the perimeter of Earth is between 40,009 km and 40,075 km, the period of the Rayleigh waves would range between 11,113 to 11,131 s (approximately 3.09 h). This duration is remarkably similar to the observed period of 3.08–3.10 h in Lake Biwa. Before the 2011TE, there were no waves with a 3.08–3.10 h period (Figure 2–6). Therefore, I concluded that the 3.08–3.10 h period of the waves in Lake Biwa was the result of a long-

period surface wave excited by the 2011TE, which was combined with the dispersion of the seismic Rayleigh waves. Under weak wind conditions, the water level of Lake Biwa oscillated for 3.08–3.10 h following the 2011TE from 12 to 14 March 2011. This oscillation was resonantly caused in Lake Biwa due to the 2011TE, as the oscillation period of 3.08–3.10 h differed significantly from the inherent oscillations in Lake Biwa.

As in this case, on 9 May 2010, a 7.3 magnitude earthquake occurred near Sumatra at 14:59 local time. The water levels in Lake Biwa, which is located approximately 5,000 km away from the epicentre of this earthquake, were measured at 60 s intervals using the same capacity-type water level gauge. The seismic seiche caused by Rayleigh waves was clearly observed in the time series data. Moreover, the water level changed significantly, exhibiting an amplitude of 15–30 mm after the main shock of the earthquake.

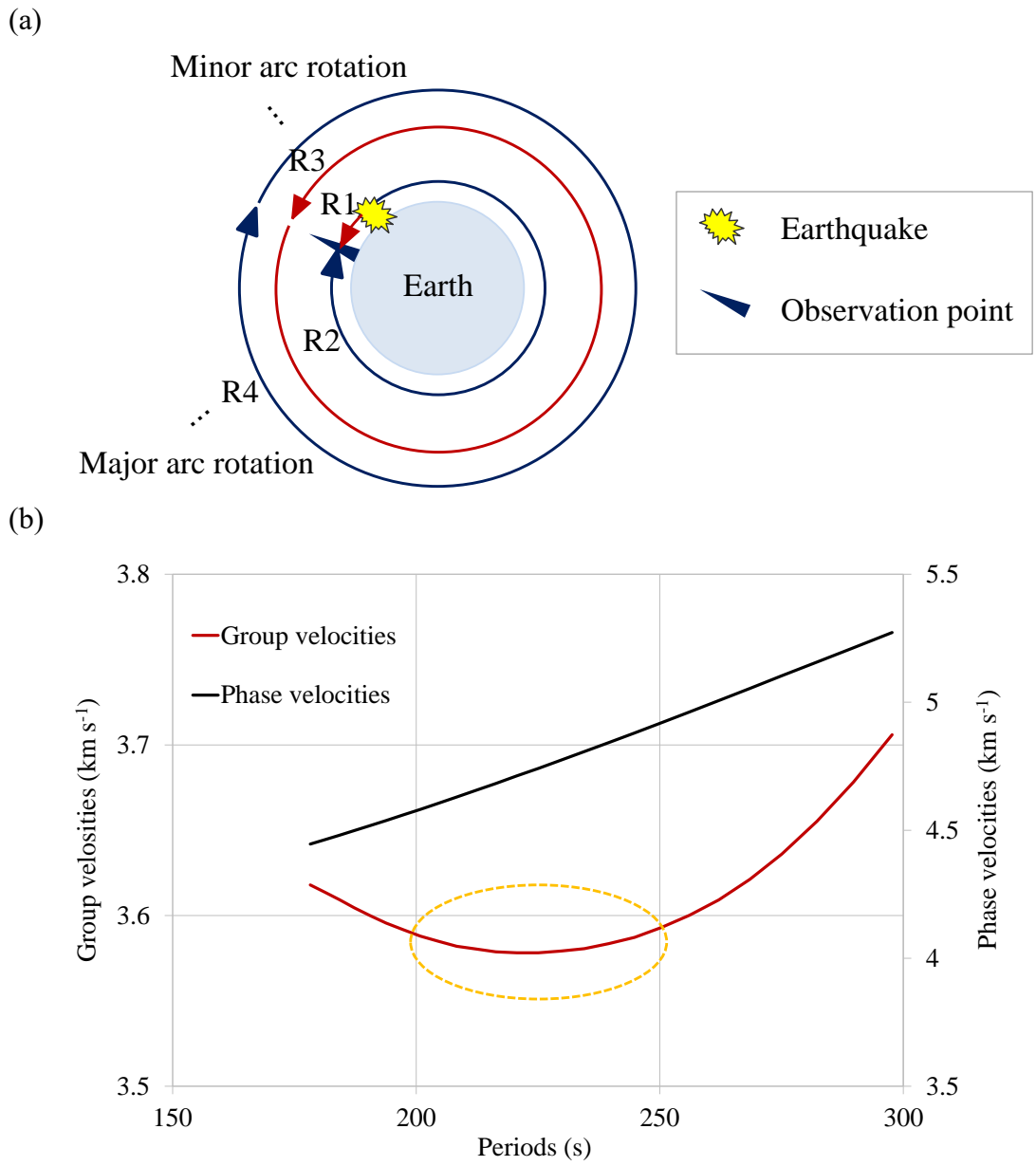


Figure 2–7. Illustration of Rayleigh waves and Rayleigh wave dispersion. (a) Illustration of the propagation of Rayleigh waves along the Earth’s surface. When an earthquake occurs, and Rayleigh waves are generated, the waves propagate along both the minor arc and major arc pathways around Earth. (b) Rayleigh wave dispersion modified from Oliver (1962), Kanamori (1970) and Dziewonski (1970). According to this model of dispersibility, the group velocity of a Rayleigh wave can be maximal near wave packets with a period of 240 s, which is approximately  $3.60 \text{ km s}^{-1}$  (Yoshizawa 2006).

## 2–4. Conclusions

This study analysed the complex water level changes in Lake Biwa created by the 2011TE earthquake using FFT and MEM spectral analyses. The results of both methods revealed previously unobserved waves with a duration of 3.08–3.10 h after the 2011TE; these waves were relatively weak under weak wind conditions. The duration of these waves satisfied the dispersion relationship of the Rayleigh waves with a 3.08–3.10 h period that were excited by the 2011TE. A subsequent MEM spectral analysis for 110 data segments showed no 3.08–3.10 h period peaks before the 2011TE and definite peaks after the 2011TE. Therefore, I deduced that the 3.08–3.10 h period waves were excited by the forced oscillation of Rayleigh waves characterised by a frequency similar to the natural frequency and a 3.08–3.10 h period after the 2011TE.

The amplitude of the seismic seiche-related oscillation excited by the forced oscillation from the Rayleigh waves was approximately 20 mm. This amplitude could have a significant impact on the ecosystem in the littoral region of the lake because the volume of water within the 20 mm thickness in Lake Biwa is more than  $1.3 \times 10^7 \text{ m}^3$ . Additionally, water level fluctuations in a lake can be amplified by forced oscillation from Rayleigh waves and are a good indicator of earthquakes with magnitude  $> 7.0$ , which may produce Rayleigh waves and an elevated tsunami.

## Appendix 2A

Table 2A. Calibration results of water level instrument used for water level measurement.

A water tank 1 m deep was filled with water and a volumetric water level instrument was fixed to the tank. Then, the voltage was recorded while adjusting the water level, and the regression equation between water level and voltage was obtained. The water level (calculated value) was calculated by the regression equation, and the error from the measured value was calculated. std indicates the standard deviation of the error. The calibration was conducted once a year in April 2010, October 2011, and May 2012.

2010/4/23			
Water Level (cm)	Volt (V)	Water Level (Calculated) (cm)	Error (cm)
-80.5	0.0559	-80.9	0.4
-76.0	0.1109	-75.7	-0.3
-68.7	0.1899	-68.2	-0.5
-58.6	0.2950	-58.2	-0.4
-48.0	0.4047	-47.8	-0.2
-39.7	0.4940	-39.4	-0.3
-30.9	0.5864	-30.6	-0.3
-21.6	0.6823	-21.5	-0.1
-12.7	0.7710	-13.1	0.4
-11.0	0.7902	-11.3	0.3
		std	0.35
2011/10/12			
Water Level (cm)	Volt (V)	Water Level (Calculated) (cm)	Error (cm)
-30.0	1.2240	-30.2	0.2
-20.0	1.3860	-19.9	-0.1
-10.0	1.5400	-10.2	0.2
0.0	1.7080	0.5	-0.5
10.0	1.8630	10.3	-0.3
20.0	2.0100	19.7	0.3
30.0	2.1710	29.9	0.1
		std	0.31
2012/5/31			
Water Level (cm)	Volt (V)	Water Level (Calculated) (cm)	Error (cm)
1.5	0.056	1.0	0.5
6.0	0.112	6.3	-0.3
13.5	0.192	13.9	-0.4
23.5	0.286	22.8	0.7
34.0	0.404	34.0	0.0
42.3	0.494	42.6	-0.3
51.0	0.586	51.3	-0.3
60.5	0.686	60.8	-0.3
69.5	0.772	69.0	0.5
71.0	0.792	70.9	0.1
		std	0.42



# Chapter 3 Estimation of the average precipitation retention time in the watershed for the surface inflows to Lake Biwa

## 3 – 1. Introduction

The knowledge of how long after a precipitation event the water level of Lake Biwa increases is important for flood forecasting and disaster prevention strategies. It is also important for forest resource management to know the delay time after precipitation until it contributes to water level increase, because it allows estimation of how long precipitation remains in the surface layer of the catchment.

In addition, because endemic fish species are affected by seasonal changes in lake water levels, changes in water levels during spawning season affect coastal ecosystems (Mizuno et al. 2010, Sato & Nishino 2010). Thus, it is important to understand the impact of lake level fluctuations on ecosystems (Yang et al. 2016). Therefore, clarifying the response of precipitation and lake levels can be useful for ecosystem conservation as well as for disaster prevention, such as flood forecasting, and for use in forest resource management.

Lake Biwa, the target of the study, is a large, deep, humid temperate lake located in the central part of Japan. With a surface area of 670.25 km<sup>2</sup>, it is the largest lake in Japan, and its maximum depth is 104.1 m (Kumagai et al. 2006). More than 450 rivers and streams flow directly into Lake Biwa, but there is only one natural outlet, the Seta River. Artificial outlets include two Lake Biwa canals and the Uji River hydroelectric power station. The outflow of the Seta River is controlled by opening and closing 10 weirs according to operational rules, which prevent flooding while maintaining a certain water level baseline suitable for fish reproduction.

The water level fluctuations in Lake Biwa are complex due to its large surface area, lake basin shape and catchment characteristics. It is difficult to identify all the factors that influence water level changes include wind waves, surface seiches, precipitation, river flow (inflow and outflow), evaporation, groundwater, others include several factors, such as direct precipitation on the lake surface, each with its own specific temporal and spatial scale. Therefore, frequency analysis over several timescales is considered to be an appropriate method for understanding the lake water level response to precipitation.

Up to the present, the calculation of delay times using impulse response functions for precipitation has been used in river and groundwater hydrology (Markus et al. 2003, Hantush 2005, Farahmand et al. 2007, Yokoki et al. 2008), however, there is no previous work on estimating precipitation retention times in lakes using impulse response functions based on the relationship between precipitation and the water level. By determining this response function, it is possible to understand how the lake level responds to phenomena such as direct precipitation and river runoff, which are considered to have relatively rapid responses.

Therefore, in this chapter, the delay time for Lake Biwa was calculated using a response function with precipitation as the input and lake water level as the output parameter, and the delay time due to direct precipitation, surface static vibration, river runoff, and return flow (fast and slow) was then used to estimate the average retention time of precipitation based on the relationship between precipitation and lake water level. The development of

this method could also lead to improved predictions of the effects of climate change in lake systems using wavelet transforms by investigating changes in delay times over long timescales (Carey et al. 2016, Woolway et al. 2020).

## 3 – 2. Method

### 3 – 2. 1. Impulse response function

Since the shape of the response function reflects the lake system itself, understanding its shape provides a better understanding of the system and processes within the lake-catchment area. Thus, information on the shape of the response function is useful to lake management. Therefore, in order to identify and separate each of the various factors that are complexly related to the effects of precipitation on the lake system, an impulse response function using the Fourier transform was used to calculate delay time for each factor. The calculation of delay time using the response function was determined by solving the integral equation in Eq. (1), as shown in (Figure 1 – 1, Iwaki et al. 2014; 2020a; 2021; 2022):

$$y(t) = \int_0^{+\infty} x(t - \tau)h(\tau)d\tau, \quad (1)$$

where  $\tau$  is the lag time (time lag).  $h(\tau)$  defines the relationship between  $x(t)$  and  $y(t)$ , so it is a response function that reflects the process of how the water level of the lake is effected by precipitation (Hidaka 1943).

More specifically, in determining the response of the lake level to precipitation, the calculation of delay time by the response function was calculated as shown in the flowchart in Figure 3 – 1.

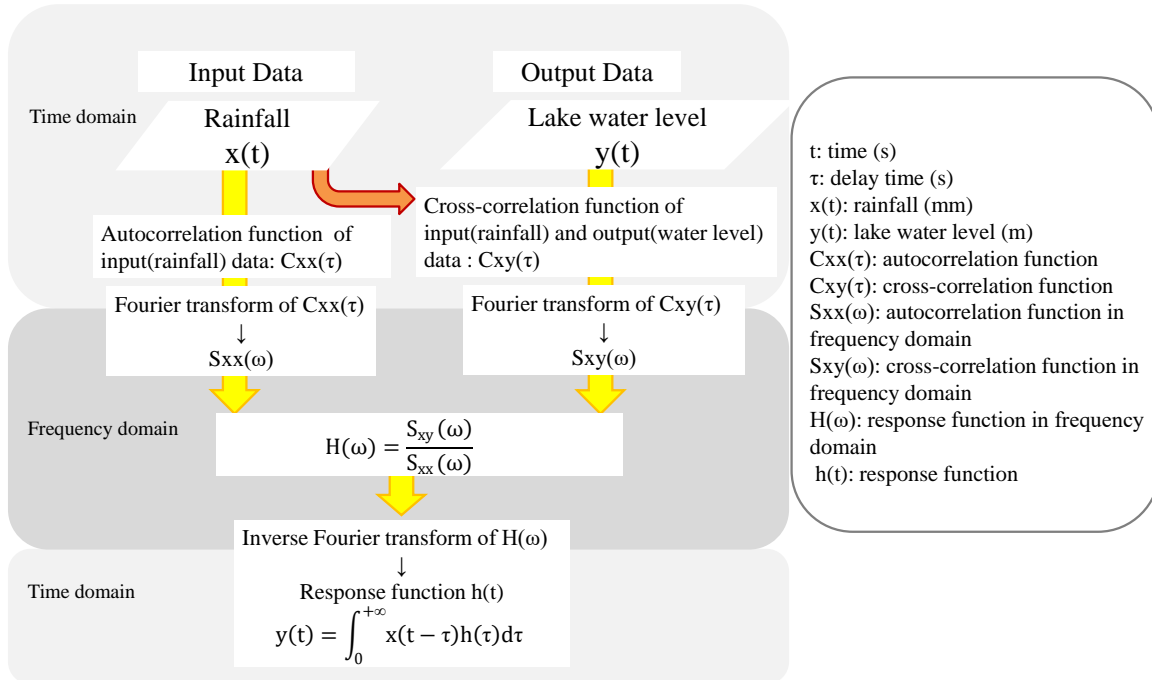


Figure 3 – 1. Flowchart of delay time calculation by response function.

$x(t)$  is the precipitation at a point representative of the lake catchment and  $y(t)$  is the lake level, both  $x(t)$  and  $y(t)$  are functions of time. Where it is assumed that  $y(t)$  can be written as a function of the integral of  $x(t)$  ( $t \geq 0$ ). In particular,  $y(t)$  is the sum of

the integral of the past precipitation  $x(t - \tau)$  multiplied by the impulse response function  $h(\tau)$  (Hidaka 1943, Hino 1977). Since  $y(t)$  and  $x(t)$  are observed values,  $h(\tau)$  can be obtained by solving the integral equation in equation (1).

The impulse response function can also be described as the response to a unit impulse. Thus, if  $x(t) = \delta(t)$  in equation (1), then  $y(t)$  equals  $y(t)$ . where  $\delta(t)$  is the delta function. The exact definition of the delta function is rather complicated, but it can be approximated as follows:

$$\delta(t) \begin{cases} = 0 & (t \neq 0) \\ = \infty & (t = 0) \end{cases} \quad \text{and} \quad \int_{-\infty}^{\infty} \delta(t) dt = 1.$$

The response function  $h(\tau)$  can then be estimated by the cross-correlation:

$$\begin{aligned} C_{xy}(\tau) &= \overline{x(t)y(t+\tau)} \\ &= \int_{-\infty}^{+\infty} h(\eta) \overline{x(t)x(t+\tau-\eta)} d\eta, \end{aligned} \quad (2)$$

where the upper bar represents the ensemble mean. Note that the autocorrelation function is defined as follows.

$$C_{xx}(\tau) = \overline{x(t)x(t+\tau)}. \quad (3)$$

The cross-correlation function is obtained by (2) and (3) as follows.

$$C_{xy}(\tau) = \int_{-\infty}^{+\infty} h(\eta) C_{xx}(\tau - \eta) d\eta. \quad (4)$$

The complex Fourier transform of the cross-correlation function  $C_{xy}(\tau)$  is a cross spectrum,

$$S_{xy}(\omega) = \frac{1}{2\pi} \int_{-\infty}^{+\infty} C_{xy}(\tau) e^{-i\omega\tau} d\tau, \quad (5)$$

and the complex Fourier transform of the autocorrelation function  $C_{xx}(\tau)$  is the power spectrum  $S_{xx}(\omega)$ .

$$S_{xx}(\omega) = \frac{1}{2\pi} \int_{-\infty}^{+\infty} C_{xx}(\tau) e^{-i\omega\tau} d\tau. \quad (6)$$

The cross spectrum  $S_{xy}(\omega)$  can be rewritten as,

$$\begin{aligned}
S_{xy}(\omega) &= \frac{1}{2\pi} \int_{-\infty}^{+\infty} C_{xy}(\tau) e^{-i\omega\tau} d\tau = \frac{1}{2\pi} \int_{-\infty}^{+\infty} \int_{-\infty}^{+\infty} h(\eta) C_{xx}(\tau - \eta) e^{-i\omega\tau} d\eta d\tau \\
&= \frac{1}{2\pi} \int_{-\infty}^{+\infty} \int_{-\infty}^{+\infty} h(\eta) e^{-i\omega\eta} C_{xx}(\sigma) e^{-i\omega\sigma} d\eta d\sigma \\
&= \frac{1}{2\pi} \int_{-\infty}^{+\infty} h(\eta) e^{-i\omega\eta} d\eta \cdot \frac{1}{2\pi} \int_{-\infty}^{+\infty} C_{xx}(\sigma) e^{-i\omega\sigma} d\sigma \\
&= H(\omega) \cdot S_{xx}(\omega),
\end{aligned} \tag{7}$$

where  $\sigma = \tau - \eta$  and  $H(\omega)$  is the system function (Fourier transform of  $h(\tau)$ ).

$$H(\omega) = \frac{1}{2\pi} \int_{-\infty}^{+\infty} h(\eta) e^{-i\omega\eta} d\eta, \tag{8}$$

Equation (7) can be replaced as follows:

$$H(\omega) = \frac{S_{xy}(\omega)}{S_{xx}(\omega)}. \tag{9}$$

The inverse Fourier transform of (9) can be used to calculate the response function  $h(\tau)$ .

By transforming  $C_{xy}(\tau)$  and  $C_{xx}(\tau)$  into  $S_{xy}(\omega)$  and  $S_{xx}(\omega)$  using the FFT of  $H(\omega)$ , and then by inverse Fourier transforming  $H(\omega)$  into  $h(\tau)$ , the response function  $h(\tau)$  was obtained (Hino 1977).

The key information needed to calculate delay time in the impulse response function is the timing and shape (response) of precipitation events (impulses) and water level changes. If the value of the response function is positive, the output value responds positively (positive value) to the impulse. This means that there is a positive correlation (a positive and large value of the delay time implies a strong response). To calculate the response function, the input precipitation  $x(t)$  and the output water level  $y(t)$  are standardized. Since the response function was calculated to examine the response to past events, a positive value for the delay time  $\tau$  ( $\tau > 0$ ) was used.

### 3-2. 2. Observation of water level

The water level of Lake Biwa is based on the Biwako Surface Line BSL; +84.371 m a.s.l.; Lake Biwa Handbook 2010). The observation point in Lake Biwa is Yanagasaki, which is located in the southern part of the lake (the observation site and data used in Chapter 3 are shown in the yellow-colored area in Figure 3-2).

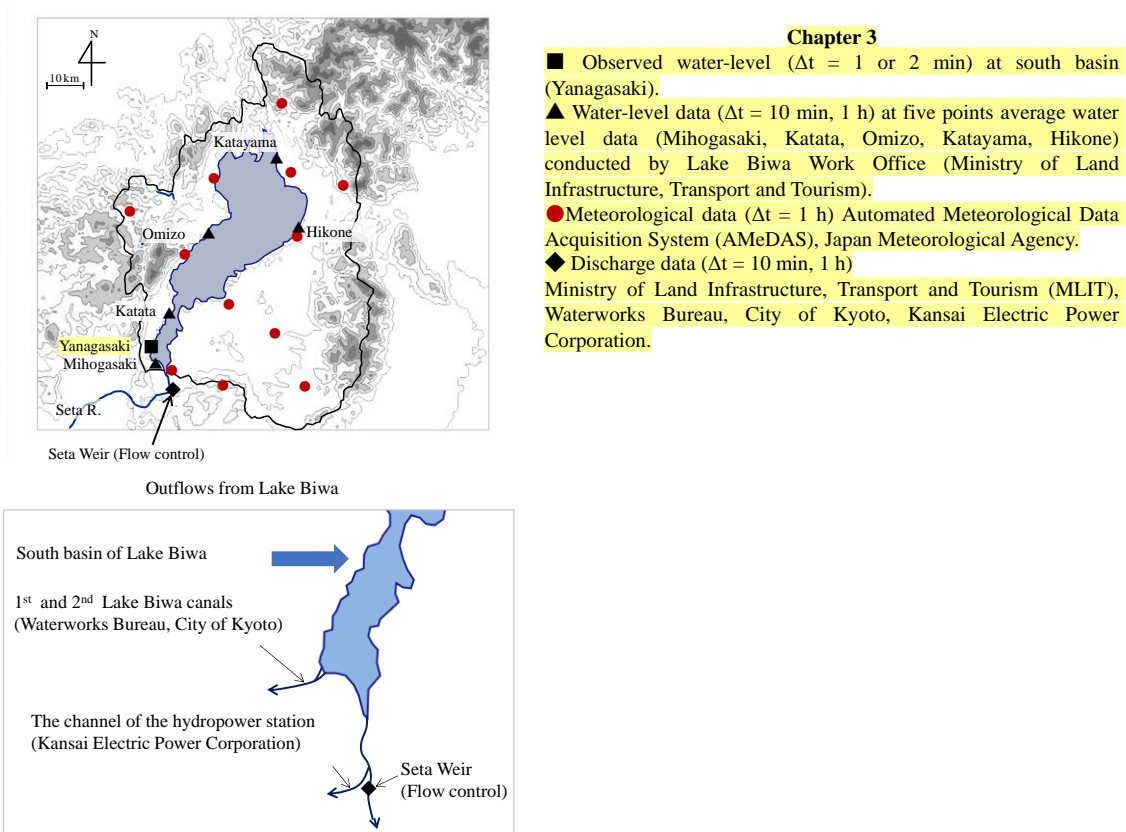


Figure 3 – 2. Observation sites and data used in Chapter 3 (sites and data related to Chapter 3 are colored yellow).

To determine water level fluctuations in Lake Biwa, I deployed a capacity-type water level gauge at the end of the Yanagasaki pier (Figure 2 – 2, Figure 3 – 3). This instrument measured water level changes using a linear relationship between the water level and a resistance–capacitance oscillator, which was developed by connecting two wires (Teflon and stainless-steel wires) in parallel. The resolution of the water level gauge was 1 mm, and the accuracy was  $\pm 3$  mm (Iwaki et al. 2014). A HIOKI data logger was used to record water level fluctuations with sampling intervals of 1 min (from 22 April to 20 May 2010 and from 1 November 2011 to 31 March 2012) and 2 min (from 21 May 2010 to 31 October 2011).



Figure 3 – 3. Capacitance type water level instrument.

### 3 – 2. 3. Other data acquisition

Precipitation, lake level, river level and discharge data

As an input data, precipitation data within the catchment area was obtained from AMeDAS of the JMA (JMA 2022). Lake level data were obtained from five stations (Katayama, Omizo, Hikone, Katada and Mihogasaki, Figure 3 – 2) provided by the MLIT to checked the input data which observed data. In addition, hourly observations of the Yasu River water level and flow rate (observation point: Hattori [downstream]) and flow rate (observation point: Yasu [near Hattori]) taken by the MLIT from June 20 to August 31, 2010, were used. These observation points and the contents of the data used are shown in Figure 3-5, as well as the major rivers flow into Lake Biwa.

All discharge data (at 10-minute intervals) for the Seta River were provided by MLIT (MLIT 2022). Outflow data from the two Biwako Sosui canals and the Uji River hydropower plant were obtained from the Kyoto City Waterworks Bureau and Kansai Electric Power Company, respectively. The outflow from the Seta River is controlled by the opening and closing of 10 weirs.

The total outflow from Lake Biwa is controlled by an operational rule so that the lake level is kept between the full water level and the lower water level shown below and is kept constant for a certain period of time, so the delay time of the lake level can be estimated using a response function. The water level of Lake Biwa is BSL+0.3 m when the lake is always full, but it can be higher during the flood season (June 15 to October 15, etc.), and the lower water level limit is set to - BSL 0.2 m from June 16 to August 31 and BSL -0.3 m from September 1 to October 15 every year (Lake Biwa Handbook Editorial Committee 2010). MLIT regulates the discharge to support the spawning and

incubation period of spring-breeding fish, and from June to September, to provide a stable supply of water for agricultural use. In addition, from September to December, the water level is adjusted only minimally because this is the fish spawning season. The effect of precipitation on the water level of Lake Biwa is mitigated by increasing the outflow through the opening and closing of weirs. The change in outflow through the operation of opening and closing weirs takes place over several hours to avoid abrupt changes, and the flow rate ranges from  $20 - 700 \text{ m}^3 \text{ s}^{-1}$ .

### 3 – 2. 4. The calculation method for delay time using response function

Using the impulse response function, the delay time for the lake level to respond to precipitation in the catchment area was calculated as  $\tau_L$ . Note that in this chapter (Chapter 3), the delay time  $\tau_R$  was used with the time series in the river, as described later, so to avoid confusion, the delay time of the lake level, calculated using the response function, was represented as  $\tau_R$  only in Chapter 3 (however, the delay time of the lake level was represented as  $\tau$  in Chapter 4). A flowchart for calculating the delay time  $\tau_L$  using the response function is shown in Figure 3-4 (delay time is represented as  $\tau_L$ ).

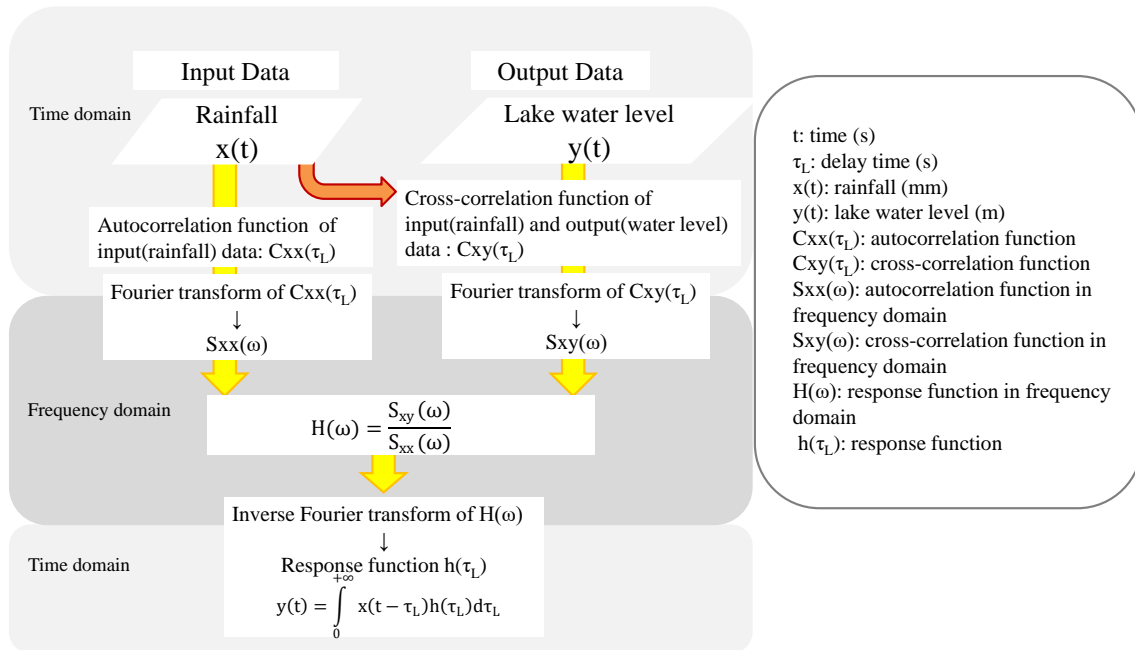


Figure 3 – 4. Flowchart for calculating delay time  $\tau_L$  using response function.

$x(t)$  is the hourly rainfall (mm) representative of the catchment (including the lake) at time  $t$ , and  $y(t)$  is the water level (m) of the lake at time  $t$ . Equation (1) applies to:

$$y(t) = \int_0^{+\infty} x(t - \tau_L)h(\tau_L)d\tau_L \quad (10)$$

where  $\tau_L$  is the delay time between the onset of precipitation and the beginning of the increase in the water level of the lake. In order to reflect how the lake level changes with

precipitation,  $h(\tau_L)$  was determined based on the flow chart (Figure 3–4) from the integral equation using Equation (10). The important information needed for the response function is the timing of precipitation onset (impulse) and the amplitude and timing of water level change (response).

Next, the delay time ( $\tau_L$ ) of the lake level calculated by the impulse response function was compared with the delay time ( $\tau_R$ ) estimated from the time series of the river level of the Yasu River. Because the Yasu River has the longest river length and the largest catchment area, it is assumed to have the largest impact on the water level of Lake Biwa and the largest delay time of all the rivers that flow into Lake Biwa. Then, the delay time  $\tau_L$  due to the river inflow of the Yasu River was identified in the calculated delay time ( $\tau_L$ ) of the lake level.

The delay time  $\tau_R$  was estimated using time-series data, which includes river level and river discharge data ( $\Delta t=1$  h, where  $\Delta t$  is the increment of time) for the Yasu River observed by MLIT (observation point, Hattori: water level, Yasu: river discharge) and precipitation data ( $\Delta t=1$  h) by JMA.

Determine the delay time to the peak,  $\tau_{R\_peak}$ , as follows. When there are multiple peaks then,

$$\tau_{R\_peak} = T_{peak} - T_0 \quad (11)$$

On the other hand, the delay time  $\tau_{R\_end}$  to return to the same water level is calculated by the following equation.

$$\tau_{R\_end} = T_{end} - T_0 \quad (12)$$

where  $T_0$  is the time just before the river level increases,  $T_{peak}$  is the peak river level during precipitation, and  $T_{end}$  is the end time when the river level returns to its previous level.

The delay time  $\tau_R$  calculated from the time series of hourly observations of the Yasu River water level at the estuary of Lake Biwa was then compared with the delay time  $\tau_L$  calculated using the response function. Since the time scale of river inflow was unknown at this stage, the water level change in Lake Biwa was divided into two time scales: (1) fast response ( $0 < \tau_L \leq 32$  h) and (2) slow response ( $32 \text{ h} < \tau_L \leq 40$  d), and each result was examined.

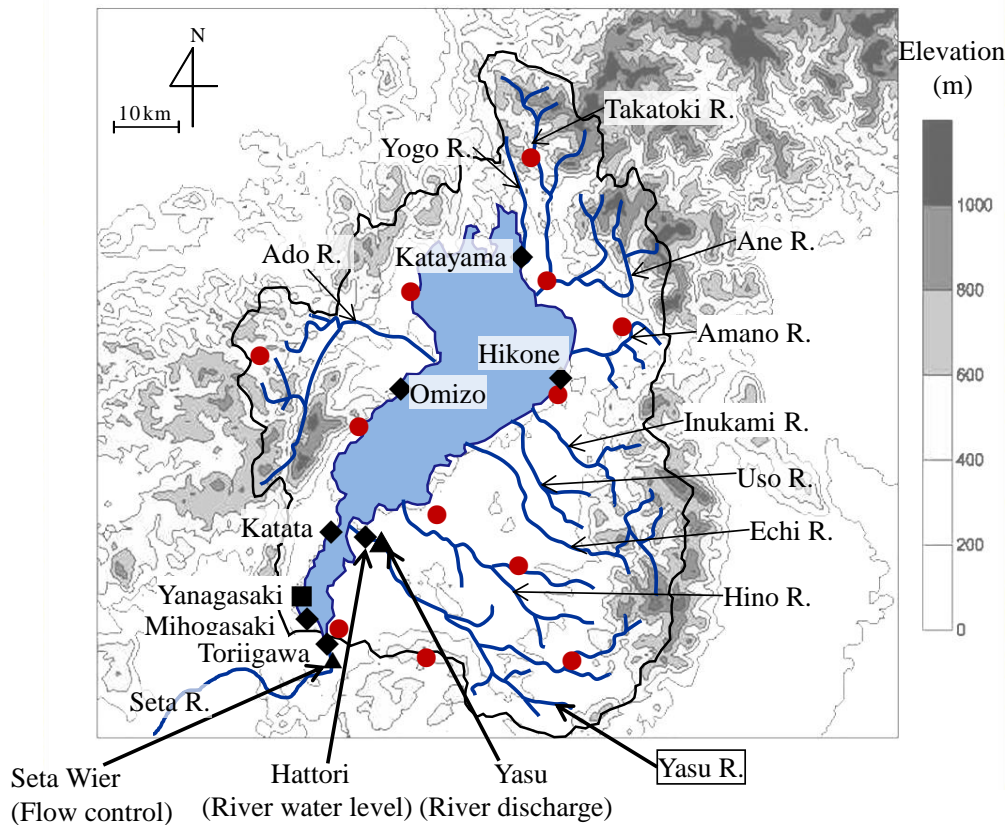


Figure 3 – 5. Major rivers flowing into Lake Biwa and points used for time series data for the Yasu River. ◆ Hattori is the river water level, ▲ Yasu is the river discharge.

The other locations shown in Figure 3 – 2 are the same as those in Figure 3 – 2 (◆ indicates the water level, ● indicates AMeDAS observation location, and ■ indicates observation points of the water level of the lake).

### 3 – 3. Results

#### 3 – 3. 1. Delay times $\tau_L$ calculated using response function

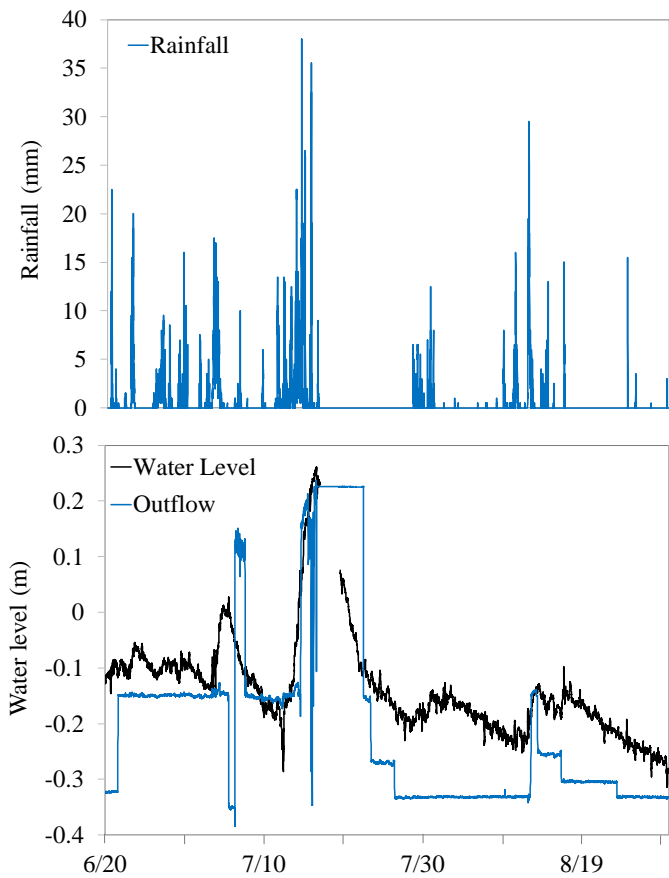
The time series of precipitation (input), water level (output), and total discharge (sum of the four discharges) into the catchment area from June to August 2010 (hereinafter referred to as "summer") and from February to May 2011 (hereinafter referred to as "winter") are shown in Figure 3 – 6a (summer) and Figure 3 – 6b (winter). Next, the delay times calculated by the response function using these data are shown in Figure 3 – 7 for delay times within 32 h ( $0 \leq \tau_L < 32$  h) and in Figure 3 – 8 for delay times within 40 days ( $0 \leq \tau_L < 40$  d).

The response function was positive in the 0.16-0.33 h interval for small values of delay time, but as the delay time became larger, the response function became negative in summer and remained positive in winter (Figures 3 – 7 and 3 – 8). In summer, peaks

existed at 0.16, 0.33, 0.8, 1.7, 2.2, 4.0-4.9, 4.6, 6.8, 8.3, 9.3, 11-12, 16-17, and 22.6 h, and the clearest peaks were at 4.6, 6.8, 8.3, 9.3, 12.6, 16, 17, 19, and 22.6 h (Figure 3 – 7, Appendix 3A). In winter, peaks were seen at 0.16, 0.33, 0.5, 2, 4.5-4.83, 10, 17, 20.5, 25, and 30 hours, but their amplitudes were smaller than those of the summer peaks (Figure 3 – 7). To identify the peaks, a two-tailed t-test was performed corresponding to the peaks of the summer response function (Appendix 3A), and each peak was treated as independent.

Next, for the case of longer delay time ( $0 \leq \tau_L < 40$  d), the calculated water level response function to average rainfall showed responses for summer on 2.0, 2.5, 3.7, 5.4, 8.3, 11.8, 16.1, 19.9, 24.5, 28.1, 31.5, and 37.8 days (Figure 3 – 8). In winter, response peaks were detected at 1-2, 9-11, 14-16, and 40-45 days (Figure 3 – 8). However, in winter, snow accumulates after snowfall in the northern part of the Lake Biwa catchment area, which is very complicated due to the warm snow accumulation area (snow melting proceeds from the lower layer even in accumulated snow conditions), and especially in winter, the northern catchment area has a heavy snow accumulation; thus, in this chapter, only summer data are discussed hereafter.

(a) Summer 2010



(b) Winter 2011

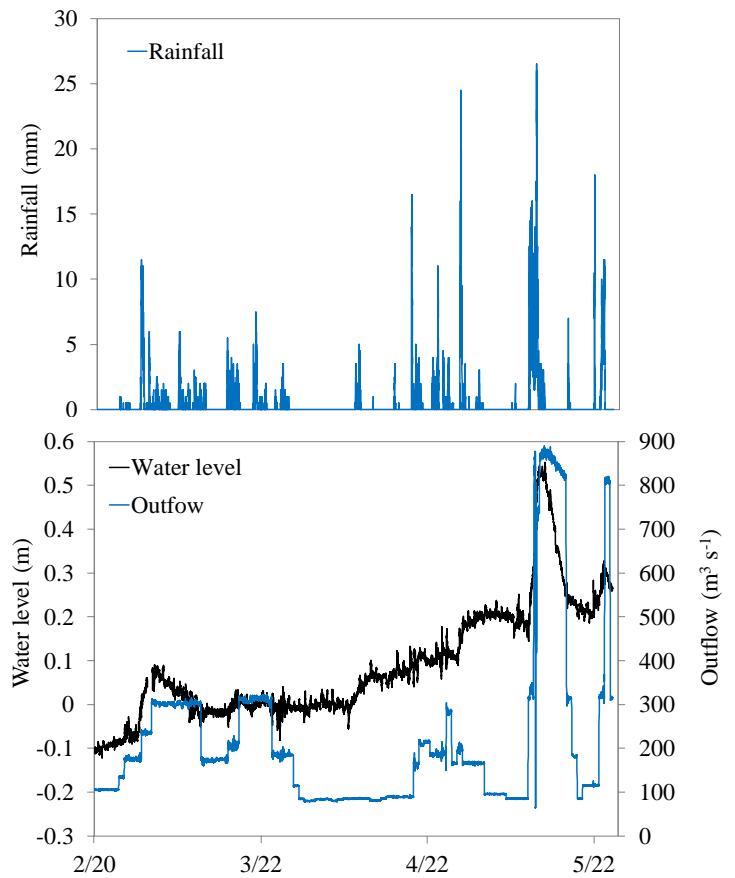


Figure 3–6. Time series of precipitation data. (a) Average precipitation from June 20, 2010, to August 31, 2010. (b) Average precipitation from February 1, 2011 to May 31, 2011 (input), water level of Lake Biwa (2-minute values are used as 10-minute average), and total discharge of Seta River (10-minute intervals). The water level of Lake Biwa is the value observed at Yanagigasaki, and the total precipitation is the AMeDAS value observed in the catchment area.

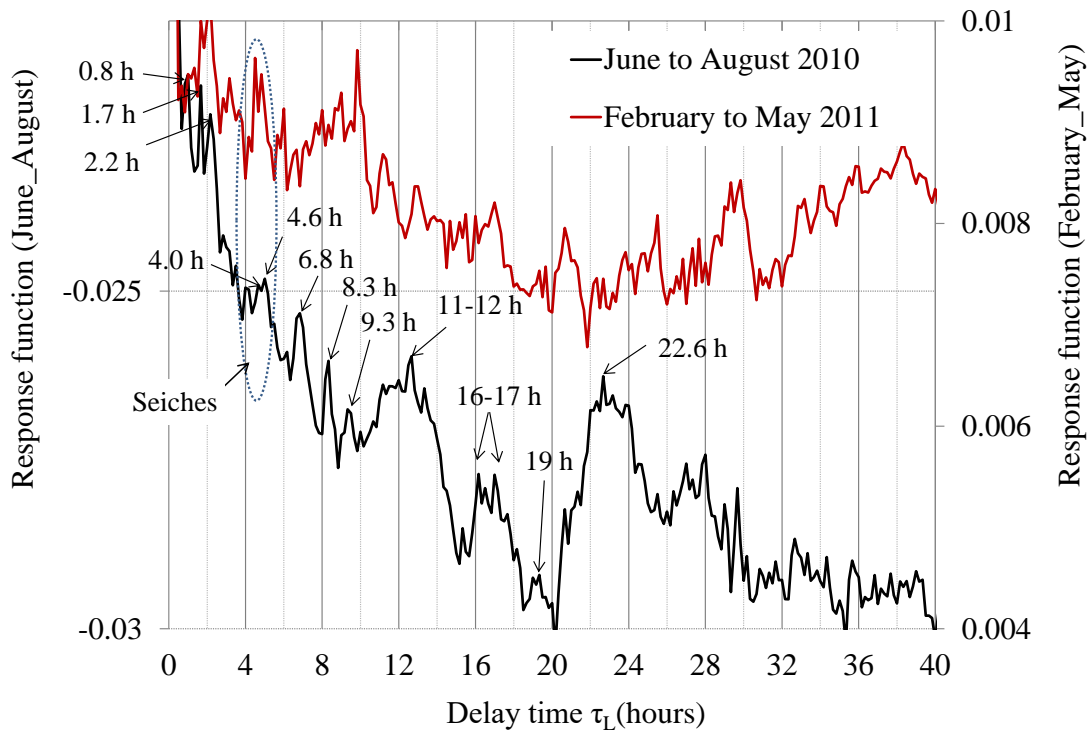


Figure 3–7. Calculated response functions of lake level ( $0 \leq \tau_L < 32$  h) to catchment average precipitation from June 20, 2010, to August 31, 2010 and from February 1, 2011 to May 31, 2011.

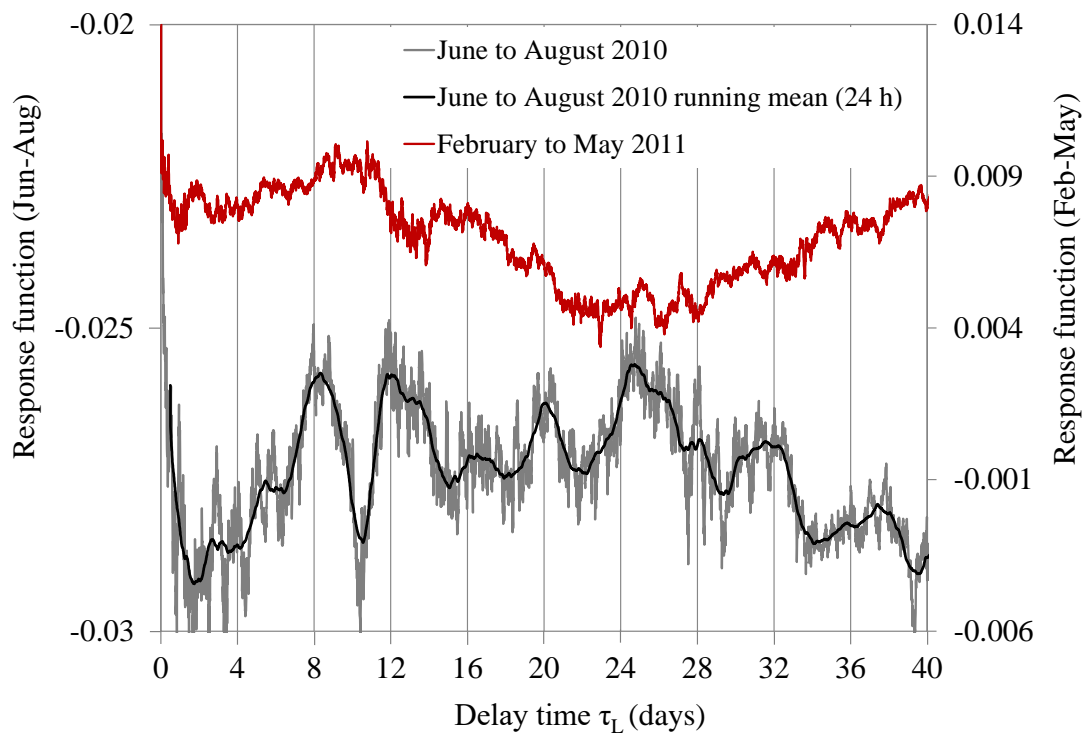


Figure 3–8. Calculated response functions of lake level ( $0 \leq \tau_L < 40$  d) to catchment average precipitation from June 20, 2010, to August 31, 2010 and from February 1, 2011 to May 31, 2011.

### 3–3. 2. Delay times $\tau_R$ estimated using time series of the incremental water level of the Yasu River

The Yasu River has the largest length and catchment area in the Lake Biwa catchment area. Therefore, the delay time due to the Yasu River is assumed to be the longest delay time in the Lake Biwa catchment area, and the delay time estimated from the time series data of river level and flow rate of the Yasu River is estimated as  $\tau_R$ . Then, the delay time  $\tau_L$  calculated from the response function was compared with  $\tau_R$  estimated from the water level change of the Yasu River, and the delay time  $\tau_L$  of the Yasu River was assumed.

The time series of water level changes in the Yasu River (65.3 km) located in the southern part of the Lake Biwa catchment area for precipitation events from June 20 to August 31, 2010 is shown in Figure 3–9a. Daily precipitation at AMeDAS stations near the Yasu River catchment area (Otsu, Tsuchiyama, and Shigaraki) are also shown in Figure 3–9b. Note that strictly speaking, the observation site Shigaraki is not included in the catchment area of the Yasu River, but is shown for reference. The daily precipitation at these three points is shown in Appendix 3B. Since it is difficult to strictly determine the correspondence between these precipitation totals and the water level, in this method, the delay time is estimated by the response function. The river level and discharge stations used (Hattori and Yasu) are located near the estuary of the Yasu River.

During this period, 14 precipitation events the delay times  $\tau_R$  estimated from 14 precipitation events are shown in Table 3–2.

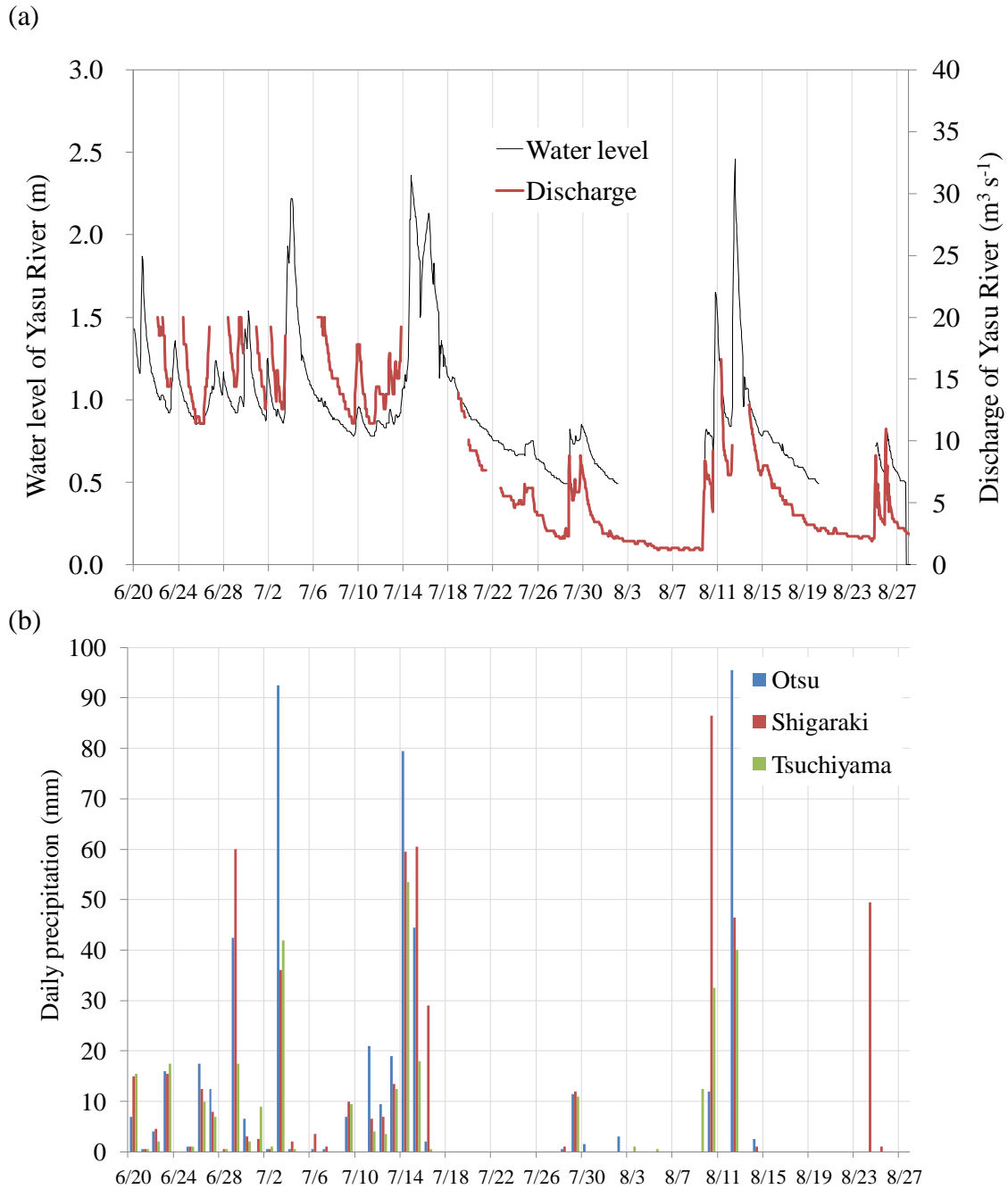


Figure 3–9. Yasu River water level and discharge (upper panel) and daily precipitation at AMeDAS stations near the Yasu River catchment area from June to August 2010 (lower panel). (a) Time series of river level (observation point: Hattori [downstream]) and discharge (observation point: Yasu [near Hattori]) in the Yasu River from June 20, 2010, to August 31, 2010. (b) Daily precipitation at AMeDAS stations (Otsu, Tsuchiyama, and

Shigaraki) around the Yasu River catchment area from June 10, 2010, to August 31, 2010. Daily precipitation data are shown in Appendix 3B (Table 3B).

The delay time calculated using a response function close to the average delay time ( $\tau_R=22.9$  h) estimated from the river level of the Yasu River was ( $\tau_L=22.6$  h) (Figure 3-7, Table 3-2). For this reason, I hypothesized that the river discharge time from the Yasu River would be approximately 24 hours. Although not verified in precise minutes, the delay time from the Yasu River was assumed to be about 24 hours. Therefore, from here on, the delay time was divided into two-time scales: (1) fast response ( $0 < \tau_L \leq 24$  h) and (2) slow response ( $24 \text{ h} < \tau_L \leq 40 \text{ d}$ ).

Table 2–2. Delay time  $\tau_R$  calculated from hourly Yasu River levels for each of the 14 precipitation events identified in Figure 2–9 from June 20, 2010, to August 31, 2010.  $T_0$ : time just before the river level increases,  $T_{\text{peak}}$ : time at the peak of the river level after precipitation,  $T_{\text{end}}$ : end time to return to the previous river level,  $\tau_{R_{\text{peak}}}$ : delay time to the peak,  $\tau_{R_{\text{end}}}$ : delay time to return to the previous river level.  $\Delta\text{water level}$ : difference between the river level just before the increase and the river level at the peak.

		Date and time	Yasu River Water Level (m)	$\tau_{R\_peak}(=T_{peak}-T_0)$	$\tau_{R\_end}(=T_{end}-T_0)$	$\Delta$ Water level (m)
①	T <sub>0</sub>	2010/6/20 13:00	1.16	6		0.71
	T <sub>peak</sub>	2010/6/20 19:00*	1.87		25	
	T <sub>end</sub>	2010/6/21 14:00	1.17			
②	T <sub>0</sub>	2010/6/23 5:00	0.92	12		0.44
	T <sub>peak</sub>	2010/6/23 17:00*	1.36		42	
	T <sub>end</sub>	2010/6/24 23:00	0.92			
③	T <sub>0</sub>	2010/6/26 7:00	0.85	25		0.39
	T <sub>peak</sub>	2010/6/27 8:00*	1.24		77	
	T <sub>end</sub>	2010/6/29 12:00	0.92			
④	T <sub>0</sub>	2010/6/29 5:00	0.92	17		0.62
	T <sub>peak</sub>	2010/6/29 22:00*	1.43	24		
	T <sub>peak</sub>	2010/6/30 5:00*	1.54		54	
	T <sub>end</sub>	2010/7/1 11:00	0.92			
⑤	T <sub>0</sub>	2010/7/1 18:00	0.87	5		0.38
	T <sub>peak</sub>	2010/7/1 23:00*	1.25		36	
	T <sub>end</sub>	2010/7/3 6:00	0.87			
⑥	T <sub>0</sub>	2010/7/3 8:00	0.86	10		1.36
	T <sub>peak</sub>	2010/7/3 18:00*	1.93	17		
	T <sub>peak</sub>	2010/7/4 1:00*	2.22		122	
	T <sub>end</sub>	2010/7/8 10:00	0.86			
⑦	T <sub>0</sub>	2010/7/9 14:00	0.78	11		0.18
	T <sub>peak</sub>	2010/7/10 1:00*	0.96		36	
	T <sub>end</sub>	2010/7/11 2:00	0.78			
⑧	T <sub>0</sub>	2010/7/11 10:00	0.78	79		1.58
	T <sub>peak</sub>	2010/7/14 17:00*	2.36	117		
	T <sub>peak</sub>	2010/7/16 7:00*	2.13		170	
	T <sub>end</sub>	2010/7/21 19:00	0.78			
⑨	T <sub>0</sub>	2010/7/24 19:00	0.67	3		0.08
	T <sub>peak</sub>	2010/7/24 22:00*	0.73	18		
	T <sub>peak</sub>	2010/7/25 13:00*	0.75		23	
	T <sub>end</sub>	2010/7/25 18:00	0.67			
⑩	T <sub>0</sub>	2010/7/28 19:00	0.49	2		0.36
	T <sub>peak</sub>	2010/7/28 21:00*	0.82	26		
	T <sub>peak</sub>	2010/7/29 21:00*	0.85		102	
	T <sub>end</sub>	2010/8/2 1:00	0.49			
⑪	T <sub>0</sub>	2010/8/9 22:00	0.74	2		0.08

		Date and time	Yasu River Water Level (m)	$\tau_{R\_peak}(=T_{peak}-T_0)$	$\tau_{R\_end}(=T_{end}-T_0)$	$\Delta$ Water level (m)
	T <sub>peak</sub>	2010/8/10 0:00*	0.82		17	
	T <sub>end</sub>	2010/8/10 15:00	0.69			
⑫	T <sub>0</sub>	2010/8/10 15:00	0.69	5		0.96
	T <sub>peak</sub>	2010/8/10 20:00*	1.65		35	
	T <sub>end</sub>	2010/8/12 2:00	0.84			
⑬	T <sub>0</sub>	2010/8/12 2:00	0.84	12		1.62
	T <sub>peak</sub>	2010/8/12 14:00*	2.46		59	
	T <sub>end</sub>	2010/8/14 13:00	0.84			
⑭	T <sub>0</sub>	2010/8/25 23:00	0.54	4		0.27
	T <sub>peak</sub>	2010/8/26 3:00*	0.81		28	
	T <sub>end</sub>	2010/8/27 3:00	0.54			
				Average delay time ( $\tau_{R\_peak}$ ) (h)	Average delay time ( $\tau_{R\_end}$ ) (h)	Average delay time $\tau_R$ (h)
Delay time to the peak (From ① to ⑭)				13.8	54.1	33.9
Delay time to the peak (Except ⑥, ⑧and ⑩)				9.3	36.5	22.9

### 3 – 3. 3. Relationship between the delay times $\tau_L$ calculated using response function and catchment scale (river length and catchment area)

The relationship between  $\tau_L$  calculated from the response function and the length (or catchment area) of the river inflowing into Lake Biwa was investigated (Figure 3 – 10, Table 3 – 3). The vertical axis is the delay time calculated by the response function, and the horizontal axis is the standardized river length and catchment area. 8 rivers used in Figure 3 – 10 are the \*\* rivers in Table 3 – 3, and 12 rivers are the 8 rivers in \*\* and 4 rivers in \*.

The largest catchment area is the Yasu River (387 km<sup>2</sup>), followed by the Anegawa River (370 km<sup>2</sup>), the Azumi River (299.2 km<sup>2</sup>), the Hino River (212 km<sup>2</sup>) and the Aichi River (208 km<sup>2</sup>). The total catchment area of these five major rivers occupies 46 % of the catchment area of Lake Biwa (Azuma 2003). Compared to  $\tau_L$  calculated from the response function,  $\tau_L$  became shorter from large to small rivers, depending on the length of the river and the size of its catchment area.

Nine rivers (Inukami, Uso, Isa, Suma, Seri, Harihata, Kita, Amano, and Daido Rivers, excluding Yogo River), which are the next largest rivers after the five major rivers, are of similar length (19 to 25 km), so I assumed that the delay times of rivers of the same size are almost similar. As for smaller rivers, linearity was assumed, and the delay time was estimated by simply calculating the ratio of the calculated delay time to the length of the river. For example, the estimated delay time for a 15 km length river (Kusatsu River) is about 4.6 hours, for a 7 km length river (Ohura River) about 2.6 hours, for a 4.4 km length river (Nose River) about 1.7 hours, and for a 2 km length river about 0.8 hours.

Next, the relationship between the delay time  $\tau_L$  calculated by the response function and the catchment size (river length and catchment area) was compared for (1) fast response ( $0 < \tau_L \leq 24$  h) and (2) slow response ( $24 \text{ h} < \tau_L \leq 40$  d) for 12 rivers, respectively. The 12 rivers are the 8 rivers that flow into Lake Biwa (8 rivers including 5 major rivers (Yasu, Ane, Ado, Hino, and Echi Rivers), Takatoki, Uso, and Inukami Rivers), and 4 smaller rivers (Kusatsu, Oura, Nose, and small rivers less than 2 km) to avoid overlapping of rivers of the same size.

A significant relationship was found for estimated delay time and river length (as well as catchment area).

- (i) For earlier responses ( $0 < \tau_L \leq 24$  h), (with river length  $n = 8$ ,  $R^2 = 0.98$ ,  $p < 0.05$ ;  $n = 12$ ,  $R^2 = 0.88$ ,  $p < 0.05$  (light blue in Figure 3-10); catchment area:  $n = 8$ ,  $R^2 = 0.87$ ,  $p < 0.05$ ;  $n = 12$ ,  $R^2 = 0.90$ ,  $p < 0.05$ ) (dark blue in Figure 3-10).
- (ii) For the slow response ( $24 \text{ h} < \tau_L \leq 40$  d),  $R^2 = 0.94$ ,  $p < 0.05$  for  $n = 8$  and  $R^2 = 0.84$ ,  $p < 0.05$  for  $n = 12$  with respect to river length (light red in Figure 3-10). For  $n = 8$ ,  $R^2 = 0.90$ ,  $p < 0.05$ , and for  $n = 12$ ,  $R^2 = 0.90$ ,  $p < 0.05$ ;) (dark red in Figure 3-10) for the catchment area.

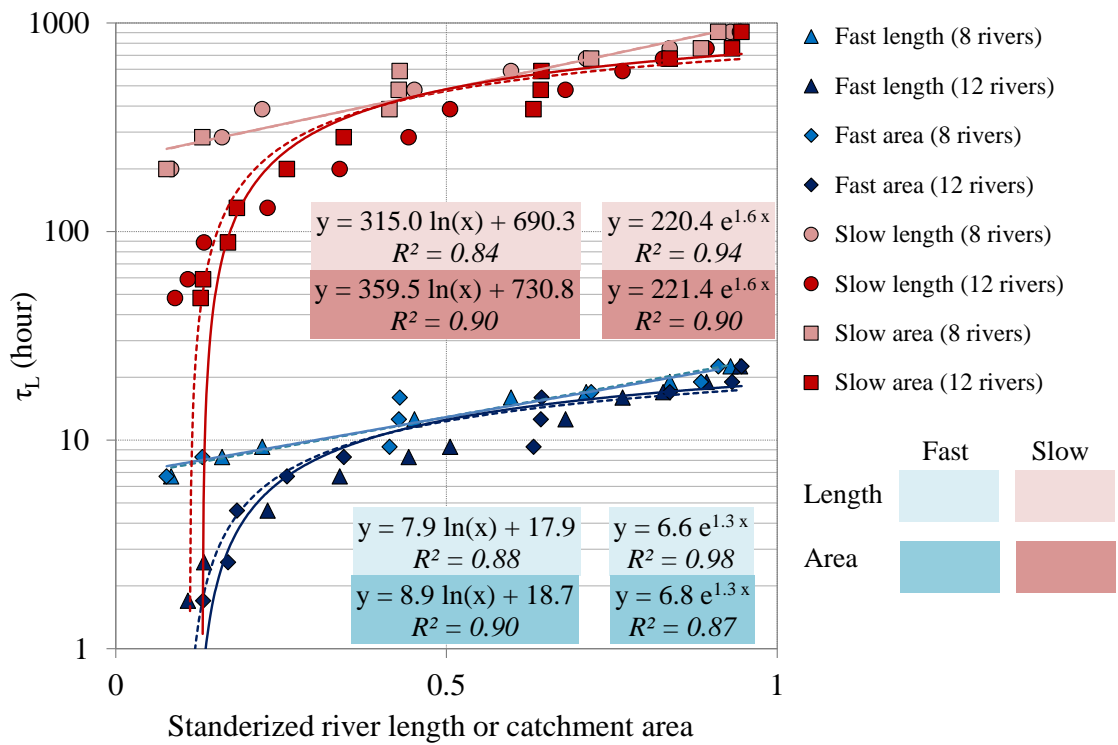


Figure 3 – 10. Relationship between river length or catchment area and lag time  $\tau_L$  for fast response ( $0 < \tau_L \leq 24$  h) and slow response ( $24 \text{ h} < \tau_L \leq 40 \text{ d}$ ) (8 rivers in \*\* in Table 3 – 3, 12 rivers in \*\* and \* in Table 3 – 3).

Table 3–3. Delay times  $\tau_L$  calculated by response functions and river lengths (as well as catchment area) of major rivers flowing into Lake Biwa (Lake Biwa Handbook, 2010). The eight rivers in \*\* are those used in Figure 3-10. The four rivers marked with \* are those used in Figure 3-10 and the eight rivers marked with \*\* are those included in the 12 rivers.

Name of rivers	River length (km)	Catchment area (km <sup>2</sup> )	Delay time ( $\tau_L$ )	
			Fast (h)	Slow (d)
Yasu River**	65.3	387.0	22.6	37.8
Ado R.**	57.9	299.2	19	31.5
Takatoki R.**	51.4	212.2	17	28.1
Hino R.**	46.7	212.6	16	24.5
Echi R.**	41.1	208.1	12.6	19.9
Ane R.**	31.3	370.1	9.3	16.1
Inukami R.**	27.9	104.7	8.3	11.8
Yogo R. (Lake Yogo)	24.9	63.5		
Uso R.**	22	69.9	6.7	8.3
Isa R. (lagoon)	21.4 (+3.7)	61.1		
Suma R.	21.3	122.6		
Seri R.	21	64.1		
Harihata R.	21.1	72.8		
Kita R.	20.1	77		
Amano R.	19	111.9		
Daido R. (lagoon)	19	41		
Ishida R.	17	53.6		
:	:	:		
Kusatsu R.*	15	33.9	4.6	5.4
Kamo R.	13.5	43.1		
Chinai R.	12	49.2		
Momose R.	12	20.2		
Hayama R.	10.3	23.3		
Yanomune R.	9.3	31.9		
:	:	:		
Ohura R.*	7	26.6	2.6	3.7
:	:	:		
Nose R.*	4.4	3.8	1.7	2.5
:	:	:		
The length shorter than 2 km*	2	1.5	0.8	2.0
:	:	:		

### 3 – 4. Discussion

In the delay time calculated by the response function, the strong positive response seen from 0.16 to 0.33 hours was determined by Iwaki et al. (2022) to be the response due to direct precipitation on the lake surface (Iwaki et al. 2022). Next, the peak in Figure 3 – 7 at about 4 hours was considered to correspond to the first mode of surface seiches (Table 1 – 1, Imasato 1984). Seiches are standing waves that may continue for several hours, and sometimes for several days (Forel 1895, Yoshimura 1937). In the case of Lake Biwa, the first mode, which has the largest amplitude, is the oscillation when the longest node is taken ( $\approx 60$  km), and the bay oscillation of the southern lake is combined with the oscillation, and the period is about 4 hours (Imasato 1970; 1971; 1972). Although the volume of lake water itself does not change, seiches are associated with a periodic change in water level (Table 1 – 1, Iwaki & Toda 2022).

The relationship between delay time calculated by the response function and catchment size (river length or catchment area) is hypothesized to be an S-curve-like line consisting of a combination of logarithmic, linear and exponential types (Figure 3-11a, b), and the three response patterns are assumed to represent differences in the runoff process. In general, the delay time of return flow is considered to be longer than that due to river inflow, and the delay time of river inflow is considered to be longer than that due to direct precipitation on the lake surface, and the delay times are considered to correspond to each of the three runoff processes.

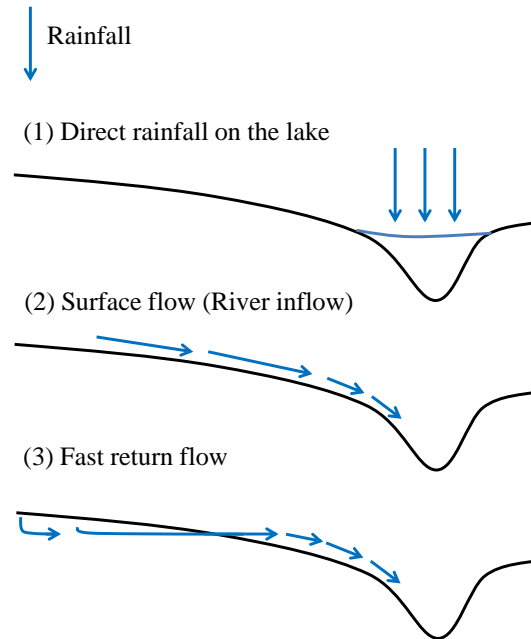
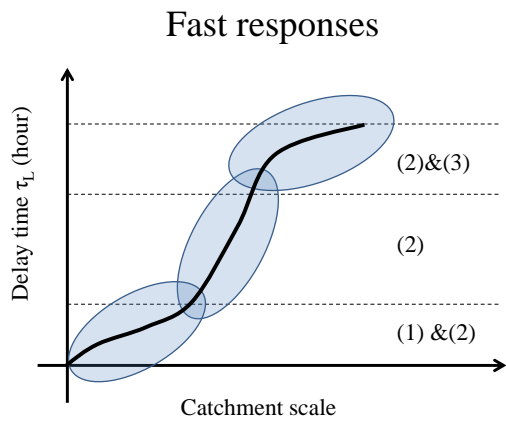
The fast response was assumed to represent three different processes: (1) direct precipitation onto the lake; (2) river inflow; and (3) fast return flow (Figure 3 – 11a). For this fast response, river runoff was considered to be the dominant runoff process.

The slow response was assumed to represent the difference in runoff processes between: (2) river inflow; (3) fast return flow; (4) slow return flow; and (5) subsurface flow. As for the slow response, it was assumed that the dominant runoff processes were those in which water percolated underground and finally returned to the surface near the lake and slow return flows from the mountains and upstream (Figure 3 – 11b; United States Department of Agriculture 2010).

These delay times and the dominant runoff processes for each time scale are based on hypotheses, however, the Yasu River has the longest and largest catchment area in the catchment area, and thus can be considered as a useful indicator to separate river runoff and return flows at around 22-23 hours. In addition, as shown in Figure 3 – 12, the delay time and the trend of the delay time are different around 23-24 hours. These differences are considered to be due to differences in the runoff process (Table 3 – 3, Figure 3 – 12).

However, not all topographic slopes and geology are the same, especially on hillslopes, where groundwater flow is the dominant runoff mechanism, even during heavy rainfall, so longer delay times need to be considered (Tani et al. 2019; 2020). In the case of Lake Biwa, the catchment area is surrounded by a mountain ridge (with steep slopes), so it would be important to consider groundwater flow in the future.

(a) Fast response



(b) Slow response

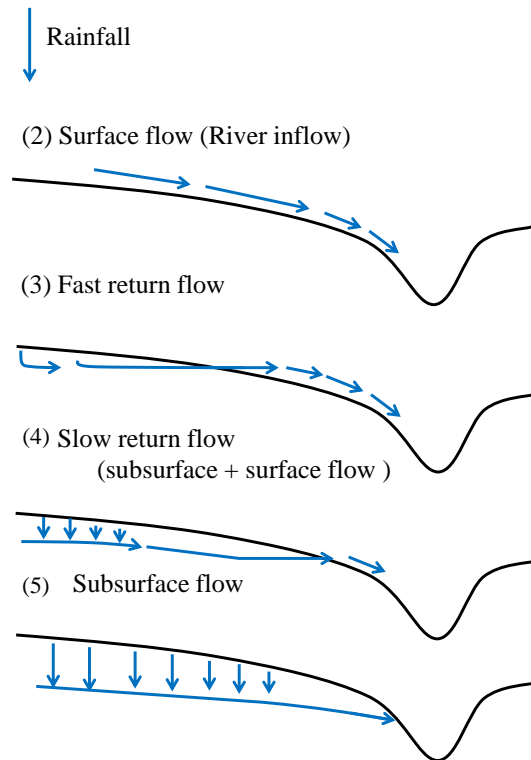
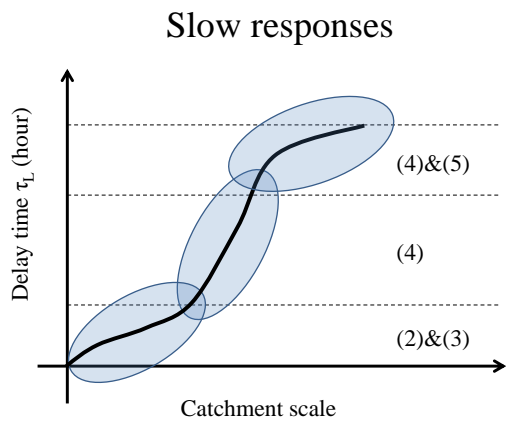


Figure 3 – 11. The left figure shows the relationship between delay time and catchment size calculated by the response function. (a) Fast response. (b) Slow response. The righthand figure shows the runoff pattern from the catchment into the lake.

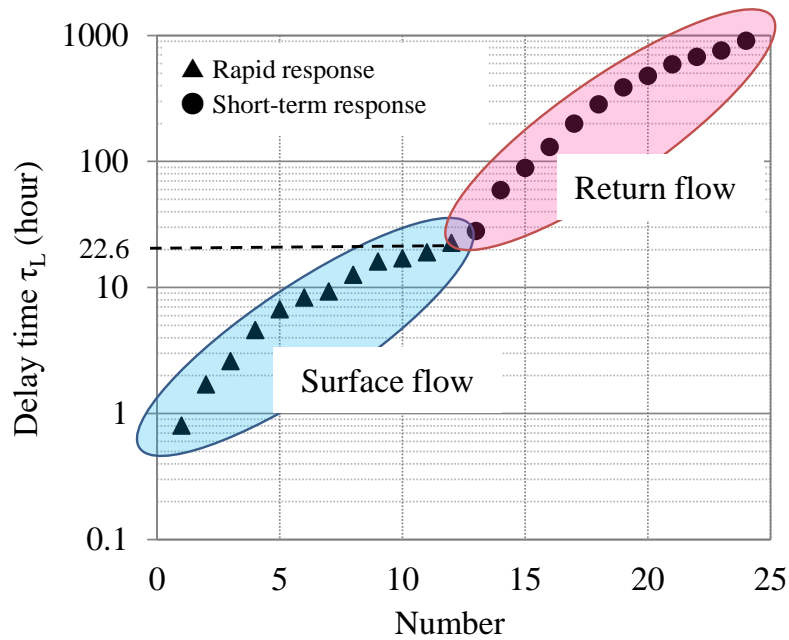


Figure 3 – 12. Delay time for two-time scales (early response and late response) in order (X-axis shows the order). Since the Yasu River is the longest river and has the widest catchment area, the delay time for the Yasu River ( $\tau_L=22.6$  h) was assumed to have the longest delay time of the fast responses.

### 3 – 5. Conclusions

In Chapter 3, the various delay times calculated by the impulse response function were considered to be due to differences in the runoff process, and the calculated delay times were compared with the runoff process that was considered to correspond to each of them. The precipitation retention times considered in this chapter are: ① direct precipitation on the lake surface; ② runoff by small rivers of about 2 km; ③ runoff by rivers of about 10-15 km; ④ runoff by rivers of similar size of about 20 km; ⑤ river runoff by the Yasu River; and ⑥ slow return flow of the Yasu River. Note that the response of ④ due to river discharge by a river of the same size has been strongly detected in previous spectral analyses (Iwaki et al. 2014, Iwaki et al. 2020b), so it is shown separately from ③ and ⑤. The water level response due to the first mode of surface seiches was observed between ② and ③.

For this chapter, the delay time was calculated from the impulse response function and the obtained delay time was correlated with the runoff process. Then, in the runoff process, precipitation retention time for direct precipitation to the lake surface, river inflow (the delay time of the incoming river was estimated according to the river size) and return flow (fast and return response) were examined.

Appendix 3A. Two-sided t-tests with correspondence between two peaks of delay times  
Two-sided t-tests were conducted for the summer response function peaks of 4.6, 6.7, 8.3, 9.3, 12.6, 16.0, 17.0, 19.0, and 22.6 hours (Figure 3 – 7, Table 3A – a). The values obtained before and after the peak values calculated were examined with a one-tailed two-tailed t-test, none of which was significant (Table 3A – a). Therefore, the values of these peaks were  $\tau = 4.6, 6.8, 8.3, 9.3, 12.6, 16.0, 17.0, 19.0,$  and 22.6 h, and these were identified as different peaks.

Two-tailed t-tests were conducted for the summer response function peaks of 2.5, 3.7, 5.4, 8.3, 11.8, 16.1, 19.9, 24.5, 28.1, 31.5, and 37.8 days (Figure 3 – 8, Table 2A). The values obtained before and after the peak were examined with a one-tailed two-tailed t-test and were not significant (Table 3A – b). Therefore, the values of these peaks were identified as  $\tau = 2.5, 3.7, 5.4, 8.3, 11.8, 16.1, 19.9, 24.5, 28.1, 31.5,$  and 37.8 days for each of these different peaks.

Table 3A. two-tailed t-tests with corresponding two peaks of delay time. n, m are the number of samples, and the subscripts represent the delay time of the target. The results shown in the right-hand column of the fast response results in (a) were tested by expanding to a significant range when the two peaks were too close together for the difference to be significant.

(a) Fast response

Two-sided t-tests with correspondence between two peaks of rapid delay times			
$n_{4.6h} = 16, m_{6.8h} = 16$	$p < 0.005$		
$n_{6.8h} = 16, m_{8.3h} = 16$	$p > 0.05$	$n_{6h} = 16, m_{8.5h} = 16$	$p < 0.05$
$n_{8.3h} = 16, m_{9.3h} = 16$	$p > 0.05$	$n_{8h} = 16, m_{10h} = 16$	$p < 0.05$
$n_{9.3h} = 16, m_{12.6h} = 16$	$p < 0.005$		
$n_{12.6h} = 16, m_{16h} = 16$	$p < 0.005$		
$n_{16h} = 16, m_{17h} = 16$	$p > 0.05$	$n_{16h} = 16, m_{18h} = 16$	$p < 0.05$
$n_{17h} = 16, m_{19h} = 16$	$p < 0.005$		
$n_{19h} = 16, m_{22.6h} = 16$	$p < 0.005$		

(b) Slow response

Two-sided t-tests with correspondence between two peaks of short-term delay times	
$n_{2.5d} = 144, m_{3.7d} = 144$	$p < 0.005$
$n_{3.7d} = 144, m_{5.4d} = 144$	$p < 0.005$
$n_{5.4d} = 144, m_{8.3d} = 144$	$p < 0.005$
$n_{8.3d} = 144, m_{11.8d} = 144$	$p < 0.005$
$n_{11.8d} = 144, m_{16.1d} = 144$	$p < 0.005$
$n_{16.1d} = 144, m_{19.9d} = 144$	$p < 0.005$
$n_{19.9d} = 144, m_{24.5d} = 144$	$p < 0.005$
$n_{24.5d} = 144, m_{28.1d} = 144$	$p < 0.005$
$n_{28.1d} = 144, m_{31.5d} = 144$	$p < 0.005$
$n_{31.5d} = 144, m_{37.8d} = 144$	$p < 0.005$

Appendix 3B. Daily precipitation at the catchment area of Yasu River from Jun 10<sup>th</sup> to Aug 31<sup>th</sup> in 2010

Date	Otsu	Shigaraki	Tsuchiyama	Σ	Date	Otsu	Shigaraki	Tsuchiyama	Σ
2010/6/10	0	0	0	0	2010/7/22	0	0	0	0
2010/6/11	0	0	0	0	2010/7/23	0	0	0	0
2010/6/12	0	0	0	0	2010/7/24	0	0	0	0
2010/6/13	24	17	9.5	50.5	2010/7/25	0	0	0	0
2010/6/14	0	0	1.5	1.5	2010/7/26	0	0	0	0
2010/6/15	16.5	15.5	15	47	2010/7/27	0	0	0	0
2010/6/16	18.5	36.5	44.5	99.5	2010/7/28	0.5	1	0	1.5
2010/6/17	0	0	0	0	2010/7/29	11.5	12	11	34.5
2010/6/18	45.5	50	31	126.5	2010/7/30	1.5	0	0	1.5
2010/6/19	5	15	9.5	29.5	2010/7/31	0	0	0	0
2010/6/20	7	15	15.5	37.5	2010/8/1	0	0	0	0
2010/6/21	0.5	0.5	0.5	1.5	2010/8/2	3	0	0	3
2010/6/22	4	4.5	2	10.5	2010/8/3	0	0	1	1
2010/6/23	16	15.5	17.5	49	2010/8/4	0	0	0	0
2010/6/24	0	0	0	0	2010/8/5	0	0	0.5	0.5
2010/6/25	1	1	1	3	2010/8/6	0	0	0	0
2010/6/26	17.5	12.5	10	40	2010/8/7	0	0	0	0
2010/6/27	12.5	8	7	27.5	2010/8/8	0	0	0	0
2010/6/28	0	0.5	0.5	1	2010/8/9	0	0	12.5	12.5
2010/6/29	42.5	60	17.5	120	2010/8/10	12	86.5	32.5	131
2010/6/30	6.5	3	2	11.5	2010/8/11	0	0	0	0
2010/7/1	0	2.5	9	11.5	2010/8/12	95.5	46.5	40	182
2010/7/2	0.5	0.5	1	2	2010/8/13	0	0	0	0
2010/7/3	92.5	36	42	170.5	2010/8/14	2.5	1	0	3.5
2010/7/4	0.5	2	0.5	3	2010/8/15	0	0	0	0
2010/7/5	0	0	0	0	2010/8/16	0	0	0	0
2010/7/6	0.5	3.5	0	4	2010/8/17	0	0	0	0
2010/7/7	0.5	1	0	1.5	2010/8/18	0	0	0	0
2010/7/8	0	0	0	0	2010/8/19	0	0	0	0
2010/7/9	7	10	9.5	26.5	2010/8/20	0	0	0	0
2010/7/10	0	0	0	0	2010/8/21	0	0	0	0
2010/7/11	21	6.5	4	31.5	2010/8/22	0	0	0	0
2010/7/12	9.5	7	3.5	20	2010/8/23	0	0	0	0
2010/7/13	19	13.5	12.5	45	2010/8/24	0	49.5	0	49.5
2010/7/14	79.5	59.5	53.5	192.5	2010/8/25	0	1	0	1
2010/7/15	44.5	60.5	18	123	2010/8/26	0	0	0	0
2010/7/16	2	29	0.5	31.5	2010/8/27	0	0	0	0
2010/7/17	0	0	0	0	2010/8/28	0	0	0	0
2010/7/18	0	0	0	0	2010/8/29	7	0	0	7
2010/7/19	0	0	0	0	2010/8/30	0	0	2	2
2010/7/20	0	0	0	0	2010/8/31	0	0	0	0
2010/7/21	0	0	0	0					



# Chapter 4 Estimation of average precipitation retention time due to subsurface flow

## 4 – 1. Introduction

Precipitation on the lake surface contributes to water level changes immediately, while precipitation in the catchment area has a lag time before it can contribute to lake level increases, due to river flows (inflow and outflow), return flows, subsurface flow, and groundwater flow. In Chapter 3, the delay times due to river inflow and fast return flow were discussed. However, because the water level observation period was 1-2 years, it was not possible to discuss the slower response, and the delay time due to slow return flow and subsurface flow (corresponding to the flow of water in the unsaturated zone above the groundwater surface) was an unsolved problem.

On the other hand, on a global scale, Lake Biwa is located in a warm and humid climatic zone, with the northern part of the lake in the Ura-Japan climate zone and the southern part in the Omote-Japan climate zone. Therefore, there are no frequent water shortages at present. However, in arid and semi-arid regions, lake water is valuable as a freshwater resource, and the shrinkage and disappearance of lakes has been reported, with water storage problems already becoming more serious (Moss et al. 2011). Indeed, lakes in such areas, such as in the Aral Sea (Micklin 1988; 2007), Lake Kinneret (Wine et al. 2019, Ostrovsky et al. 2013), Lake Urmia (AghaKouchak et al. 2015), and Lake Abert (Moore 2016), are also shrinking or disappearing, much effort is devoted to the study of water level changes, and furthermore, they are fragile to climate change. Some factors causing water shortages include the balance between inflows and outflows, and other anthropogenic influences such as increased water withdrawals during droughts and excessive agricultural water use in catchments (Ostrovsky et al. 2013).

In arid regions where water is not available at the surface, it is important to estimate the retention time of precipitation by subsurface flow. However, estimating subsurface flow in arid regions is often difficult because it is not known whether the water is present at all times. On the other hand, water level fluctuations in Lake Biwa, which is located in a humid region, are complicated due to its vast area and complex catchment characteristics, but the total discharge is artificially controlled. Therefore, there is a high potential for understanding the volume of discharge and estimating the precipitation retention time due to subsurface flow.

In this chapter, I estimated the precipitation retention time due to subsurface flow. Using 31 years of water level data of Lake Biwa and its catchment area from 1983 to 2013, and precipitation data in the catchment area of Lake Biwa, I calculated the delay time due to subsurface flow by using an impulse response function to estimate the precipitation retention time due to subsurface flow.

Changes in the delay time every four months were also examined here. Understanding the time scale of the average precipitation retention time due to subsurface flow and the approximate average precipitation retention time will contribute to water and forest management, since it will allow us to determine the delay time that contributes to water level increase some time after a precipitation event.

## 4–2. Methods

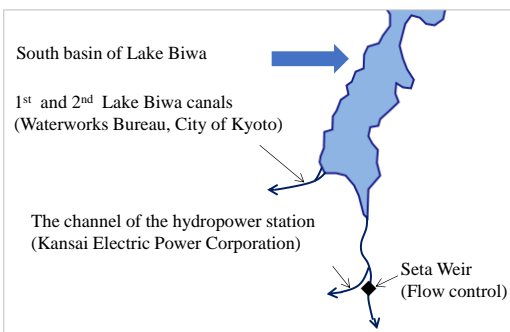
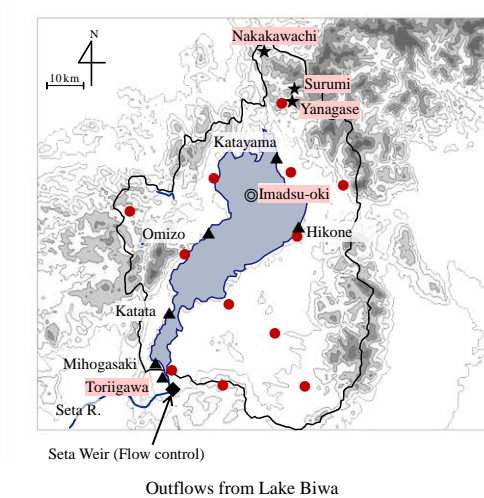
Lake Biwa has some 140 years of water level observations. For the purpose of understanding the shape of the response function, I focused on the period after the 1980s, when precipitation data from AMeDAS at many sites in Shiga Prefecture were obtained. For this reason, I used 31 years of Lake Biwa water level and precipitation data in the Lake Biwa catchment area from 1983 to 2013 to calculate the delay time using an impulse response function and discuss the average precipitation retention time. The method for calculating the delay time using the impulse response function is the same as that described in the Methods of Chapter 3 (section 3–2).

### 4–2. 1. Data Assimilation and Calculation of the Response Function

#### 4–2. 1. 1. Water level

The water level of Lake Biwa has been observed by the Ministry of Land, Infrastructure, Transport and Tourism since February 4, 1874. In this study, I used water level data of Lake Biwa observed at 6:00 a.m. daily from January 1, 1983, to December 31, 2013. In general, the water level of Lake Biwa represents the height of the water relative to the Lake Biwa Standard Level (BSL; +84.371 m) of  $\pm 0$  m (Lake Biwa Handbook 2010).

Until March 1992, the lake level at the Toriigawa (place name) observation point was used as BSL (Figure 4–1). However, after 1992, the BSL now represents the average water level at five observation points (Katayama, Omizo, Hikone, Katada, and Mihogasaki; Figure 3–1). Therefore, the effect of the station changes in BSL around 1992 was examined and is shown in Appendix A (Figure 4A–1).



#### Chapter 4

▲ Water-level data ( $\Delta t = 1$  day) at five points average water level data (Mihogasaki, Katata, Omizo, Katayama, Hikone, Torigawa) conducted by Lake Biwa Work Office (Ministry of Land Infrastructure, Transport and Tourism).

● Meteorological data ( $\Delta t = 1$  day) Automated Meteorological Data Acquisition System (AMeDAS), Japan Meteorological Agency.

◆ Discharge data ( $\Delta t = 1$  day)

Ministry of Land Infrastructure, Transport and Tourism (MLIT), Waterworks Bureau, City of Kyoto, Kansai Electric Power Corporation.

★ Observed snow water equivalent (1–2 times/week) at the northern catchment are of Lake Biwa (Yanagase, Surumi, Nakakawachi).

◎ The water temperature and dissolved oxygen (DO) (1 times/2week) at eight depths in northern part of Lake Biwa (Imadsu-oki) conducted by Lake Biwa Work Office (Ministry of Land Infrastructure, Transport and Tourism).

Figure 4 – 1. Observation sites and data used in this thesis (locations and data related to Chapter 4 are colored red).

#### 4 – 2. 1. 2. Precipitation

Twelve JMA AMeDAS daily precipitation stations located in the catchment area from January 1, 1983, to December 31, 2013, were summed and used as the daily precipitation. However, the influence of snowfall is observed in terms of snow depth but is not easily reflected as precipitation due to the time lag and snow density described below.

Since the effect of snowfall is taken into account in Section 4.2.1.3. below, after this section, the term "rainfall" is used to distinguish between the precipitation that takes into account rainfall and snowfall, and is used as the daily rainfall in the catchment area (Figure 4 – 1).

The type of rain gauge is a tipping-mass rain gauge with a resolution of 0.5 mm. However, the tipping-mass rain gauge has a slight time lag relative to the actual time of precipitation during snowfall and snowmelt events. In addition, because snow accumulates on top of the rain gauge during winter, when snowfall causes snow to accumulate on top of the rain gauge, the snow is melted by a heater and counted as rainfall, resulting in a time lag with the time when snowfall is actually occurring. To compensate for this time lag, I used the snow depth at an AMeDAS station (Yanagigase) observed by the JMA (Figure 4 – 1).

#### 4–2. 1. 3. Snow density and snow water equivalent

Snow density was converted using snow depth and snow weight. To calculate snow density, 16 observations of snow cover were made at Surumi (marked with ★ in Figure 4–1) during the winter of 2001 (Iwaki et al. 2010). For the snow depth observation, snow depth and snow weight were observed and the average snow density was calculated from snow weight (weight) and snow depth (height), as shown in Table 4–1 (only for the snow-melting season). Based on the snow observation results, the average snow density during the snowmelt season in this northern part of the Lake Biwa catchment area was calculated to be about  $0.43 \text{ g cm}^{-3}$  (Table 4–1). The amount of snowfall was calculated as follows (Iwaki et al. 2011):

$$\text{Daily Snowfall (g cm}^{-2}\text{)} = \text{snow density (g cm}^{-3}\text{)} \times \Delta \text{snow depth (cm)}$$

$$\text{Precipitation} = \text{rainfall} + \text{snowfall.}$$

In addition, from 2009 to 2010, snow conditions, snow depth and snow weight were observed at the two locations marked with ★ (Yanagase in the mid-mountain area and Nakanokawachi in the mountain area) in the catchment area of northern Lake Biwa (Figure 4–1), as observed by Surumi in 2001/2002, and the snow density was calculated.

Table 4–1. Average snow density in the northern catchment of Lake Biwa during winter 2001<sup>†</sup>.

Date	Weather	Snow depth (cm)	Snow water equivalent (mm)	Snow density (g-cm <sup>-3</sup> )	Air temperature (°C)	Surface snow temperature (°C)
2002/2/24	Sun	82.6	36.5	0.442	2.9	-1.0
2002/2/28	Cloud	74.6	32.9	0.441	1.7	-0.9
2002/3/5	Cloud	59.4	25.9	0.436	1.5	-2.1
2002/3/14	Rain	20.5	8.6	0.418	5.4	-2.2
2002/3/17	Sun	10.1	4.6	0.454	13.2	-3.0

<sup>†</sup>Only the snowmelt season is shown (cited from Iwaki et al. 2008, Iwaki et al. 2010, and Iwaki et al. 2011; the observation point is Surumi★ in Figure 4–1).

#### 4–2. 1. 4. Dissolved oxygen and water temperature

The calculated delay time was evaluated by evaluating the effect of snowmelt water on dissolved oxygen (DO) concentrations in the lake based on changes in water temperature. For this purpose, I used data observed by Shiga Prefecture every two weeks from October 9, 2009, to May 10, 2010 at the center of Imazu-oki in the northern part of Lake Biwa. Water temperature (°C) and DO (mg/L) values observed at eight depths (0.5 m, 5 m, 10 m, 15 m, 20 m, 30 m, 40 m, 60 m, 80 m, and 1 m from the bottom) in the center of Imazu-

oki were used (Figure 4-1; Shiga Prefecture Environmental White Paper 2009-2010).

Figure 4 – 1 shows the snow water volume observed in the area, which is located in the catchment area of the Ane River (Takatoki River); snowmelt water in this catchment area flows into Lake Biwa through the Ane River. In the northwestern part of Lake Biwa, the distance from the mountains to the lake is short and steep. On the other hand, characteristics of the lake basin in the northeastern part of Lake Biwa are different from those in the northwestern part. The shape of the lake basin in the northeastern part of Lake Biwa has a gradual gradient, and because of this, the lake gradually deepens toward the deepest part of the lake.

The data observation point in the center of Imazu-oki is located at the end of the deep basin of Lake Biwa where river water from the Ane River and other sources penetrate toward the deeper layers of the lake. Although there are various flows in the lake, the snowmelt water is turbid during snowmelt season, and therefore, when used together with turbidity, it is possible to examine the timing of the influence of river water penetrating deep into the lake due to density currents (Hasegawa 2012).

However, since river inflow due to turbidity is also caused by rainfall, it is difficult to distinguish the effect from that caused by snowmelt. Therefore, dissolved oxygen concentration was used. Although dissolved oxygen concentration is not a conserved property, it was used as an indicator of the impact of river water on the lake because the dissolved oxygen concentration in river water during the snowmelt season is very high. Water temperature was used to confirm the depth of the water temperature thermocline layer (to determine to what depth the river water penetrated and mixed into the lake), and water temperature and dissolved oxygen concentration were used to determine the effects of snowmelt.

#### 4 – 2. 2. The calculation method for delay time using a response function

Precipitation (input) and water level (output) data from January 1, 1983, to December 31, 2013 were standardized. The observed data in Lake Biwa and its catchment area are the values from the locations shown in Figure 4 – 1. Next, I calculated the autocorrelation function for the input data (precipitation) and the cross-correlation function between the input data and the output data (water level). Then, the delay time was calculated by the response function, and the average precipitation retention time was discussed. Finally, I evaluated the appropriateness of the calculated delay times (identified in the discussion), focusing on the snow accumulation and melting processes in the catchment area and the changes in water temperature and dissolved oxygen concentration in the lake.

First, the response functions were calculated using records of daily precipitation and daily lake level (6:00 a.m. values) for all 31 years from 1983 to 2013. The input data are precipitation data (before calibration ("rainfall") and after calibration (total precipitation converted from rainfall and snowfall into water volume by snow density, "precipitation"), and the output data are daily lake water levels.

Next, using the impulse response function, the rainfall (rainfall only) - water level delay time and the precipitation (taking into account the effect of snowfall) - water level delay time were calculated and compared, respectively. To determine the positive peak (= delay time) of the calculated response function, a one-paired two-tailed t-test was also performed to examine the deviation between the mean of the peak values and the mean of the non-peak values (a test that indicates that the peaks of the response function do not

correspond to peak and non-peak values). The three peaks of focus (45, 63, and 71 days) were also distinguished in the same way and were verified with a corresponding paired two-tailed t-test, which showed that none of them were significant, so they were used as the values of different peaks. From these tests, the values of the respective peaks of the response function were identified and discussed as delay times.

Then, precipitation-water level and precipitation-water volume response functions were calculated every 4 months using precipitation (taking snowfall into account) and water level, and the calculated results for 31 years are shown for each 4-month period. The delay time (peak of the response function) was then discussed from the calculated response functions. Here, the water volume is the volume converted from the water level. Since there are too many records to read over the 31-year period, the mean, median, and 25 – 75 % of the calculated range are shown for each year. Finally, the validity of the delay time calculated using the response function was discussed using water temperature, DO concentration, and snow water equivalent observations, focusing on the water flow of the snowmelt water.

#### 4–2. 3. Other factors

I focused on the response of the relationship between precipitation and water level in order to determine the precipitation retention time. However, the complexity of considering all factors made it necessary to simplify the calculation. For this reason, I treated several factors as constants, including lake surface area, groundwater, and evaporation, which seem reasonable approximations for the following reasons. The Lake Biwa catchment lies in a humid region, and therefore the lake area changes little because of much lesser evaporation compared to lakes in arid regions of the world (Saijo 1995). Groundwater infiltration into the lake is very slow compared to river inflow (Taniguchi 1995, Fujii 2000, Takahashi et al. 2004). Furthermore, the ratio of lake surface evaporation to Lake Biwa discharge is estimated to be 5-10% (Fujino 1980; Tsurumaki & Kobayashi 1989). The fluctuations in evaporation are periodic and are detected using the FFT. However, the area around Lake Biwa is a humid region, and unlike arid regions, daily water levels are not greatly affected by evaporation (Kotoda 1977, Ikebuchi et al. 1988). Also, since evaporation depends basically on temperature, it needs to be taken into account with respect to the daily and yearly periods, but as in this study, it was necessary to consider it constant or for simplicity to identify the lag time or to filter out this effect. However, in order to filter it, it is possible if there has been enough continuous research accumulated in the past or the periodicity is clearly known, but at this time, there were many difficulties and unknowns in the measurement of the evaporation itself. Therefore, deep groundwater recharge and water evaporation from the lake surface were considered as constant for the purposes of this study (about 2 – 3 months).

### 4–3. Results and Discussion

#### 4–3. 1. Data assimilation and calculation delay time using impulse response function

The time series of precipitation (input) and water level of Lake Biwa (output) are shown in Figure 4–2. In 1992, the BSL was changed from Toriigawa to the average of five

points (Katayama, Omizo, Hikone, Katada, and Mihogasaki) (Figure 4 – 1). For this reason, the relationship between the daily water level of the Toriigawa and the average five points is shown in Figure 4A – 1. The value of  $R^2$  was 0.91 from 1993 to 2013 ( $m_{\text{Toriigawa}} = 7634$ ,  $n_{5 \text{ points}} = 7634$ ,  $m$  is the number of samples when BSL is the average of Toriigawa observation points,  $n$  is the number of samples when BSL is the average of the above 5 points.). Therefore, the effect of the change in BSL from one point at Toriigawa to five average observation points is not completely negligible. However, I regarded the difference as not serious enough to invalidate the use of the data as the same data and treated the data as continuous water level data of Lake Biwa.

I calculated and compared two response functions based on the relationship between precipitation and water level (including Toriigawa) from 1983 to 2013 and precipitation (five-point average) and water level from 1993 to 2013 (Fig.4 – 3). In both response functions calculated by the response function, the response due to direct rainfall on the lake surface (< 1 day) and river inflow on 1-3 days (Iwaki et al. 2020; 2021; 2022), and other peaks were identified on 45 and 63-71 days (Figure 4 – 3). In addition, in order to confirm the effect of discharge, an outflow-water level response function was also calculated (Figure 4 – 3). No significant peaks were identified before 130 days (when the response function is close to 0), other than the peak immediately after the discharge, and therefore were not taken into account.

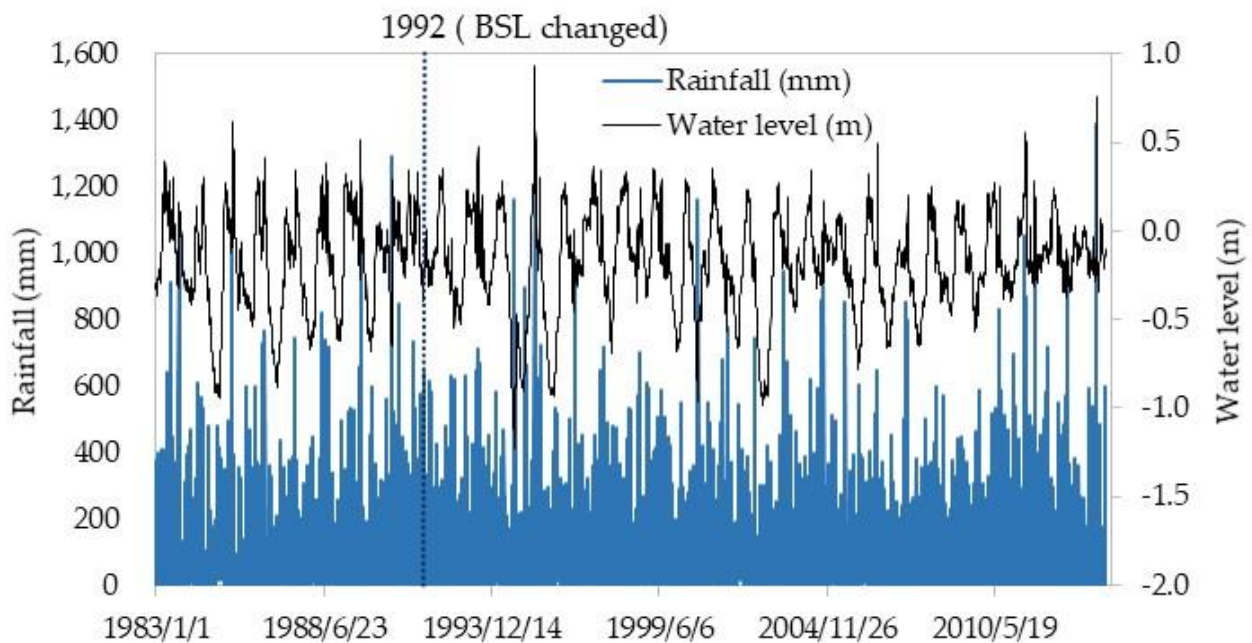


Figure 4 – 2. Time series data of input (rainfall; left axis) and output (daily water level of Lake Biwa; right axis) from 1983 to 2013.

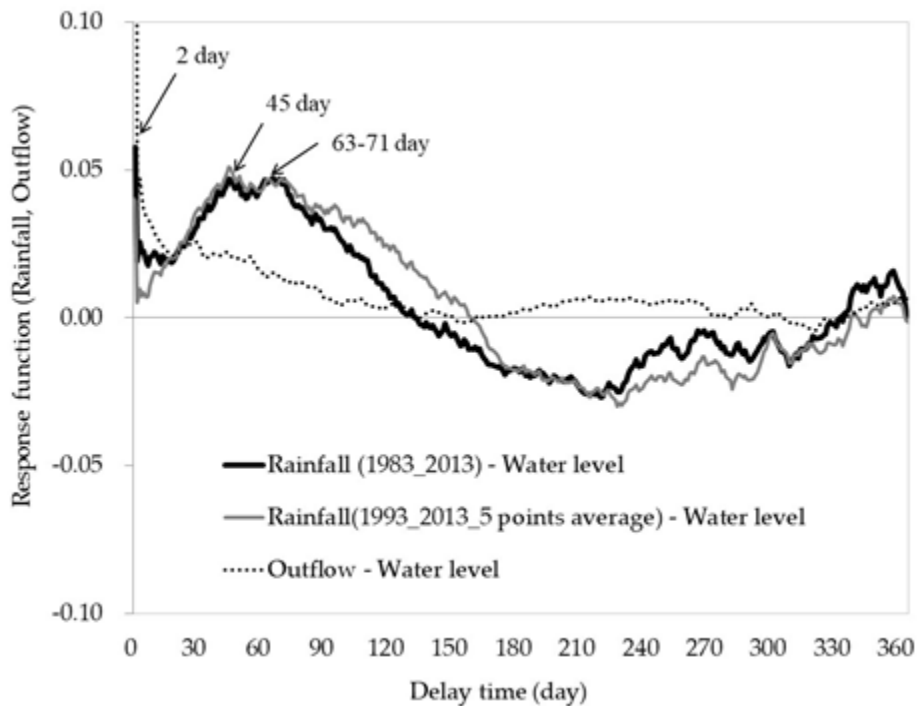


Figure 4–3. Delay times calculated from the rainfall-water level. relationship using the impulse response function (the dashed line is the response function calculated from the outflow-water level relationship). All input data are standardized (following the same pattern as below).

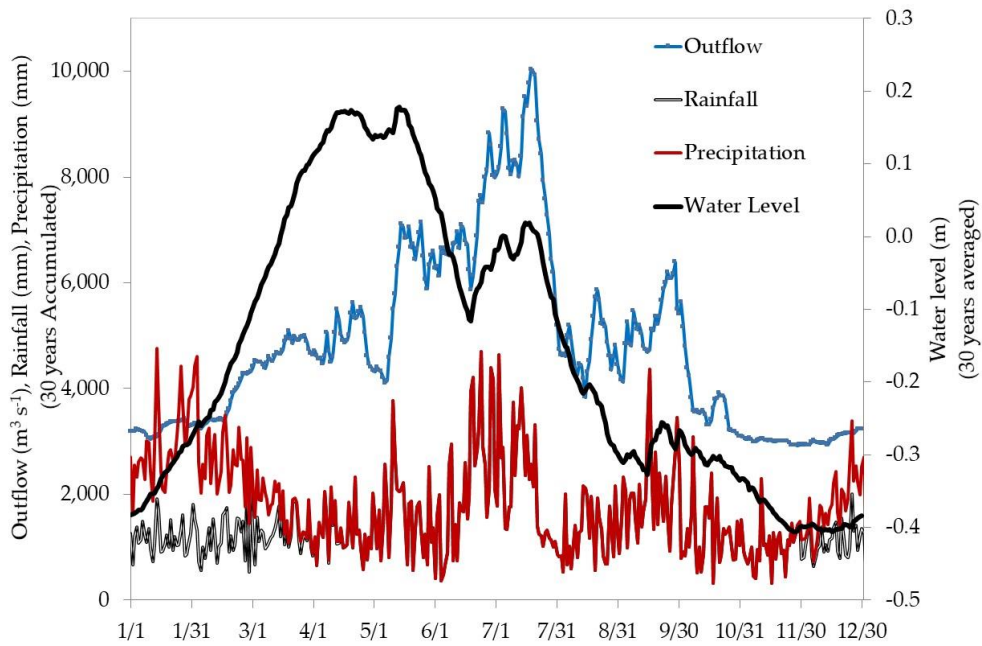
#### 4–3. 2. Determination of delay time calculated by impulse response function using precipitation including the effect of snowfall

The precipitation data from AMeDAS may have underestimated the effect of snowfall (Figure 4–4a). Therefore, the response function with respect to the water level for each of the precipitation, considering the snowfall, was calculated and compared with the response function with respect to the average rainfall shown in Figure 4–3 (Figure 4–4b).

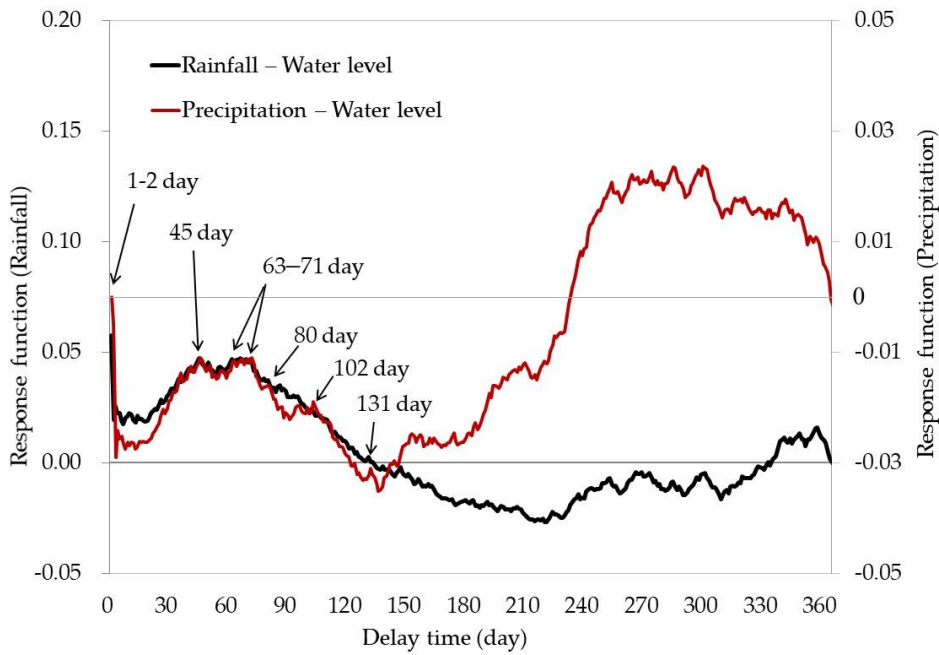
The shape of response function of precipitation-water level was similar to that in Figure 4–3 until approximately 131 days. For the case where the input is rainfall and for the case where the input is precipitation (including snowfall) and for the shapes of days 1-131, the value of R2 for the two response functions is 0.95. (Figure 4–4b, Figure 4C–1). Similar to the case of Figure 4–3, river inflow from the catchment area showed the clearest peak on approximately 1–3 days (Figure 4–4b). And the next clear peaks after 1–3 days were obtained at 45, 63–71, and 102 days. There were few differences in delay times shorter than 131 days when the input was rainfall and snowfall, but only in

the case of snowfall there was a peak around 102 days. As for the test of the peaks, the same method was used as in the case where the input was rainfall (section 4 – 3. 1), and significant differences were found in the means of the four peaks at 45, 63, 71, and 102 days, so these were considered to be four different peaks.

On the other hand, for delay times longer than 131 days, the differences were significant. This suggested that for delay times greater than 131 days, the differences could be due to the effects of snow accumulation and snowmelt, or other factors not considered that have longer time scales, such as evaporation or groundwater.



(a)



(b)

Figure 4—4. The response function with respect to the water level for each of the precipitation, considering the snowfall, was calculated and compared with the response

function with respect to the average rainfall shown in Figure 4–3.

(a) Seasonal water level (average; right axis), outflow (integrated; left axis), rainfall (integrated; left axis), and precipitation (integrated; left axis) for Lake Biwa and its catchment area from 1983 to 2013. Average snow density ( $0.43 \text{ g cm}^{-3}$ ) was used to convert changes in snow depth into snowfall (Table 4–1).

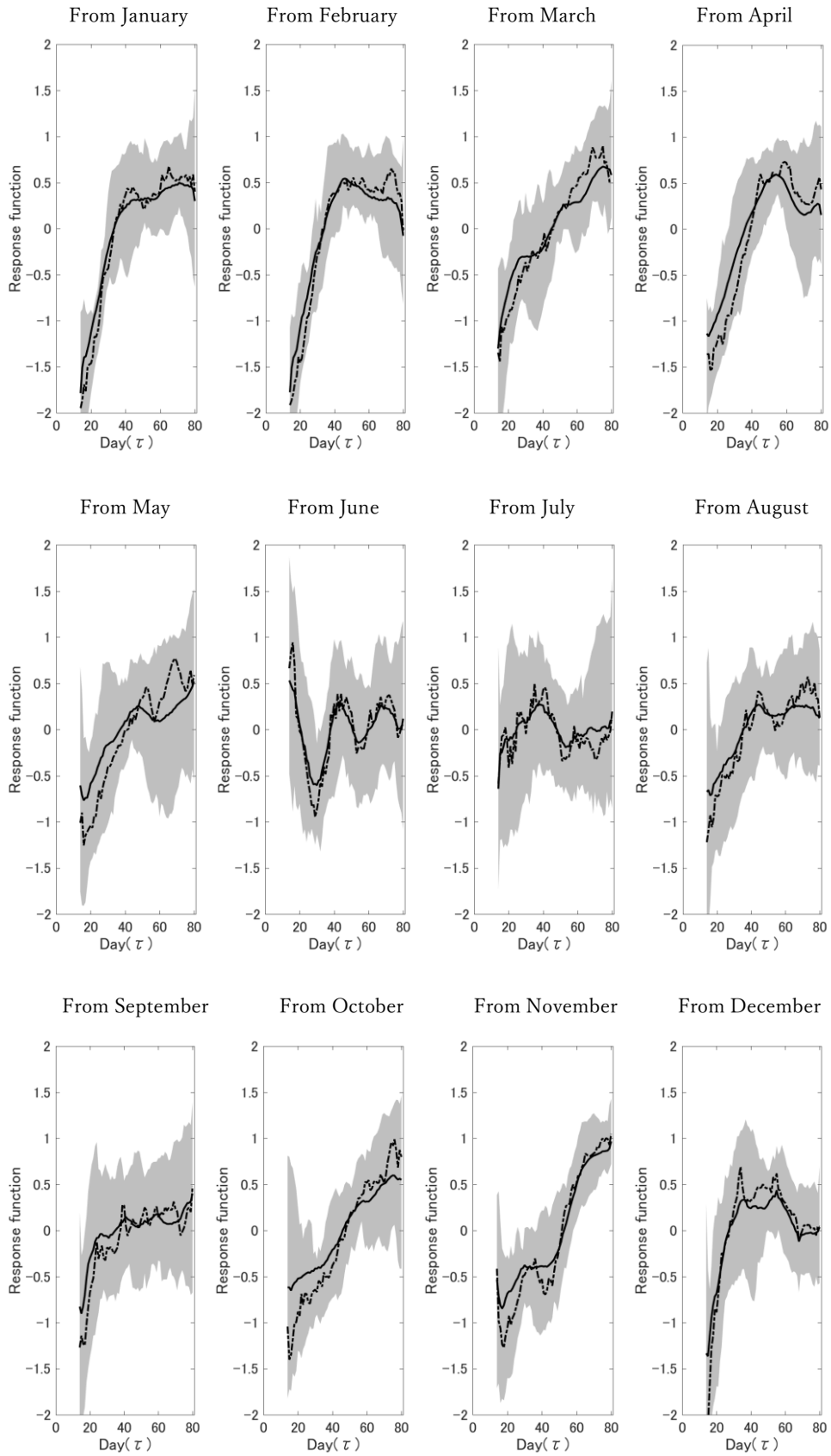
(b) The red line shows the delay time calculated from the precipitation-water level response function. The black line shows the delay time for rainfall-water level (1983–2013) in Figure 4–3, which is shown for comparison.

### 4–3. 3. Calculation of the Seasonal Response Function for each month

Figure 4–5a and b show the results of the precipitation-water level and precipitation-water volume response functions for 31 years of data from 1983 to 2013, with the average, median, and 25–75 % of the calculated range (due to the legends, which are difficult to read.) for each of the 31 years, every 4 months (Fig. 4–5a and b). For example, the heading "From January" in Figure 4–5a represents the period from January to April.

In summary, these results suggest that the response due to subsurface flow has a delay time in the range of 25–70 days, although it varies with the season. The results of the delay time for each four-month period indicate that the average precipitation retention time due to subsurface flow varies from 25 to 70 days. Even in those 25–70 day delay times, there were differences depending on the season, but the average was taken as about 45 days with regular peaks identified before and after the snowmelt season. The response during the snowmelt season was assumed to be early. On the other hand, during the snowmelt season, the delay time was slightly earlier, 25–35 days, and during the slightly drier season (around September), which is neither the rainy season (around June) nor the snowmelt season (around March), the delay time was slightly slower, about 60–70 days (Figure 4–3, Figure 4–4, Figure 4–5a,b).

(a)



(b)

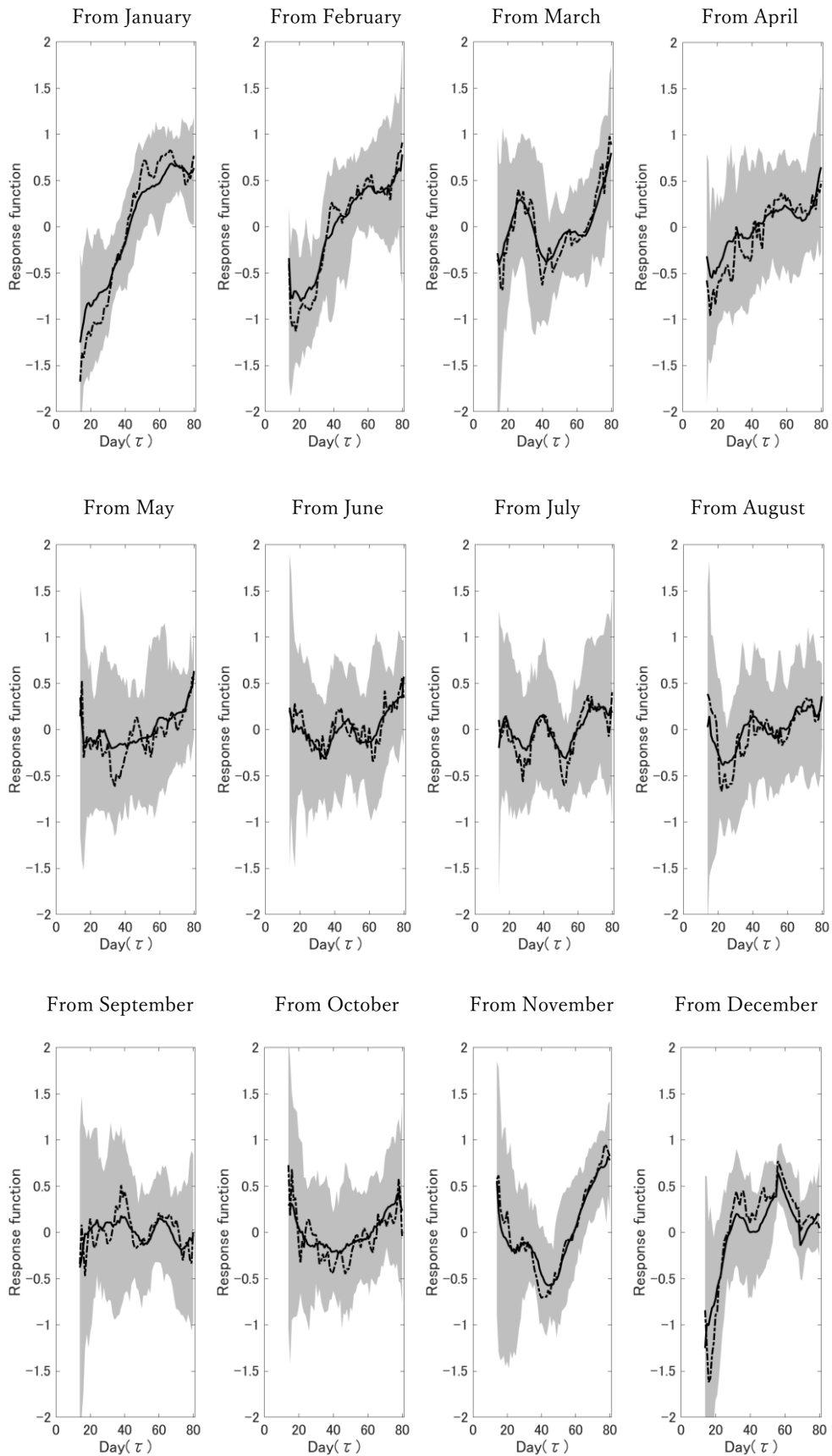


Figure 4–5. Calculations of delay time from (a) precipitation - water level and (b) precipitation - water volume (volume) response functions for a 4-month period for 31 years of data from 1983 to 2013. The plot with the heading "From January" covers the period from January to April, and in the same way, all the other plots represent a four-month period. The bold line represents the mean value of the calculated response function, and the dotted line represents the median value of the calculated response function. The shaded area represents 25 – 75 % of the calculated range.

#### 4–3. 4. Inflow due to snowmelt water

Figure 4–6 shows the observed snow water equivalent in the mid-mountain (Yanagase in Figure 4–1) and mountainous (Nakakawachi in Figure 4–1) areas in the northern part of the Lake Biwa catchment from December 2009 to March 2010 (Iwaki et al. 2010; 2011). Here, the mid-mountain area indicates a relatively high elevation area (about 200-300 m above sea level) between plains and mountains, while the mountain area indicates a high elevation area (about 500 m above sea level) including mountainous areas. I compared these snow cover observations with the peak delay time calculated by the response function.

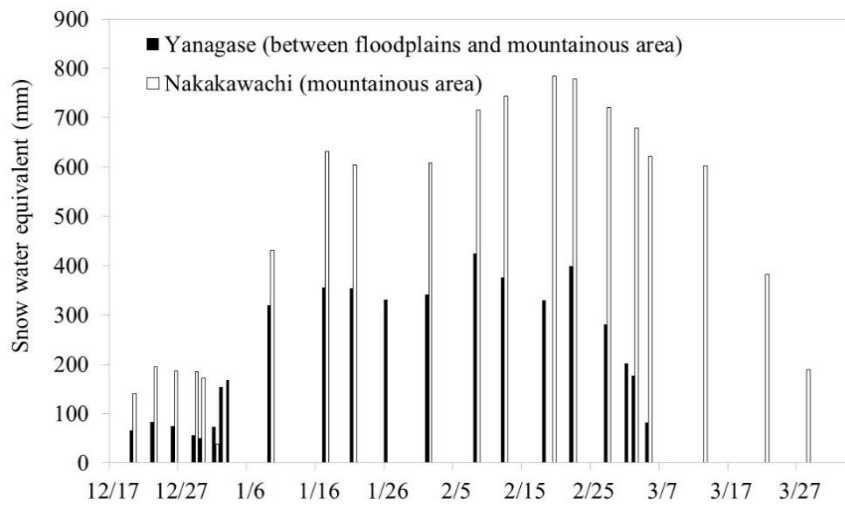
During the snow season from January to early March, especially in February and March, the peak appeared around 45 days (Figure 4–4b and Figure 4–5a). During the snowmelt season (late March), two peaks appeared around 25–35 days and 45 days (Figure 4–5b). These results suggest that precipitation retention time may be shorter during the snowmelt season than at other times of the year because the soil becomes saturated with snowmelt water.

In addition, I describe in the following as the snow in mid-mountain and mountainous areas at this catchment area of Lake Biwa during the winter season. The snow at the catchment area of Lake Biwa, compared to other cold regions such as Hokkaido and the Tohoku, is a warm snow area where rain, snowfall and snowmelt flooding occur simultaneously even in winter (Arai 2004). Typically, the northern catchment area has a larger amount of snow cover than the southern catchment area of Lake Biwa.

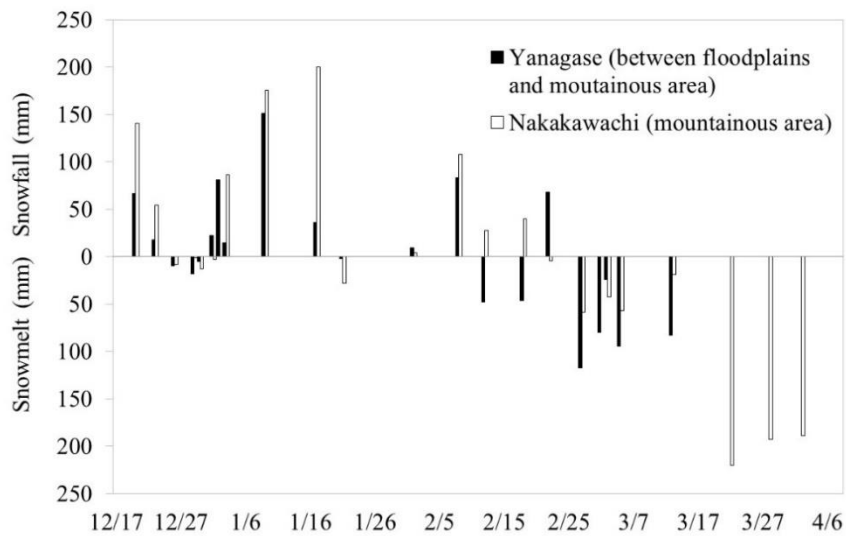
The snowfall begins in mid-December in this area. However, in high elevation mountainous areas (Nakakawachi in Figure 4–1), snow sometimes accumulates as a persistent snowpack, whereas in lower altitude plain areas, snow almost never forms a lasting snowpack and melts quickly (Figure 4–6a, b; Iwaki et al. 2011; Kumagai & Fushimi, 1995). Peak snowfall in the northern part of the Lake Biwa catchment area is from late January to mid-February (Figure 4–6a). In the lower elevation plains, snowmelt occurs soon after snowfall, and the snowmelt water either flows into rivers or percolates into the ground. On the other hand, in the mid-mountainous areas (Surumi and Yanagase in Figure 4–1), after snow has accumulated, snowmelt occurs a little when solar radiation and temperatures are high, but because of low temperatures, snowmelt occurs in late February and early March, when temperatures are increasing. When the temperature increases, snow accumulation in mountainous areas often melts all at once. For this reason, snowmelt flooding is observed at the mouth of the Anegawa River in years when snow accumulation is high over a wide area in mid-mountainous areas. In the

higher elevation mountain areas, snow melting occurs from late March to early April when the temperature increases more, and this can also cause snowmelt floods. Therefore, in years when snow cover is heavy, there may be two snowmelt floods, one in the mid-mountain area and the other in the mountain area (Figure 4–6b). Although the problems associated with this snowmelt are quite complex, there have been efforts to estimate the amount of snowmelt using various models (Kumagai & Fushimi 1995, Chaffe et al. 2010; 2011; 2012).

When the effect of snowfall is included in precipitation, it is possible to discuss the delay time due to two snow cover patterns, one in the mid-mountain region and the other in the mountain region, and the following can be estimated from the observation of snow water volume in the northern Lake Biwa catchment area in 2009/2010 (Figure 4–6a). In the northern part of the Lake Biwa catchment area, the snow cover period was  $\approx 80$  days in the mid-mountain region (Yanagase) and  $\approx 100$  days in the mountainous area (Nakanokawachi) (Figure 4–6a,b). These are considered to be delayed response times due to the retention of snow cover on the land surface itself. Figure 4–4b shows that there is a large peak around 240–300 days, hypothetically assuming a snow accumulation period of 80–100 days (delay due to snow accumulation in mid-mountain areas: 80 days and delay due to snow accumulation in mountain areas: 100 days) and a precipitation retention time of 25–70 days, the maximum precipitation retention time due to snow accumulation would be about 105–170 days. Therefore, the longer delay time (around 240–300 days) shown in Figure 4–4b may have been caused by other factors (e.g., response due to groundwater and evaporation assumed to be constant), which would need to be identified in the future.



(a)



(b)

Figure 4–6. Seasonal changes of snow water equivalent and snowmelt in the northern Lake Biwa catchment area from December 2009 to March 2010, based on (a) the observed snow water equivalent (1–2 times/week) and (b) the estimated increase/decrease in snow water accumulation. (a) Seasonal snow water equivalent observations in Yanagigase (mid-mountainous area) and Nakagawachi (mountainous area) from December 2009 to March 2010. (b) Seasonal changes in measured snow water equivalent and estimated snow melt from December 2009 to March 2010 in Yanagigase and Nakagawachi,

calculated from Figure 4—6a (Iwaki et al. 2010).

Then, the calculated average precipitation retention time was verified using water temperature and dissolved oxygen (DO) concentrations observed at different depths in Lake Biwa. Before the snow melt season, surface water temperature gradually decreases, but DO begins to recover (increase again) in winter when snow falls in December and snow melt begins in February and March at the depth of 60-80 m and at the bottom of the lake (Table 4—2). The deepening of the thermocline, indicating the depth of the lake mixing can be explained by the observed water temperature (Table 4—2). In addition, the recovery of DO was slower for approximately one month at around 80 m than at depths as deep as 15 m (Table 4—2). The recovery of DO in the lake bottom can be explained by lake mixing, since the DO concentration of snowmelt water from rivers is significantly higher than that of lake water (Yamashiki et al. 2003, Akitomo et al. 2004, Chaffe et al. 2010; 2011; 2012). In addition, snowmelt water from rivers is muddy, and snowmelt water discharged from rivers submerges deeper than the surface layer of the lake (Kumagai & Fushimi 1995). Even though the observation interval was about 2 weeks, the delay time is estimated to be about 25—35 days. Furthermore, the recovery of DO ceased since May 2010, which means that the supply of snowmelt water was delayed by 30—45 days. This result suggests that the estimated delay time may be acceptable. Therefore, I conclude that the calculated mean precipitation retention time is one of the factors affecting the lake ecosystem because it is response to river inflow and subsurface flow, and their effects appear in the recovery of DO of the lake bottom.

Table 4–2. Water temperature and DO<sup>†‡</sup> observed in Lake Biwa from 2009 to 2010 (Shiga Prefecture White Paper, 2009–2010). In the table, the yellow color in the table refers to the deepening of thermocline, indicating the depth of lake mixing.

		Water temperature (°C)															
Observation point	Depth\Month-Year	Oct-09		Nov-09		Dec-09		Jan-10		Feb-10		Mar-10		Apr-10		May-10	
The center of Imadsu-oki	0.5m	22.7	20	17.7	14.6	13.4	11.4	10.0	8.7	8.3	7.9	8.2	8.1	9.1	10.4	14.4	16.8
	5 m	22.6	19.6	17.0	14.6	13.4	11.4	10.0	8.7	8.3	7.9	7.9	8.1	8.6	9.1	12.9	12.9
	10 m	22.6	19.6	17.0	14.6	13.4	11.4	10.0	8.7	8.3	7.9	7.9	8.1	8.2	8.8	12.4	11.1
	15 m	22.2	19.6	16.9	14.6	13.4	11.4	10.0	8.7	8.3	7.9	7.8	8.0	8.2	8.7	11.5	10.6
	20 m	13.9	17.4	16.8	14.6	13.4	11.4	9.9	8.7	8.3	7.9	7.9	7.9	8.2	8.7	11.2	10.1
	30 m	9.8	9.8	10.5	11.2	10.2	11.4	9.9	8.6	8.3	7.9	7.9	7.9	8.2	8.6	9.4	9.4
	40 m	8.8	8.5	8.9	8.8	8.8	10.1	9.9	8.6	8.3	7.9	7.9	7.8	8.2	8.4	8.8	8.9
	60 m	8.3	8.0	8.1	8.2	8.1	8.4	8.8	8.6	8.3	7.9	7.6	7.7	8.0	8.1	8.3	8.5
	80 m	8.2	7.9	7.9	7.9	7.9	8.2	8.3	8.4	8.3	7.7	7.5	7.6	7.6	7.9	8.0	7.9
	1m above from the bottom of the lake	8.1	7.8	7.8	7.9	7.9	8.1	8.2	8.3	8.3	7.6	7.5	7.6	7.6	7.8	7.8	7.9

		Dissolved oxygen (mg/L)															
Observation point	Depth\Month-Year	Oct-09		Nov-09		Dec-09		Jan-10		Feb-10		Mar-10		Apr-10		May-10	
The center of Imadsu-oki	0.5m	8.7	9.2	9.4	10.0	10.4	10.5	9.8	9.7	10.6	11.1	11.6	12.0	12.0	12.1	11.3	10.6
	5 m	8.7	9.2	9.6	9.9	10.3	10.5	9.8	9.7	10.6	11.1	11.6	12.0	12.0	12.3	11.8	11.1
	10 m	8.5	9.0	9.4	9.9	10.2	10.5	9.8	9.6	10.5	11.0	11.6	11.9	12.0	12.4	11.6	10.9
	15 m	7.7	8.9	9.4	9.9	10.3	10.4	9.7	9.7	10.5	11.0	11.7	11.8	12.0	12.3	11.6	10.9
	20 m	5.9	7.5	8.8	9.8	10.3	10.4	9.7	9.6	10.5	11.0	11.6	11.8	11.9	12.1	11.6	10.6
	30 m	7.8	7.7	7.1	7.1	8.9	10.3	9.6	9.6	10.5	11.0	11.6	11.8	11.8	12.0	11.2	10.5
	40 m	8.1	8.6	7.3	6.8	7.3	9.3	9.1	10.1	10.5	11.0	11.2	11.6	11.8	11.8	11.0	10.3
	60 m	9.2	9.0	8.3	7.0	6.6	7.0	6.4	10.1	10.5	10.9	11.2	11.0	11.2	11.5	10.7	10.2
	80 m	6.9	7.6	7.2	5.8	4.1	5.2	5.6	6.9	10.4	11.2	11.0	10.9	10.1	10.6	9.9	9.2
	1m above from the bottom of the lake	2.5	3.6	4.1	3.8	3.6	2.8	5.0	3.9	10.2	11.1	11.0	11.0	10.0	10.2	9.3	8.8

		Snow Water Equivalent (mm)															
Observation point	Month-Year	Oct-09		Nov-09		Dec-09		Jan-10		Feb-10		Mar-10		Apr-10		May-10	
						12/1	12/23	1/9	1/21	2/8	2/22	3/5	3/22	4/2			
Yanagase (between mountainous and floodplain)						0	84	320.1	354.2	424.1	398.2	82.61	0	0			
Nakakawachi (mountainous)						0	195	431.7	604	715.8	779.2	621	382	0			

† DO: dissolved oxygen. ‡ These measurements were conducted every two weeks at eight depths in the northern part of the lake at the center of Imadsu-oki (Shiga Prefecture White Paper 2009–2010, Figure 4–1).

#### 4–4. Conclusions

I calculated the delay time (precipitation as the input variable; water level as the output variable) using an impulse response function with 31 years of water level and precipitation data from 1983–2013 in Lake Biwa and its catchment area, and obtained the average precipitation retention times due to subsurface flow with a longer delay time than that of river inflows. The delay times calculated by the precipitation-water level response function confirm a strong response due to direct rainfall on the lake surface and river inflow for approximately 1–3 days, followed by peaks at 25–35 days, 45 days, and 60–70 days. Therefore, based on Iwaki et al. (2020), the delay time due to slow return flow in the Yasu River, which has the longest river length and largest catchment area, was estimated to be about 35–38 days. These results suggest that the delay time due to subsurface flow is approximately in the range of 25–70 days. Furthermore, from the delay times calculated every four months by the response function for water level and precipitation over 31 years, the average precipitation retention time for the Lake Biwa catchment was estimated to be about 45 days. In addition, results suggest that precipitation retention time during snowmelt (around March) is 25–35 days, which is shorter than 60–70 days during dry seasons (e.g., September), except during the paddy irrigation season (May–August), which is complicated slightly due to artificial influences. Although the retention time of precipitation varies depending on the season and surface conditions, I conclude that the average precipitation retention time due to subsurface flow is approximately 45 days. The precipitation retention time estimated in this chapter is close to and supports the results shown in Sayamara 2007, which was about 70 days when there was no rainfall and about 20 days when there was rainfall.

The shape of the response function represented the specific lake system of Lake Biwa, and allowed the delay time to be determined. The findings obtained in this study help us understand Lake Biwa as a lake system, and will be useful for lake management, forest management and disaster prevention. Furthermore, this method may be applied to other lakes and thereby contribute to their water and forest management.

Appendix 4A. Effects of the change in the baseline observation points of BSL

As for BSL, BSL is defined as the observed water level data of Toriigawa before 1992, and after 1992 BSL is redefined as the average of the water levels at five sites (Katayama, Omizo, Hikone, Katada, and Mihogasaki; Figure. 4 – 1). For this reason, the effect of changes in water level observation points was investigated. The Toriigawa water level data from 1993 to 2013 (before) and the average water level at five points (after) were compared (Figure 4 – 1). A one-tailed paired t-test was performed, and the value of Pearson's correlation coefficient was calculated.

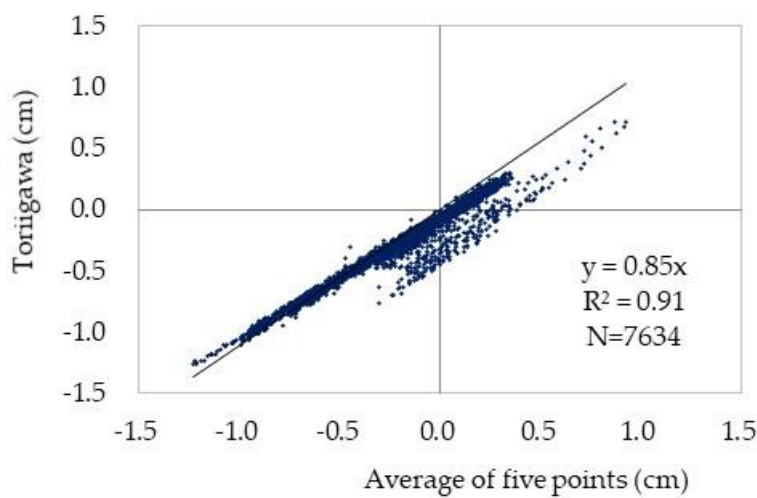


Figure 4A – 1. The relationship between the Toriigawa and five sites (Katayama, Omizo, Hikone, Katada, and Mihogasaki; Figure 4 – 1). Before 1992, BSL used the data of Toriigawa; after 1992, BSL used the averaged data of five sites.

Appendix 4B. Discussion on the change of the baseline observation points of BSL

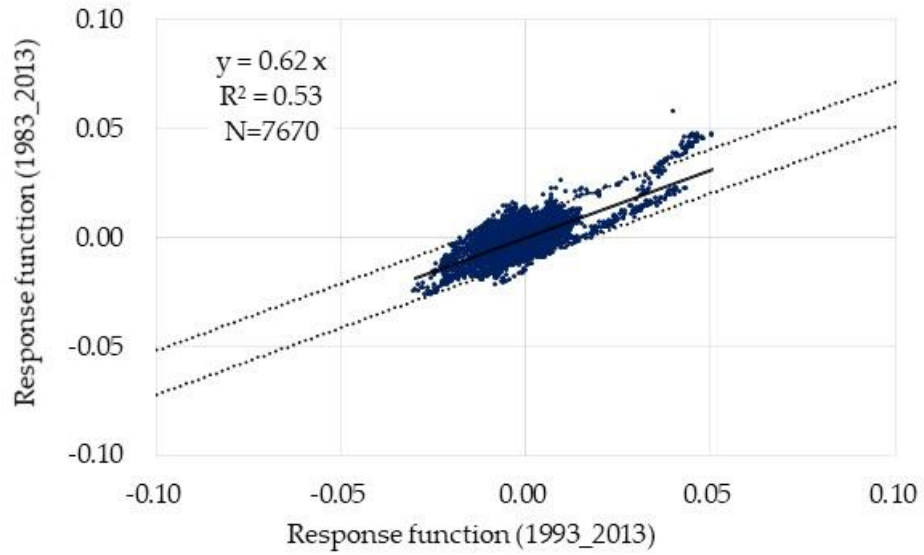


Figure 4B – 1.

The relationship between the calculated results of the response functions from 1983 to 2013 and from 1993 to 2013. The dotted lines represent 95 % confidence intervals for the data.

Appendix 4C. Relationship between rainfall-water level and precipitation-water level of delay times from 1 to 131 days calculated using impulse response function

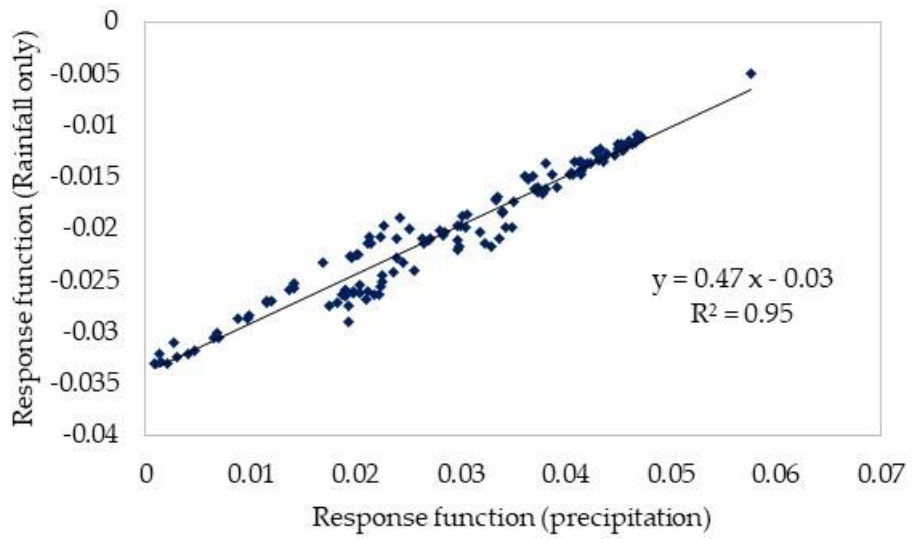


Figure 4C – 1. The relationship between rainfall-water level and precipitation-water level calculated using the impulse response function for the delay time 1 – 131 days.

## Chapter 5 Conclusions

In this thesis, the precipitation retention time was defined as the time from the start of direct precipitation to the end of subsurface flow for a given water mass. Then, the delay time  $\tau$  was calculated using the impulse response function with the lake level of Lake Biwa and the data of the average precipitation in the catchment area, and the precipitation retention time in the catchment area of Lake Biwa was estimated (Iwaki et al. 2014; 2020a; 2020b; 2021; 2022, Iwaki & Toda 2022).

Based on the results obtained in Chapters 3 and 4, the precipitation retention times were (in order of fastest response): ① direct precipitation on the lake surface; ② river inflow by small rivers approximately 2 km in length; ③ river inflow by rivers approximately 10–15 km; ④ the strong response river inflow by overlapping rivers of similar scale approximately 20 km; ⑤ river inflow by Yasu River; ⑥ fast return flow and ⑦ slow return flow by Yasu River; and ⑧ average subsurface flow. As for the water level response of ④, it was treated separately from ③ and ⑤, because the response was well defined by spectral analysis in our previous studies (Iwaki et al. 2014; 2020b).

Based on the findings in Chapter 2, the water level response due to surface seiches was observed between ② and ④, and the water level response due to internal seiches was observed between ⑤ and ⑦. However, surface seiches and internal seiches were not included as precipitation retention time because they are inherent oscillations of the lake and were not related to the changes (increases or decreases) of total lakewater volume. The precipitation retention times from ① to ⑧ above obtained in this thesis are shown schematically in Figure 5–1 (Iwaki et al. 2014; 2020a; 2020b; 2021; 2022).

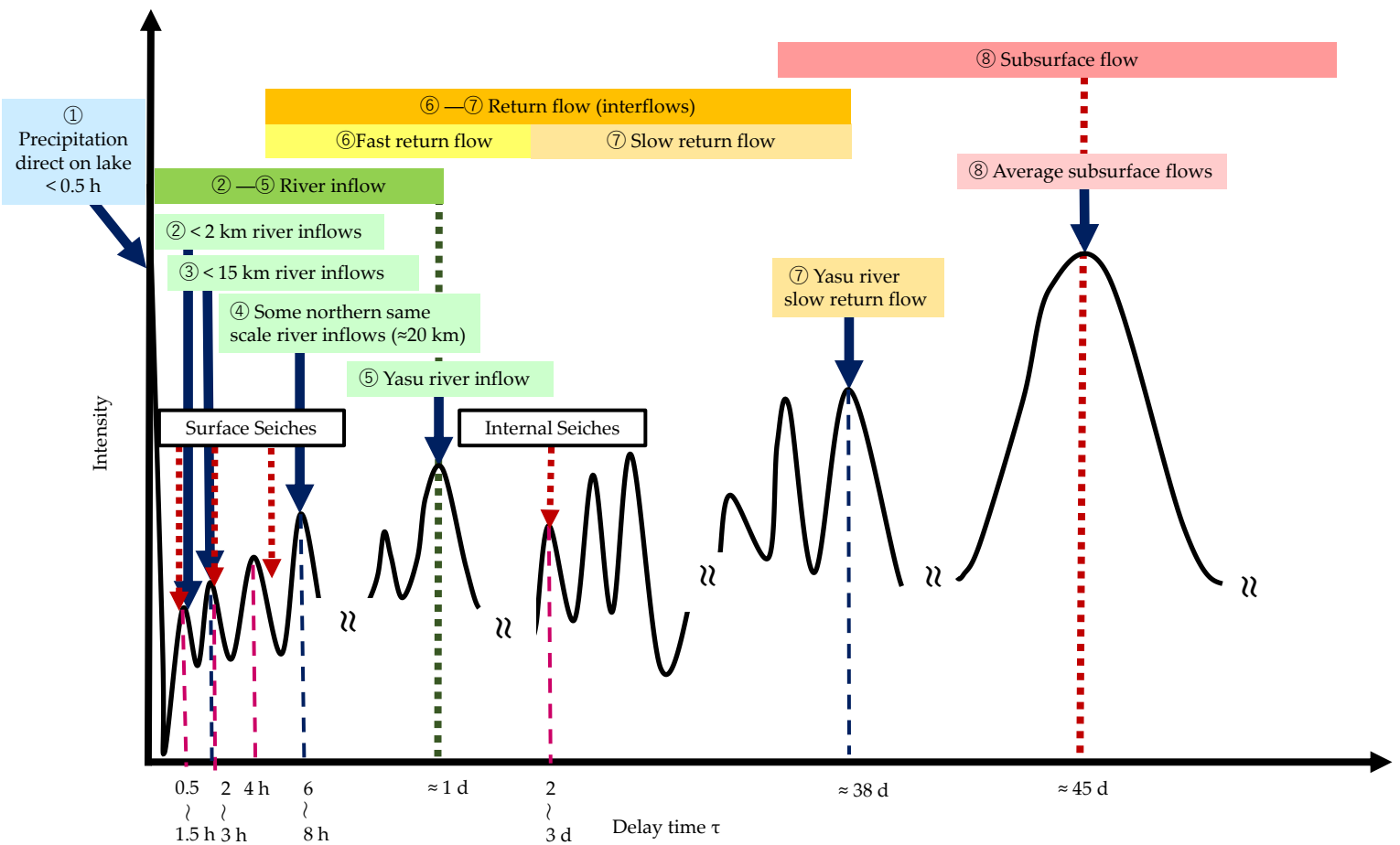


Figure 5 — 1. Schematic diagram of the precipitation retention times (delay times) determined in this thesis.

It is expected that the knowledge obtained in this thesis on several delay time identification methods would contribute to flood forecasting and prevention in catchment areas. It may also help to protect downstream environments and their key ecological processes, for example the spawning activities of aquatic organisms living in estuarine areas, which are sensitive to changes in water levels, from the perspective of water level regulation. This method may also be useful for the analysis the advection and diffusion of mass and heat in lakes and for consideration of materials circulated in the littoral zone of lakes.

The knowledge obtained through this thesis contributes to the important fields of land hydrology and limnology, and is a contribution toward water management, forest resource management and conservation, flood forecasting and disaster prevention.



## References

- AghaKouchak, A., Norouzi, H., Madani, K., Mirchi, A., Azarderakhsh, M., Nazemi, A., Nasrollahi, N., Farahmand, A., Mehran, A., Hasanzadeh, E. Aral Sea syndrome desiccates Lake Urmia: Call for action. *J. Great Lakes Res.* **2015**, *41*, 307–311. <https://doi.org/10.1016/j.jglr.2014.12.007>
- Akitomo, K., Kurogi, M., Kumagai, M. Numerical study of a thermally induced gyre system in Lake Biwa. *Limnology*, **2004**, *5*, 103–114.
- Arai, T. Hydrology of heat and water balance analysis for local analysis, Kokin–Shoin, Tokyo, **2004**.
- Azuma Y. Meteorology and hydrology of the Lake Biwa watershed, Lake Biwa Research Institute; Commemorative Edition, **2003**, 22:9–17.
- Bakker, M., Maas, K., Schaars, F., Asmuth, J. R. Analytic modeling of groundwater dynamics with an approximate impulse response function for areal recharge. *Adv. Water Resour.* **2007**, *30*, 493–504. <https://doi.org/10.1016/j.advwatres.2006.04.008>
- Barberopoulou, A., Qamar, A., Pratt, T. L., Creager, K. C., Steele, W. P. Local amplification of seismic waves from the Denali Earthquake and damaging seiches in Lake Union, Seattle, Washington. *Geophys. Res. Lett.* **2004**, *31*, L03607. <https://doi.org/10.1029/2003GL018569>
- Barberopoulou, A. A seiche hazard study for Lake Union, Seattle, Washington. *Bull. Seismol. Soc. Am.* **2008**, *98*, 1837–1848. <https://doi.org/10.1785/0120070153>
- Berninghausen, W. M. H. Tunamis and seismic seiches reported from the eastern Atlantic south of the Bay of Biscay. *Bull. Seismol. Soc. Am.* **1964**, *54*, 439–442. <https://doi.org/10.1785/BSSA0540010439>
- Berninghausen, W. M. H. Tunamis and seismic seiches reported from regions adjacent to the Indian Ocean. *Bull. Seismol. Soc. Am.* **1966**, *56*, 69–74. <https://doi.org/10.1785/BSSA0560010069>
- Berninghausen, W. M. H. Tunamis and seismic seiches of southeast Asia. *Bull. Seismol. Soc. Am.* **1969**, *59*:289–297. <https://doi.org/10.1785/BSSA0590010289>
- Biwako Handbook. (Eds.) Fluctuation of Lake Biwa. In *Biwako handbook*; Shiga Prefecture: Shiga, Japan, **2010**; pp. 192–192.
- Bondevik, S., Gjevik, B., and Sørensen, M. B. Norwegian seiches from the giant 2011 Tohoku earthquake, *Geophysical Research Letters*, **2013**, *40*, 3374–3378. <https://doi.org/10.1002/grl.50639>

- Burg, J. P. Maximum Entropy Spectral Analysis. PhD dissertation, Stanford Univ., **1975**.
- Carey, C. C., Hanson, C. P., Lathrop, C. R, Amand, L. Using wavelet analyses to examine variability in phytoplankton seasonal succession and annual periodicity. *J. Plankton Res.* **2016**, 38, 27–40. <https://doi.org/10.1093/plankt/fbv116>
- Chaffe, P.L.B., Yamashiki, Y., Takara, K., Kato, M., Iwaki, M. Influence of the Ane River Basin on Dissolved Oxygen Concentration of Lake Biwa: Sensitivity Study of the Biwa–3D model. *Anu. Dis. Prev. Res. Inst. Kyoto Univ.* **2010**, 53B, 91–96. <http://hdl.handle.net/2433/129421>
- Chaffe, P.L.B., Yamashiki, Y., Takara, K., Iwaki, M. A comparison of simple snowmelt models for the Ane River Basin. *Anu. Dis. Prev. Res. Inst. Kyoto Univ.* **2011**, 54B, 113–118. <http://hdl.handle.net/2433/151079>
- Chaffe, P.L.B., Yamashiki, Y., Takara, K., Iwaki, M. Measurement and modeling of the snowmelt in the Ane river basin. *J. Japan Soc. Civil Eng.* **2012**, 68, 223–228. [https://doi.org/10.2208/jscejhe.68.I\\_223](https://doi.org/10.2208/jscejhe.68.I_223)
- Delbart, C., Valdés, D., Barbecot, F., Tognelli, A., Couchoux, L. Spatial organization of the impulse response in a karst aquifer. *J. Hydrol.* **2016**, 537, 18–26. <https://doi.org/10.1016/j.jhydrol.2016.03.029>
- Dooge, J. C. I. Linear Theory of Hydrologic Systems. Technical Bulletin 1468. US Department of Agriculture, Washington, D.C., **1973**, 3–29.
- Dziewonski, A. M. On Regional Differences in Dispersion of Mantle Rayleigh Waves. *Geophys. J.R. astr. Soc.* **1970**, 22:289–325. <https://doi.org/10.1111/j.1365-246X.1971.tb03601.x>
- Farahmand, T., Fleming, S. W., Quilty, E. J. Detection and visualization of storm hydrograph changes under urbanization: an impulse response approach. *J. Environ. Manag.* **2007**, 85, 93–100. <https://doi.org/10.1016/j.jenvman.2006.08.004>
- Forel, F-A. *Le Léman. Monographie limnologique, Vol. 2*. Lausanne F. Rouge. **1895**, pp, 39–213.
- Fujii, S. Physics of Lake Biwa, In: Somiya I., eds. Lake Biwa, 2-6, pp 66-82, Gihoudou publish, Tokyo, **2000**.
- Fujino, Y. Water Budget. An Introduction to Limnology of Lake Biwa, Mori, S., Ed., Kyoto, Japan, **1980**, pp. 19–26.
- Furukawa, M., Kaneki R. Development and Application of a Water Quality Model for a Lagoon. *Irrigation, Drainage and Rural Engineering Journal*, 232, **2004**, pp. 411–417.
- Geospatial Information Authority of Japan. Report of crustal deformation after 2011 TE,

**2011.**

Gronewold, A. D., Rood, R. B. Recent water level changes across Earth's largest lake system and implications for future variability. *Journal of Great Lakes Research*, **2019**, *45*(1), 1–3. <https://doi.org/10.1016/j.jglr.2018.10.012>

Haga, H. Confirmation of surface area of the southern basin of Lake Biwa Japan. *Jpn. J. Limnol.* **2006**, *67*, 123–126. <https://doi.org/10.3739/rikusui.67.123>

Hantush, M. M. Modeling stream–aquifer interactions with linear response functions. *J. Hydrol.* **2005**, *311*, 59–79. <https://doi.org/10.1016/j.jhydrol.2005.01.007>

Hasegawa N. Estuary boundary process, In: Nagata, T., Kumagai, M., Yoshiyama, K., eds. *Limnology of Global Warming, 2.5*, pp 87–98, Kyoto university publish, Kyoto, **2012**.

Hayami, S. On the propagation of flood waves. *Bulletins, Disaster Prevention Research Institute, Kyoto Univ.*, **1951**, *1*, 1–16. <http://hdl.handle.net/2433/123641>

Hidaka, K. *The Theory of Applied Integral Equation*, Kawakita Press, Tokyo, Japan, **1943**.

Hikosaka, S. *Physical in Oceanography* (ed. Masuzawa, J.) III 173–196. Tokai University, **1971**.

Hino, M. *Spectrum Analysis*; Asakura Press: Tokyo, Japan, **1977**.

Hocking, M. and Kelly, B.F.J. Groundwater recharge and time lag measurement through Vertosols using impulse functions. *J. Hydrol.* **2016**, *535*, 22–35. <https://doi.org/10.1016/j.jhydrol.2016.01.042>

Hofmann, H., Lorke, A., Peeters, F. Temporal scales of water-level fluctuations in lakes and their ecological implications. *Hydrobiologia.* **2008**, *613*, 85–96. [https://doi.org/10.1007/978-1-4020-9192-6\\_9](https://doi.org/10.1007/978-1-4020-9192-6_9)

Honda, K., Terada, T., Yoshida, Y. & Isitani, D. Secondary undulations of oceanic tides. *J. Coll. Sci. Imp. Univ. Tokyo* *24*, 1, **1908**.

Ichinose, G. A., Anderson, J. G., Satake, K., Schweickert, R. A., Lahren, M. M. The potential hazard from tsunami and Seiche waves generated by large earthquakes within Lake Tahoe. California–Nevada. *Geophys. Res. Lett.* **2000**, *27*, 1203–1206. <https://doi.org/10.1029/1999GL011119>

Ikebuchi, S., Seki, M., Ohtoh, A. Evaporation from Lake Biwa. *J. Hydrol.* **1988**, *102*, 427–449. [https://doi.org/10.1016/0022-1694\(88\)90110-2](https://doi.org/10.1016/0022-1694(88)90110-2)

Imasato, N. Study of seiche in Biwa-ko [I] – on the numerical calculation by Defant's method. *Contrib. Geophys. Inst. Kyoto Univ.* **1970**, *10*, 93–103.

Imasato, N. Study of seiche in Biwa-ko [II] – on a numerical experiment by nonlinear two-dimensional model. *Contrib. Geophys. Inst. Kyoto Univ.* **1971**, *11*, 77–90.

Imasato, N. Study of seich in Biwa-ko [III] – some results of numerical experiments by nonlinear two-dimensional model. *Contrib. Geophys. Inst. Kyoto Univ.* **1972**, *12*, 63–75.

Imasato, N. Seiche. In: Horie S., ed. *Lake Biwa*. Dr. W. Junk Publishers, Dordrecht, **1984**, pp. 238–256.

Imasato, N., Kanari, S., Kunishi, H. A numerical experiment of water motion in Lake Biwa-ko – on the two-dimentional one layer model –. *Contrib. Geophys. Inst. Kyoto Univ.*, **1971**, *14*, 451–464.

Imasato, N., Kanari, S., Kunishi, H. Study of seiche in Biwa-ko [IV] – observation with a new portable long period water level gauge. *Contrib. Geophys. Inst. Kyoto Univ.*, **1973**, *13*, 65–72.

Iwai S., Ishiguro M. Applied Hydrodynamic Statistics, Morikita publish, Tokyo, **1970**.

Iwaki, M., Saijyou, M., Hida, Y., Ueno, K. Estimation of Snow Water Equivalent at North Catchment Area of Lake Biwa. Abstract of 1<sup>st</sup> World Lake Student Conference, **2008**.

Iwaki, M., Furukawa Y., Sakai S. Seasonal changes in snow water equivalent and snowmelt at the northern part of the catchment area of Lake Biwa, Abstract of 75<sup>th</sup> Jpn J limnology, **2010**.

Iwaki, M., Hida, Y., Ueno, K., Saijyo, M. Observation of snow water equivalent in the north catchment area of Lake Biwa. *Lakes Reserv. Res. Manag.* **2011**, *16*, 215–221. <https://doi.org/10.1111/j.1440-1770.2011.00454.x>

Iwaki, M., Kumagai, M., Nishi, K. The water level fluctuations of Lake Biwa - water level changes after the 2011 TE, Abstract of Japan society of hydrology and water resources meeting, **2011**.

Iwaki, M., Kumagai, M., Kitazawa, D., Nishi, K., Jiao, C. The surface seiche of Lake Biwa. Abstract of Association for the Sciences of Limnology and Oceanography Aquatic Sciences meeting, **2012**.

Iwaki, M., Kumagai, M., Jao, C., Nishi, K. Evaluation of river inflows during heavy precipitation based on water level changes in a large lake. *Jpn J Limnol*, **2014**, *75*:87–98. <https://doi.org/10.3739/rikusui.75.87>

Iwaki, M.<sup>a)</sup>, Yamashiki, Y., Muraoka, K., Toda, T., Jiao, C., Kumagai, M. Effect of rainfall-influenced river influx on lake water levels: Time scale analysis based on impulse response function in the Lake Biwa catchment area. *Inland Waters*, **2020**, *10*, 283–294. <https://doi.org/10.1080/20442041.2020.1712952>

Iwaki, M.<sup>b)</sup>, Hayakawa, K., Goto, N. How the precipitation to the catchment effect on the lake water level using depth meter moored in north Lake Biwa. Abstract of JpGU - AGU Joint Meeting, **2020**.

Iwaki, M.<sup>a)</sup>, Yamashiki, Y., Toda, T., Jiao, C., Kumagai, M. Estimation of the average retention time of precipitation at the surface of a catchment area for Lake Biwa. *Water*, **2021**, *13*, 1711. <https://doi.org/10.3390/w13121711>

Iwaki, M.<sup>b)</sup>, Takamura, N., Nakada, S., Oguma, H. Monitoring of lake environment using a fixed point and time-lapse camera—Case study of south basin of Lake Biwa. *Journal of The Remote Sensing Society of Japan*, **2021**, *41*;5, 563–574. <https://doi.org/10.11440/rssj.41.563>

Iwaki, M., Hayakawa, K., Goto, N. An estimation of precipitation retention time using depth metres in the northern basin of Lake Biwa. *Atmosphere* **2022**, *13*, 724. <https://doi.org/10.3390/atmos13050724>

Iwaki, M., Toda, T. Seismic seiche-related oscillations in Lake Biwa, Japan, after the 2011 Tohoku earthquake. *Sci Rep.* **2022**, *12*, 19357. <https://doi.org/10.1038/s41598-022-23939-7>

Japan Meteorological Agency. Improved soil rainfall index and watershed rainfall index, Textbook for training on forecasting technology in 2012, **2013**, 122-131. <https://www.data.jma.go.jp/obd/stats/etrn/> (Accessed 2022.1.1)

Japan Meteorological Agency. 20<sup>th</sup> Report of as for Study of Tunami forecasting method. **20**, **2022**.

Japan Ministry of Land Infrastructure of Biwako Office, Available online: <https://www.kkr.mlit.go.jp/biwako/index.php> (Accessed 2022.1.1)

Japan Ministry of Land Infrastructure, **2014**, *2*, 1–31. Available online: <https://www.kkr.mlit.go.jp/river/iinkaikatsudou/kensyou/datatenkenkawaniu.html> (Accessed 2022.1.1).

Japan Ministry of Land Infrastructure, Report of Kinki Regional Development Bureau, 2014, *2*; 1–31. Available online: <https://www.kkr.mlit.go.jp/river/iinkaikatsudou/kensyou/datatenkenkawaniu.html> (Accessed 2022.1.1).

Jiao, C., Kumagai, M. Large amplitude nonlinear internal surge in Lake Biwa. *Jpn. J. Limnol.* **1995**, *56*, 279–289. <https://doi.org/10.3739/rikusui.56.279>

Kanamori, H. Velocity and Q of mantle waves. *Phys. Earth Planet. Interiors.* **1970**, *2*;259–275.

Kanari, S. Internal waves in Lake Biwa (I)-The responses of the thermocline to the wind

- action. *Bull. Disaster Prev. Res. Inst.* **1970**, *19*, 19–26. <http://hdl.handle.net/2433/124777>
- Kanari, S. The long-period internal waves in Lake Biwa. *Limnol. Oceanogr.* **1975**, *20*, 544–553. <https://doi.org/10.4319/lo.1975.20.4.0544>
- Kawabata, H. Groundwater infiltration into the lake. *Environ. Sci. Res. Rep.* **1982**, *S704*, 29–36.
- Khono, N. About meteo-tsunami, Tenki, Explanation of new terminology, **2014**, *61*;6, 58–60.
- Koike, S. Scientific Computation in C, CQ Press, Tokyo, **1997**.
- Kvale, A. Seismic seiches in Norway and England during the Assam earthquake of August 15, 1950. *Bull. Seismol. Soc. Am.* **1955**, *45*. <https://doi.org/10.1785/BSSA0450020093>.
- Kotoda, K. The estimation method of lake evaporation using climatological data. In *Report of the Hydraulic Experiment University of Tsukuba Environmental Research Center Papers*; University of Tsukuba: Tsukuba, Japan, **1977**, 53–65.
- Kondo J., Honya K., Matsushima, D. A study on annual variations of the soil water content and water equivalent of snow in a watershed, runoff and the river water temperature by use of the new bucket-model, Tenki, **1995**, *42*;12, 821–831.
- Kumagai, M. and Fushimi, H. Inflows due to snowmelt. In: Okuda, S., Imberger, J., Kumagai, M., eds., *Physical Processes in a Large Lake: Lake Biwa, Japan. Coastal and Estuarine Studies*, *48*. The American Geophysical Union, Washington, **1995**, pp. 129–139.
- Kumagai, M., Okubo K., Jiao C., Sou, G. Comparison of Fuxian Lake and Lake Biwa in terms of geophysical characteristics and environmental dynamics. In: Sakamoto, m., Kumagai, M., eds., *Lakes and Drainage Basins in East Asia Monsoon Area*; Nagoya University Press, Nagoya, **2006**, pp. 186–202.
- Manabe S. Climate and the ocean circulation, I, The atmospheric circulation and the hydrology of the earth's surface, *Mon. Weather Rev.* **1969**, *97*;11, 739–774. [https://doi.org/10.1175/1520-0493\(1969\)097<0739:CATOC>2.3.CO;2](https://doi.org/10.1175/1520-0493(1969)097<0739:CATOC>2.3.CO;2)
- Markus, W., McGlynn, B. L., McGuire, K. J., McDonnell, J. J. How does rainfall become runoff? A combined tracer and runoff transfer function approach. *Water Resour. Res.* **2003**, *39*, 1315. <https://doi.org/10.1029/2003WR002331>
- McGarr, A. & Vorhis, R. C. Seismic seiches from the March 1964 Alaska earthquake, *US. Geol. Surv. Prof. Pap.* **1968**, *544*, E1–43.
- Micklin, P. P. Desiccation of the Aral Sea: A water management disaster in the Soviet Union. *Science*, **1988**, *241*(4870), 1170–1176.

<https://doi.org/10.1126/science.241.4870.1170>

Micklin, P. M. The Aral Sea disaster. *Annual Review of Earth and Planetary Sciences*, **2007**, 35(1), 47–72. <https://doi.org/10.1146/annurev.earth.35.031306.140120>

Minami, S. *Waveform Data Processing for Scientific Technique*, CQ Press, Tokyo, **1997**.

Miyazawa, M. Detection of seismic events triggered by P-waves from the 2011 Tohoku-Oki earthquake. *Earth Planets Space*. **2012**, 64, 1223–1229.  
<https://doi.org/10.5047/eps.2012.07.003>

Mizuno, T., Otuska, T., Ogawa, M., Funao, T., Kanao, S., Machata, M. Spawning migration triggers in round crucian carp *Carassius auratus glandoculis* and water level fluctuations in Lake Biwa. *Jpn. J. Conserv. Ecol.* **2010**, 15;2, 211–217.  
[https://doi.org/10.18960/hozen.15.2\\_211](https://doi.org/10.18960/hozen.15.2_211)

Moore, J.N. Recent desiccation of Western Great Basin Saline Lakes: Lessons from Lake Abert, Oregon, U.S.A. *Sci. Total Environ.* **2016**, 554–555, 142–154.  
<https://doi.org/10.1016/j.scitotenv.2016.02.161>

Moss, B., Kosten, S., Meerhoff, M., Battarbee, W. R., Jeppesen, E., Mazzeo, N., Havens, K., Lacerot, G., Liu, Z., Meester, D. L. Allied attack: climate change and eutrophication. *Inland Waters*. **2011**, 1, 101–105. <https://doi.org/10.5268/IW-1.2.359>

Moussa, R. Geomorphological transfer function calculated from digital elevation models for distributed hydrological modelling. *Hydrol. Process.* **1997**, 11, 429–449.  
[https://doi.org/10.1002/\(SICI\)1099-1085\(199704\)11:5<429::AID-HYP471>3.0.CO;2-J](https://doi.org/10.1002/(SICI)1099-1085(199704)11:5<429::AID-HYP471>3.0.CO;2-J)

Murakami M. A method for estimating discharge and the Kamo River flood of 1935, *Chikyū*, **1936**, 25;6, 425–451.

Nakakita, E., Sugahara, T., Okada, N., Ikebuchi, S. Temporal-spatial Rainfall Distribution Characteristics Depending on Topographical Features. *Anu. Dis. Prev. Res. Inst. Kyoto Univ.* **1997**, 40, 275–287.  
<https://repository.kulib.kyoto-u.ac.jp/dspace/bitstream/2433/80277/1/a40b2p20.pdf>

Nakakita E. Suzuki Y., Ikebuchi S. Hierarchical time-scale structure independency of rainfall distribution on topography. *Proceedings of hydraulic engineering*, **2000**, 44, 91–96. [https://www.jstage.jst.go.jp/article/prohe1990/44/0/44\\_0\\_91/\\_pdf/-char/ja](https://www.jstage.jst.go.jp/article/prohe1990/44/0/44_0_91/_pdf/-char/ja)

Nakakita E., Yoshikai T., Kim S. Application of error-ensemble method to a short-term rainfall prediction with transration model considering orographic rainfall. *Annuals of Disas. Prev. Res. Inst., Kyoto Univ.*, **2010**, No.53B, 447–458.  
<https://www.dpri.kyoto-u.ac.jp/nenpo/no53/ronbunB/a53b0p49.pdf>

Nakamura, S., Honda, K. Seiches in some lakes of Japan. *J. Coll. Sci. Imp. Univ. Tokyo*, **1902**, 28; 1–95.

Obara, K. New detection of tremor triggered in Hokkaido, northern Japan by the 2004 Sumatra-Andaman earthquake, *Geophysical Research Letters*. **2012**, *39*;20, 20305. <https://doi.org/10.1029/2012GL053339>

Okada K., Makihara Y., Shimpo A., Nagata K., Kunitsugu M., Saitoh K. Soil Water Index (SWI), *Tenki*, **2001**, *48*, 349356.

Oliver, J. A summary of observed seismic surface wave dispersion. *Bull. Seismol. Soc. Am.* **1962**, *52*, 81–86. <https://doi.org/10.1785/BSSA0520010081>

Ostrovsky, I., Rimmer, A., Yacobi, Z.Y., Nishri, A., Sukenik, A., Hadas, O., Zohary, T. Long-term changes in the Lake Kinneret ecosystem: The effects of climate change and anthropogenic factors. In: Goldman, R.C., Kumagai, M.M., Robarts, D.R., eds. *Climatic Change and Global Warming of Inland Waters: Impacts and Mitigation for Ecosystems and Societies*, John Wiley and Sons, West Sussex, UK, **2013**, pp. 271–291.

Saijo, Y. Investigation of lake morphology, In: Saijyo Y., Mitamura O., eds. *Guideline Limnological Research*. Koudansya. Tokyo, **1995**.

Sato K., *Method for Calculating Flood Discharge*, Sankaido publish, Tokyo, **1982**.

Sato, Y., Nishino, M. Model analysis of the impact on spawning of cyprinid fishes by water level manipulation and prediction of the effect of measures. *Wetl. Res.* **2010**, *1*, 17–31.

Sayama T., Tachikawa Y., Takara K. Gause-rader rainfall composition with incorporating estimation uncertainty by using cokriging-type sequential Gaussian simulation. *J. Journal of JSCE*, **2005**, *803*, 1–11. [https://www.jstage.jst.go.jp/article/jscej/2005/803/2005\\_803\\_803\\_1/\\_pdf/-char/ja](https://www.jstage.jst.go.jp/article/jscej/2005/803/2005_803_803_1/_pdf/-char/ja)

Sayama T., Tatsumi K., Tachikawa Y., Takara K. Hydrograph separation based on spatiotemporal record of stream flow in a distribution rainfall-runoff model. *J. Japan Soc. Hydrol & Water Resour.* **2007**, *20*;3, 214–225. <https://doi.org/10.3178/jjshwr.20.214>

Shiga Prefecture. *White Paper on the Environmental of Shiga Prefecture*; Shiga Prefecture, **2009–2010**.

Sugawara M. *Hydrology Lecture 7 Runoff Analysis Method*, Kyoritsu publish, Tokyo, **1972**.

Sugawara M. *Runoff Analysis of the Lake Biwa Basin*, Water science, **1973**, *89*, 1–41.

Sugawara M. *Hydrology Lecture additional volume Sequential Runoff Analysis Method*, Kyoritsu publish, Tokyo, **1979**.

Takahashi Y. River Engineering, University of Tokyo Press, Tokyo, **1990**.

Takahashi, T., Tsumoto, K., Kobayashi, M. The flux distribution and amount of groundwater sprung from a bottom in south basin of Lake Biwa. Abstract of 15<sup>th</sup> Jpn J limnology of Kinki, **2004**.

Tani, M., Matsushi, Y., Sayama, T., Kojima, N. Characterization of the vertical unsaturated flow for an integrated prediction of the storm runoff response and landslide initiation on a hillslope, Abstract of Japan Geoscience Union 2019 meeting. **2019**, HGM04-05.

Tani, M., Matsushi, Y., Sayama, T., Sidle, R. C., Kojima, N. Characterization of vertical unsaturated flow reveals why storm runoff responses can be simulated by simple runoff-storage relationship models. *J. Hydrol.* **2020**, 588;3, 124982.  
<https://doi.org/10.1016/j.jhydrol.2020.124982>

Taniguchi, M. Change in groundwater seepage rate into Lake Biwa, Japan, *Jpn. J. Limnol.*, **1995**, 56;4, 261–267.

Taniguchi, M., Fukuo, Y. An effect of seiches on groundwater seepage rate into Lake Biwa, Japan, *Water Resources Research*, **1996**, 32; 2, 333–338.  
<https://doi.org/10.1029/95WR03245>

Tokiwano, K., Ohtomo, N. & Tanaka, Y. The Time Series Analysis Using Maximum Entropy Method, Hokkaido University Press, **2002**.

Tsai, C., Miki, T., Chang, C.W., Ishikawa, K., Ichise, S., Kumagai, M., Hsieh, C.H. Phytoplankton functional group dynamics explain species abundance distribution in a directionally changing environment. *Ecology* **2014**, 95, 3335–3343.  
<https://doi.org/10.1890/13-1946.1>

Tsurumaki, M., Kobayashi, M. Interaction of lake and ground water case study of Lake Biwa. *Jpn J. Geogr.* **1989**, 98:53, 77.

United States Department of Agriculture. Time of concentration. Part 630, hydrology. National Engineering handbook, Chapter 15. *Nat. Res. Conserv. Serv.* **2010**, 15, 1–11.

Utsu, T. Seismology, Kyoritsu publish, Tokyo, **2001**.

Wine, M.L., Rimmer, A., Laronne, J.B. Agriculture, diversions, and drought shrinking Galilee Sea. *Sci. Total Environ.* **2019**, 651, 70–83.  
<https://doi.org/10.1016/j.scitotenv.2018.09.058>

Woolway, I. R., Kraemer, M. B., Lenters, D. J., Merchant J C., O'Reilly, M. C., Sharma, S. Global lake responses to climate change. *Nat. Rev. Earth Environ.* **2020**, 1, 388–403.  
<https://doi.org/10.1038/s43017-020-0067-5>

Yamashiki, Y., Kumagai, M., Jiao, C., Nezu, I., Matsui, S. Numerical simulation of thermally induced gyres in Lake Biwa, *Hydrol. Proc.*, **2003**, *17*, 2947–2956. <http://hdl.handle.net/2433/8436>

Yamamoto S. Hydrology Lecture 1 Comprehensive Hydrology, Kyoritsu publish, Tokyo, **1972**.

Yang, J., Lv, H., Yang, J., Liu, L., Yu, X., Chen, H. Decline in water level boosts cyanobacteria dominance in subtropical reservoirs. *Sci. Total Environ.* **2016**, 557–558, 445–452. <https://doi.org/10.1016/j.scitotenv.2016.03.094>

Yokoki, H., Tomura, T., Hanawa, N., Kuwahara, Y., Mimra, N. Estimation of the Future River Flood and Inundation Risk Due to Climate Change-Analyses on Naka River and Kuji River in Ibaraki Prefecture, Japan. *Chikyu Kankyo Assoc. Int. Res. Initiat. Environ. Stud.* **2008**, *16*, 87–93. <https://doi.org/10.2208/proge.16.87>.

Yomogida, K., Yoshizawa, K., Koyama, J., Tsuzuki, M. Along-dip segmentation of the 2011 off the Pacific coast of Tohoku earthquake and comparison with other megathrust earthquakes. *Earth Planets Space.* *63*, 697–701, **2011**; <https://doi.org/10.5047/eps.2011.06.003>

Yoshimura, S. Limonology, Sanseido publish, Tokyo, **1937**.

Yoshizawa, K. Multi-orbit surface waves generated by the 2004 great Sumatra earthquake. *Geophys. Bull*, Hokkaido Univ., Sapporo, **2006**, *69*:15–21.

Zohary, T., Ostrovsky, I. Ecological impacts of excessive water level fluctuations in stratified freshwater lakes. *Inland Waters.* **2011**, *1*, 47–59. <https://doi.org/10.5268/IW-1.1.406>